MODULATING INNATE IMMUNITY IMPROVES OUTCOMES IN ACUTE LUNG INJURY

Julia Louise Malik Dunn

A dissertation submitted to the faculty at the University of North Carolina at Chapel Hill in partial fulfillment of the requirements for the degree of Doctor of Philosophy in the Department of Microbiology & Immunology in the School of Medicine.

Chapel Hill
2016

Approved by:

Bruce A. Cairns

Robert Maile

Tom Kawula

Claire Doerschuk

Janelle Arthur

Ed Miao

ABSTRACT

Julia Louise Malik Dunn: Modulating Innate Immunity Improves Outcomes in Acute Lung Injury
(Under the Direction of Bruce A. Cairns)

Pulmonary inflammation following traumatic injury disrupts the lung architecture, leading to impaired oxygen exchange and rendering patients susceptible to life threatening bacterial infections. Innate immunity is central to the resolution of infection; however, excessive immune responses cause unresolved inflammation that exacerbate tissue damage. We hypothesize that partially attenuating recruitment of innate immune cells without impairing their function *in situ* will improve outcomes for patients diagnosed with acute lung injury (ALI) following burns and smoke inhalation by restoring homeostasis. Using mouse models of injury, we characterized the innate immune response in the lung following burns and smoke inhalation to establish mechanistic relationships that drive inflammation and to test therapeutic interventions. We show that significant neutrophil recruitment to the lung following burn injury is driven by damage associated molecular patterns (DAMPs); however, this recruitment does not result in improved bacterial clearance following pulmonary infection. To explore the factors that drive inflammation in a clinically relevant direct lung injury model, we developed and validated a novel murine model of acute smoke inhalation. This model mimics granulocyte recruitment, anti-inflammatory cytokine profile, DAMP release, and susceptibility to bacterial infection that are important drivers of outcome in patients. Using this model, we differentiate between correlative and causative inflammatory relationships in ALI. First, we demonstrate that inducible nitric

oxide synthase is required for upregulation of interleukin-10 (IL-10), monocyte chemotactic protein 1, and hyaluronic acid (HA) following inhalational injury, but not for bacterial clearance. Thus, we propose that the relationship between elevated IL-10 and the onset of bacterial infection in patients may be correlative rather than causative. Furthermore, we demonstrate that neutrophil recruitment is driven by the chemokine CXCL1 as well as leukotriene B4, and we present data that granulocyte NADPH oxidase (NOX2) rapidly eliminates these signals and prevents excessive inflammation. Finally, we demonstrate that a 50% decrease in early neutrophil recruitment to the lung after smoke inhalation leads to decreased tissue damage and improved outcomes following bacterial challenge. Collectively, these data demonstrate the clinical relevance of our experimental model and suggest that downstream targets of NOX2 activity are promising candidates for accelerating resolution of inflammation in patients.

To my mom.
To my dad.

ACKNOWLEDGEMENTS

In 2006, Deb Siwik inspired me to aspire to a career in academic research, and that inspiration has helped me to overcome obstacles and push through hard times ever since.

When my time as a graduate student almost came to an untimely end, countless friends, colleagues, and mentors came to my rescue. Kevin Blauth and Danny Bruce never stopped believing in me. Neither did Bob Bourret or Bill Goldman, who were the greatest advocates I could have ever hoped for, and who have continued to support me ever since. I will always be grateful to Rob Maile and Bruce Cairns, who decided to take a chance on me and to offer me their uncompromising support professionally and personally. Many thanks to my mentees, Karli, Kelly, Janice, Marci, Amber, and Maddy –their growth and success motivate me to overcome the long odds on the road to professorship. Last but not least, nobody could ask for a more supportive friend and colleague than Laurel Kartchner.

Ultimately, none of this would have happened without my best friend turned husband, Michael. From helping me label tubes at midnight to always knowing what to say to make me feel stronger than my challenges and insecurities, Michael's support never wavers. Michael helps me believe that I will create positive change in the world through science, education, and communication, and in the words of Mahatma Ghandi, "if I have the belief that I can do it, I shall surely acquire the capacity to do it even if I may not have it at the beginning."

TABLE OF CONTENTS

LIST OF TABLES

LIST OF FIGURES

LIST OF ABBREVIATIONS

ALI	Acute lung injury
ARDS	Acute respiratory distress syndrome
BALF	Broncho-alveolar lavage fluid
CARS	Compensatory anti-inflammatory response syndrome
CXCL1	Chemokine (C-X-C motif) ligand 1
CXCL2	Chemokine (C-X-C motif) ligand 2
CXCR2	Chemokine (C-X-C motif) receptor 2
DAMP	Damage-associated molecular pattern
dsDNA	Double stranded deoxyribonucleic acid
HA	Hyaluronic acid
HIF1α	Hypoxia inducible factor 1α
IκBα	Inhibitor of NFκB
IL	Interleukin
LPS	Lipopolysaccharide
MCP1	Monocyte chemoattractant protein 1
MIP2	Macrophage inflammatory protein 2
MMP	Matrix metalloprotease
MMW	Medium molecular weight
mRNA	messenger ribonucleic acid
MTD	Mitochondrial DAMPs
mtDNA	Mitochondrial deoxyribonucleic acid
NFκB	Nuclear factor κB
NO	Nitric oxide
NOS	Nitric oxide synthase

NOX2	Nicotinamide adenine dinucleotide phosphate (NADPH) oxidase 2
PPAR	Peroxisome proliferator-activated receptor
PS	Phosphatidylserine
RNS	Reactive nitrogen species
ROS	Reactive oxygen species
RONS	Reactive oxygen and nitrogen species
SDF	Stromal-derived factor
SIRS	Systemic inflammatory response syndrome
SOD	Superoxide dismutase
TLR	Toll-like receptor
TRIF	TIR-domain-containing adaptor-inducing interferon-β
VILI	Ventilator-induced lung injury

CHAPTER 1: INNATE IMMUNITY IS CRITICAL FOR SURVIVAL FOLLOWING TRAUMA

Introduction

Traumatic injury is the leading cause of death in Americans under 44 years of age, and poses a threat to human health that will never be eliminated as long as people continue to drive cars, live inside flammable[1] structures, or go to war. Recovery from traumatic injury requires the body to accomplish two objectives: first, to combat the threat of infection that results from damage to normal physiological barriers, and second, to replace injured tissue with new, healthy tissue. Both processes are orchestrated by the immune system and in most cases they occur sequentially. In the early stages of inflammation, immune cells are recruited to damaged tissue and infectious threats are neutralized. Resolution can then occur, during which phase the immune system clears dead or damaged cells and debris, promotes proliferation of local stromal cells, and restructures the extracellular matrix. Failure to initiate the initial inflammatory response can lead to infectious complications. Failure to progress to the resolution phase leads to scar tissue, fibrosis, and may increase the extent of tissue damage. Immune activity that causes tissue damage or interferes with organ function is referred to as immunopathology, which can be associated with a hyperactive inflammatory phase or persistent inflammation that fails to resolve. A well-orchestrated innate immune response is a critical determinant of patient outcomes following traumatic injury, and presents a constellation of potential therapeutic targets.

Our central hypothesis is that some aspects of the innate immune response following trauma are beneficial and assist in efficient progress from the inflammatory to the resolution phase during recovery,

[1] Despite popularity of 'flame retardant' materials, especially textiles, evidence suggests that in a structural fire these materials inevitably catch fire. Additionally, the compounds that they contain to make them 'flame retardant' are toxic.

while aberrant responses either fail to clear infection or interfere with resolution. Our objective is to identify opportunities for intervention by examining the relationship between inflammation and outcomes in patients and animal models of injury. This study outlines research aimed at understanding how the lung is impacted by burn and inhalational injuries, and how immune activity can be modulated to promote successful transition from inflammation to resolution.

Inflammation drives outcome in trauma patients.

For many years it was thought that traumatic injury resulted in a biphasic inflammatory response that has been extensively characterized following sepsis. This paradigm suggests an initial systemic inflammatory response syndrome (SIRS) marked by pro-inflammatory cytokines and a hyperactive immune state. The SIRS phase was thought to be followed by a compensatory anti-inflammatory response syndrome (CARS), in which the anti-inflammatory cytokine profile limits tissue damage due to immunopathology. Novel methodologies of the '-omics' age have enabled a more nuanced analysis, which suggests that pro- and anti-inflammatory genes are expressed simultaneously after trauma (1-6).

Traumatic injury causes differential expression of >80% of genes in the human genome within 28 days (1). Remarkably, the type of injury (i.e. blunt trauma vs. burn) is of only marginal importance to the genetic changes that occur, indicating that the physiological responses to these injuries are more alike than they are different. Despite the presence of anti-inflammatory cytokines during the early phase and pro-inflammatory cytokines during the late phase, which contradict the straightforward SIRS/CARS paradigm, it remains true that patients are at the greatest risk of developing organ failure secondary to shock early after injury and of succumbing to fatal opportunistic infections late after injury (4, 7, 8).

Changes in serum levels of cytokines, chemokines, and immunogenic growth factors persist for years after burn injury, especially in pediatric patients (9). Because of the prolonged inflammatory and hypermetabolic state that follows burn injury, patients experience many physiological problems associated with persistent inflammation, including metabolic dysregulation and cardiovascular stress (9-

11). Interference with aberrant inflammatory processes after trauma is therefore likely to improve long-term prognosis for trauma patients by promoting a prompt and complete return to homeostasis.

Excessive inflammation leads to organ dysfunction. Damaged tissue and the tissue-resident immune cells release a battery of signals into circulation that impact tissues beyond the initial damage site. Increased systemic circulation of damage-associated molecular patterns (DAMPs) as well as cytokines, chemokines and growth factors in serum have been observed following burn injury in both humans and animal models (12-15). Inflammatory signals from the burn wound exit the site of damage through venous circulation and cause inflammation in secondary organs, with the heart and lungs being chief collateral targets because they receive the greatest concentration of inflammatory factors in the blood (16, 17).

Presence of a burn wound increases sensitivity to inflammatory and infectious signals such as C5a and LPS, and this sensitivity disrupts normal organ function by promoting edema and congestion of microvasculature. Attenuating inflammation after trauma in animal models by depleting complement or neutrophils either prior to or shortly after burn injury significantly reduces –or eliminates entirely –the collateral damage to distal organs (18, 19). These results have failed to translate to the clinic because they do not account for the opportunistic infections that would swamp patients if their innate immune functions were so completely abolished. They do, however, illustrate the power of immune modulation in alleviating organ dysfunction after injury.

Aberrant inflammatory response leads to infectious complications. Anti-inflammatory signals present in patient biofluids, specifically serum and broncho-alveolar lavage fluid (BALF), are predictive of outcomes in patients diagnosed with burns and inhalational injury (3, 12, 20). Interleukin 10 (IL-10) is a hallmark anti-inflammatory cytokine and its elevation in patients with inhalational injury predicts the onset of infection (20). In a murine model of burn injury, an abundance of innate immune cells expressing IL-10 was associated with failure to control bacterial growth following a skin infection (21).

Moreover, administration of flagellin stimulated innate immune activation through toll-like receptor (TLR) ligation, reversed the anti-inflammatory immune polarization following burn injury, and improved bacterial clearance (21). These data illustrate two points. First, that despite immune hyperactivity sufficient to cause organ damage, the immune system struggles to clear even minimally invasive pathogens such as *Pseudomonas aeruginosa*. Second, that it is possible to modulate the immune response to improve detection and clearance of certain pathogens.

The lung is a key site of immunopathology and infection that hinders patient outcomes.

In the latter half of the 20th century significant gains were made in improving survival and prognosis in burn patients through improved wound excision and grafting strategies and resuscitation techniques (22, 23). Whereas burn wound infections had long been the main challenge to patient recovery, this clinical threat has been overtaken by bacterial pneumonia, which today accounts for the majority of burn unit fatalities (8).

The lung presents a two-fold challenge after trauma (24, 25). First, immune infiltration disrupts gas exchange and can lead to acute lung injury (ALI) or acute respiratory distress syndrome (ARDS) (26). Second, despite significant immune cell recruitment, immunological surveillance fails to control bacteria and patients often develop life-threatening bacterial pneumonia (8). The leading cause of pneumonia in burn patients is *P. aeruginosa*, which is an opportunistic bacterium that is rapidly cleared by neutrophils in healthy individuals (8, 27).

ALI follows trauma. ALI is defined in humans as the presence of bilateral infiltrates to the lung tissue and impaired oxygen exchange (25, 28). Progressively more severe impairment in oxygen exchange marks a transition from ALI to ARDS (28). ALI/ARDS can be brought on by a spectrum of stimuli including infection and damage, which affect the lung either directly or indirectly (Table 1.1). The cellular and molecular characteristics of ALI are similarly variable, though they all involve disruption

of the alveolar/capillary barrier and damage to the airway epithelium either in the alveoli or in larger airways.

Mouse models of ALI mirror the complexity and non-uniformity of the human disease, comprising a full spectrum of stimuli and resulting in a wide array of outcomes (29-31). Measurement of ALI is somewhat different in mice compared to humans in large part because few laboratories have access to the equipment required to measure oxygen saturation in the blood or to observe lung infiltrates in real-time (29). Small animal models of ALI are therefore defined by the extent to which they fulfill each of four broadly defined categories: perturbation of the alveolar/capillary barrier, evidence of an inflammatory response, histological evidence of tissue damage, and disrupted lung function.

A direct pulmonary insult is not required for progression to ALI. Inflammatory signals from an injury that are released into the blood invariably make their way via venous circulation to the heart before being pumped into pulmonary circulation. The lung is therefore a target for organ damage subsequent to injury because it receives 100% of cardiac output, therefore it sees more highly concentrated inflammatory mediators than other organs such as the liver or kidney. C5a release after burn injury causes an increase in vascular ICAM-1 expression in pulmonary microvasculature (19), which causes neutrophil accumulation in the capillaries and contributes to vascular permeability (18). Inhibiting complement activation or depleting complement factors prevented sequestration of neutrophils in pulmonary microvasculature after burn injury, however because sequestration occurs within minutes of the injury it is only possible to inhibit it through prophylactic treatment, which is impractical for the treatment of burn injuries outside of the laboratory (18, 19).

Neutrophils accumulating in the pulmonary microvasculature cause damage to the endothelial-capillary barrier that can be prevented by administration of catalase or superoxide dismutase, which inhibit reactive oxygen species activity (18). Damage to the endothelium results in leakage of serum proteins and fluid from the vasculature, causing either thickening of the interstitium, fluid buildup in the

alveoli, or both. In summary, release of inflammatory mediators from damaged tissue precipitates complement activation, resulting in changes to the pulmonary microvasculature and accumulation of activated neutrophils that degranulate and cause tissue damage that culminates in ALI.

Immune function in the lung is altered by injury.

Inhalational injury presents a significant clinical challenge. Inhalational injury is a common comorbidity observed in burn patients. The impact of inhalational injury on the outcome of trauma is significant, as it increases mortality and, in survivors, leads to a three-fold increase in the duration of hospitalization and a substantial increase in healthcare costs (32). Despite its frequency, inhalational injury is not a straightforward diagnosis because disease presentation depends on the smoke source, which varies from structure to structure, as well as concentration and duration of exposure (20, 33, 34). Additionally, the rate and severity of inhalational injuries are increasing as structures transition to synthetic building materials, because many synthetics burn faster and release more airborne toxics than wood or stone structures (24).

Due to the significant cost of treating inhalational injuries without targeted therapies, it is imperative that ongoing research attempt to address this patient population. Optimal immune function in the lung plays a pivotal role in the two primary challenges that face patients, specifically combatting infection and healing damaged tissue. We therefore propose that it is imperative to characterize the immune response in the lung following injury, specifically burns and inhalational injury, and to explore treatments to modulate that response.

Significant work has been done to characterize and quantify the immune response in the lung in different models of ALI including pulmonary infection, sepsis, and ventilator-associated (mechanical) lung injuries (29, 31, 35-45). Although these injuries differ significantly from acute smoke inhalation, it is instructive to consider the results of those studies in order to outline themes and patterns as well as to identify points of comparison between patients and animal models. Here we discuss the state of the

literature surrounding immune function in various models of ALI, and have divided the analysis into six categories: transcription factors, proteases, reactive oxygen and nitrogen species (RONS), toll-like receptors, cytokines, and chemokines.

Transcription factors. Nuclear Factor (NF)-κB signaling in both epithelial cells and myeloid cells in the lung play a significant role in the etiology of ALI. Introduction of a viral vector to promote expression of IκBα attenuated NFκB signaling in epithelial cells in a lipopolysaccharide (LPS) model of ALI (35). This attenuated neutrophil recruitment resulted in decreased IL-6 expression and protein leakage in the BALF (35). Additionally, low concentrations of nitric oxide (NO) promote NFκB activation, which promotes iNOS expression to generate a positive feedback loop that increases pro-inflammatory cytokine and chemokine production (46).

PPARγ is required for the maturation of anti-inflammatory "alternately" activated macrophages, which drive resolution and tissue repair (47). In a mouse model of asthma, agonists of peroxisome proliferator-activated receptor (PPAR)-α and -γ attenuated inflammation by reducing the recruitment of neutrophils and eosinophils to the airway (48).

Proteases. Matrix metalloproteinase 8 (MMP8), also referred to as neutrophil collagenase, is an enzyme released by activated neutrophils upon extravasation from the vasculature to render the extracellular matrix more permissive to cellular migration and tissue remodeling. MMP8 is upregulated in peripheral leukocytes from trauma patients within 12h of injury (1). Furthermore, MMP8-deficient mice were partially protected from injury in a ventilator-induced lung injury (VILI) model, and MMP8 inhibitors exhibited a similar protective effect in VILI and a burn-blast injury (31, 49, 50).

MMP9, also known as Gelatinase B, is produced as neutrophils differentiate and mature in the bone marrow and is stored in granules. When neutrophils degranulate, MMP9 is released and acts on the extracellular matrix as well as on chemokines, such as IL-8, and cytokines, such as IL-1β, to increase their activity and binding affinity (51). The feed-forward mechanism, wherein MMP9 activity promotes

IL-8 potency, which promotes neutrophil recruitment/degranulation and therefore MMP9 activity, results in compounded inflammation. The ability of MMP9 to promote runaway inflammation may be why MMP9 deficiency was found to be protective against septic shock in an endotoxemia model (51).

Reactive oxygen and nitrogen species. Reactive oxygen species (ROS) and reactive nitrogen species (RNS) are highly reactive small molecules that serve a variety of effector functions. Under physiological conditions, reactive oxygen and nitrogen species (RONS) are potent signaling molecules that can act in an autocrine or paracrine manner and are especially important in regulating vascular tone to promote healthy blood pressure. When activated, phagocytic cells pump ROS into phagosomes in order to degrade microbial pathogens and scavenged debris (52). ROS are potent antimicrobial effector molecules that can cause unwanted tissue damage when they are produced in excess, as is the case in the lung following injury (18, 36, 37). ROS and RNS react with one another to generate peroxynitrite, which is an especially potent oxidizing agent (53).

ROS in the lung after injury can be produced by multiple processes. In addition to xanthine oxidase, which becomes activated following damage to the airway epithelium and produces ROS, infiltrating phagocytes express NADPH oxidase 2 (NOX2), a potent source of both intra- and extracellular ROS (19, 52). NOX2 exists as an inactive complex in the plasma membrane that becomes part of the phagosome when the membrane folds during phagocytosis (52). Upon activation, the NOX2 machinery fully assembles on the cytoplasmic side of the membrane and results in an electron transport chain that generates ROS inside the phagosome (52). In some activated cells, the NOX2 machinery assembles at the cytoplasmic membrane, resulting in generation of extracellular ROS (52).

Neutrophil accumulation and activation are associated with oxidative tissue damage in an ovine model of cotton smoke inhalation and bacterial infection (36). Superoxide dismutase (SOD), which converts superoxide into hydrogen peroxide, is increased in the macrophage proteome of humans with ARDS in the early phase after diagnosis compared to resolution phase, suggesting an attempt by local

cells to cope with the elevated burden of ROS (2). The relative success of antioxidants derived from Vitamin E, most notably γ-tocopherol, in attenuating ALI after smoke inhalation further implicates ROS in immunopathology (24). Similarly, administration of a peroxynitrite scavenger in a mouse model of cotton smoke inhalation with burn injury inhibited protein oxidation and resulted in a concomitant increase in IL-10 production as well as decreased damage to lung architecture (37). Extracellular ROS leads to oxidation of proteins and lipids, which can alter or abrogate their function and may render them immunostimulatory. Oxidized lipids are detected by TLR4 to promote inflammation (38).

There are several established mechanisms by which ROS production promotes resolution of inflammation by decreaseing neutrophil recruitment, promoting neutrophil apoptosis, and increasing efferocytosis. Leukotriene B4 (LTB4), a small molecule with potent activity as a neutrophil chemoattractant, is inactivated in the presence of ROS, potentially reflective of a self-limiting immune mechanism (54). NOX2-dependent ROS production in neutrophils is critical for upregulation of modified phosphatidyl serine (Lyso-PS) on the cell surface, which leads to clearance of local neutrophils (55). In a model of peritonitis using mice lacking the main transmembrane subunit of the NOX2 machinery, gp91phox, local neutrophils were not cleared and recruitment continued, resulting in sustained inflammation (55).

The role of neutrophil derived ROS in limiting inflammation has been similarly suggested by a murine model of experimental colitis, which is marked by recruitment of activated neutrophils (56). In this model, depletion of local oxygen by neutrophils generating ROS resulted in stabilization of hypoxia-inducible factor 1α (HIF1α) in stromal cells, which promoted resolution of inflammation and a return to tissue homeostasis. This mechanism was disrupted when colitis was induced in mice deficient for NOX2 activity, leading to increased tissue damage that was partially reversible through pharmacological stabilization of HIF1α (56). In summary, ROS are potent antimicrobial molecules that can cause immunopathology via tissue oxidation when released in excess, however a growing body of evidence suggests that ablation of ROS production inhibits resolution of inflammation.

A hallmark RNS nitric oxide (NO) is a key regulator of vascular dynamics and, though interactions with the vascular endothelium, inflammation. NO is produced by nitric oxide synthases (NOS) of which there are three known isoforms: endogenous (eNOS), inducible (iNOS), and neuronal (nNOS). iNOS is expressed by activated leukocytes, especially myeloid cells and granulocytes, and NO derived from iNOS is associated with changes in cytokine and chemokine production and signaling as well as leukocyte migration and apoptosis (46, 53, 57-59). NO regulates iNOS expression, promotes leukocyte adhesion to –and rolling on –the vascular endithelium, modulates chemokine production (including MCP1 and MIP2) and activity (IL-8), and promotes neutrophil degranulation and ROS production (46, 53). In certain cell types high concentrations of NO promote apoptosis; however, NO differentially impacts macrophage survival and function to allow macrophages to persist during inflammation, when NO concentrations are elevated, and to apoptose during resolution when NO concentrations abate (59). NO has been used as a highly sensitive real time biomarker of inflammation and immune competence, and can be measured directly in exhaled gases or blood (30, 60).

The signals that induce iNOS expression and activity are incompletely understood, in part because the impact of certain stimuli appears to depend largely on concentration. Under resting conditions, epithelial cells and alveolar macrophages express Arg2, which counteracts iNOS expression and activity; however, iNOS is expressed in these cell types following sepsis (61). Upregulation of iNOS expression and production of NO are hallmarks of acute lung injury in a variety of models, including smoke inhalation (40, 57, 61, 62). Increased iNOS expression and activity in the airway were observed in a mouse model of cotton smoke inhalation with and without burn injury (40). Moreover, NO derived from iNOS contributed to cardiac dysfunction following smoke inhalation and burn injury in sheep (41).

Toll-like receptors. Toll-like receptors (TLR) recognize conserved molecular patterns associated with bacterial or viral structures and are the first line of defense for detecting infection. TLR4 is responsible for detecting LPS and is also known to respond to DAMPs including oxidized lipids and hyaluronic acid (HA) (38, 63, 64). Signaling via TLR4 presents a double-edged sword in the onset and

resolution of ALI. On one hand, detection of oxidized lipids and signaling via TLR-TRIF-NFkB in myeloid cells promotes ALI in an acid aspiration model (38). On the other hand, deficient TLR signaling adversely effects survival in a *Pseudomonas*-induced model of ALI (42).

Changes in expression of TLR and sensitivity to TLR ligation on immune cells following burn injury have been described previously in both humans and mice (1, 21, 65, 66). Administration of flagellin, a TLR5 ligand, following burn injury improved clearance of *P. aeruginosa* in mice (21, 67). In another study neutrophil recruitment to the lung after bacterial challenge was positively correlated with bacterial clearance and survival, in connection with TLR4 signaling (42).

Cytokine production and secretion. Interleukin (IL)-6 has been extensively described for its role in the acute pro-inflammatory response following burn and inhalational injury (38, 68-70). IL-6 concentration is tightly correlated with tissue damage, persistent inflammation, and the onset of fibrosis (71). Most evidence suggests that IL-6 may be more relevant in burn and combined injuries as opposed to inhalational injuries, alone. IL-6 signaling is upregulated in trauma patients (1), however it was not found to be elevated in BALF from patients with inhalational injury, alone (4). More sensitive methods do point to some role of IL-6 in pulmonary inflammation. Patient BAL-derived leukocytes produced IL-6 following *ex vivo* LPS stimulation (4), and IL-6 mRNA was detected in lung tissue within 24 h of injury and infection in an ovine model of cotton smoke exposure (45).

A hallmark anti-inflammatory cytokine, IL-10, has been correlated with outcomes in multiple studies of patients with inhalational injury. Like TLR4 expression and signaling, IL-10 is prominent as having conflicting roles in ALI, as it has been shown to suppress antimicrobial responses but may also help prevent immunopathology. Our group examined BALF from patients diagnosed with inhalational injury and identified elevated IL-10 in patients with compromised lung function who were at risk of developing pneumonia (20). Others have observed elevated IL-10 in non-survivors compared to survivors (4). In a model of LPS-induced lung injury, a tolerizing dose of LPS was found to be

efficacious in reducing tissue damage due to IL-10 production by macrophages upon subsequent challenge (43). IL-10^{+}IL-12^{-} neutrophils that appear following burn injury have been implicated in susceptibility to infection, however they can be eliminated by treatment with a TLR ligand, leading to improved response to bacterial challenge (21).

Chemokine production and secretion. IL-8, also known as CXCL8 in humans, is a chemokine produced by granylocytes and epithelial cells that acts on neutrophils and other granulocytes to promote migration and phagocytosis. IL-8 is elevated in burn patients, even more in severe burns than mild injuries (72). Furthermore, while levels of IL-8 dropped off following injury without infectious complications, sepsis resulted in a second peak in IL-8 (73). IL-8 was elevated in patients diagnosed with inhalational injury, with higher concentrations observed in survivors compared to non-survivors (4).

Mice have two homologues of IL-8; CXCL1, also known as KC, and CXCL2, also known as macrophage inhibitory protein 2 (MIP2). In an animal model, inhibition of CXCL1 secretion into the serum following burn led to a decrease in several markers of lung injury (74). It has been shown that diesel exhaust particles exacerbate asthma symptoms in mice by upregulating expression of CXCL1 and CXCL2, and that inhibition of these signals suppressed pulmonary inflammation and improved outcomes (75). Both CXCL1 and CXCL2 are recognized by CXCR2, and blockade of either the ligands or receptor significantly attenuated pulmonary damage in a murine model of ventilator-induced lung injury (VILI) (44). Moreover, CXCR2 agonists have been found to be relevant in several models of direct lung injury including acid aspiration, VILI, and LPS instillation (31).

Expression of CCL2, also known as monocyte chemoattractant protein 1 (MCP1), is elevated early following thermal injuries and is associated with recruitment of pro-inflammatory "classically activated" macrophages to the site of injury and the acute hyper-inflammatory response that can precipitate shock in patients (47, 76, 77). Examination of BALF from patients diagnosed with inhalational injury indicated that MCP-1 was elevated but not to an extent that achieved statistical significance (4). Finally, ubiquitin

and stromal-derived factor (SDF)1α, which are elevated in patient BALF, are agonists of CXCR4 and are thought to have a protective, anti-inflammatory effect (78).

Optimized innate immune function would improve patient outcomes.

Correct resolution of inflammation requires the coordination of tissue resident macrophages and recruited immune cells. Neutrophils are typically the first cells recruited, and once activated they phagocytose bacteria, release neutrophil extracellular traps to kill extracellular pathogens, and modulate the response of other immune cells. Macrophage numbers do not change between the acute (inflammatory) phase and resolution of ARDS, while a significant decrease is observed in neutrophil numbers (2). During resolution, neutrophils initiate apoptosis and signal to macrophages to phagocytose and degrade the dying cells through a process known as efferocytosis. Clearance of apoptotic neutrophils causes macrophages to adopt an anti-inflammatory phenotype to suppress further immune cell recruitment and repair local tissue that may have been damaged by the initial insult, ensuing infection, immunopathology, or any combination thereof.

In modulating the immune response to promote resolution without impairing antimicrobial function, it is important to visualize a return to homeostasis rather than "skewing" towards either a pro- or anti-inflammatory response. Suppressing immunopathology will not benefit patients if it renders them immunologically paralyzed so that they succumb to infection. Conversely, prompting phagocytes to clear bacteria and debris must be achieved without causing collateral damage and thereby creating more debris, potentially leading to lung failure.

Experimental Approach to Study Lung Injury in Mice

There is substantial criticism of mouse models for their imperfection in mimicking human disease, however they remain the most effective tool for achieving mechanistic insight into complex disease processes and developing therapeutic interventions. Despite differences in magnitude, innate immune responses to stress in mice and humans are largely similar, including cytokine and chemokine

production, leukocyte circulation and activation (79). Nevertheless, model selection and design must be approached with care to ensure that results of mouse studies are translationally relevant. Existing studies of acute lung injury, particularly subsequent to smoke inhalation, exhibit disagreement between clinical data and animal data (24). The majority of research into acute inhalational injury has relied on cotton smoke inhalation in either rats, mice, or sheep (36, 37, 40, 41, 45, 80, 81). It has been shown, however, that there are differences between injury induced by cotton smoke, wood smoke, and plastic smoke (81). Because the majority of acute inhalational injuries that result in hospitalization do not result from the combustion of pure cotton toweling, as is used in the above animal studies, we propose that a novel model is needed to study inhalational injury.

There is a diverse and extensive array of animal models of ALI –for this reason the American Thoracic Society produced a document outlining standards, characteristics, and measurements that should be present in any model (29). We used these guidelines to design an appropriate animal model and to define parameters that would be used to determine success of any therapeutic intervention.

We started by approaching the impact of systemic inflammation subsequent to cutaneous burn injury on the immunological environment of the lung. Because infections after burn injury pose the greatest clinical threat late after injury, we conducted initial studies two weeks after burn injury. Chapter 2 describes how systemic immune dysfunction following burn injury correlates with bacterial clearance in the lung. In chapter 3 we investigated metabolic control of innate immunity in the lung and identified a distinction between neutrophil recruitment and neutrophil RONS production in bacterial clearance. These studies highlight changes in innate immune function after burn injury that impact immunological surveillance in the lung.

In order to explore factors that lead to long-term immune dysfunction in the lung after injury, we studied acute responses in order to gain insight into the chain of events that results in failure to resolve inflammation. Our objective was to compare ALI that develops in patients with severe injuries but no

direct lung insult with ALI that develops following inhalational injury. We therefore chose to utilize both direct and an indirect injury models in mice. In chapter 4 we describe the impact of systemic damage on pulmonary inflammation by measuring the ability of intravenous DAMPs to induce ALI. We show that damage from a 20% total body surface area (TBSA) burn, alone, did not induce ALI, but supplementation with exogenous DAMPs promoted leakage of serum proteins and recruitment of neutrophils to the airway. Observation of these phenotypes without either a pathogenic signal or a direct insult to the lung is a novel finding and represents a meaningful step in the study of ALI in trauma patients who are not diagnosed with inhalational injury.

To study the consequences of a direct pulmonary challenge, specifically inhalational injury, we developed and characterized a novel model of wood smoke inhalation. In chapter 5 we identified early neutrophilia as a source of tissue damage that leads to susceptibility to systemic bacterial challenge and showed that partial inhibition of neutrophil chemotaxis can reduce damage without adversely impacting bacterial clearance. Finally, the results outlined in chapter 6 address granulocyte function by quantifying neutrophil RONS production and characterizing the response to inhalational injury in mice deficient for NOX2. The results of these studies highlight the importance of the novel model of smoke inhalation, which reproduces many key characteristics of patients diagnosed with inhalational injury, represents an opportunity to develop therapeutic interventions, and adds meaningfully to existing literature on murine models of ALI.

TABLES

Table 1.1: Challenges that lead to Acute Lung Injury (ALI).

	Pathogen Signal	Damage Signal
Systemic	**Sepsis**	**Severe Burn Injury** **Blunt Force Trauma**
Pulmonary	**Influenza** **Pneumonia**	**Acid Aspiration** **Inhalational Injury** **Ventilator-Induced Lung Injury**

REFERENCES

1. Xiao W, Mindrinos MN, Seok J, Cuschieri J, Cuenca AG, Gao H, Hayden DL, Hennessy L, Moore EE, Minei JP, Bankey PE, Johnson JL, Sperry J, Nathens AB, Billiar TR, West MA, Brownstein BH, Mason PH, Baker HV, Finnerty CC, Jeschke MG, Lopez MC, Klein MB, Gamelli RL, Gibran NS, Arnoldo B, Xu W, Zhang Y, Calvano SE, McDonald-Smith GP, Schoenfeld DA, Storey JD, Cobb JP, Warren HS, Moldawer LL, Herndon DN, Lowry SF, Maier RV, Davis RW, Tompkins RG, Inflammation, Host Response to Injury Large-Scale Collaborative Research P. A genomic storm in critically injured humans. J Exp Med. 2011;208(13):2581-90. doi: 10.1084/jem.20111354. PubMed PMID: 22110166; PMCID: PMC3244029.

2. Dong H, Li J, Lv Y, Zhou Y, Wang G, Hu S, He X, Yang P, Zhou Z, Xiang X, Wang CY. Comparative analysis of the alveolar macrophage proteome in ALI/ARDS patients between the exudative phase and recovery phase. BMC Immunol. 2013;14:25. doi: 10.1186/1471-2172-14-25. PubMed PMID: 23773529; PMCID: PMC3727986.

3. Finnerty CC, Jeschke MG, Herndon DN, Gamelli R, Gibran N, Klein M, Silver G, Arnoldo B, Remick D, Tompkins RG, Investigators of the I, the Host Response Glue G. Temporal cytokine profiles in severely burned patients: a comparison of adults and children. Mol Med. 2008;14(9-10):553-60. doi: 10.2119/2007-00132.Finnerty. PubMed PMID: 18548133; PMCID: PMC2424320.

4. Davis CS, Albright JM, Carter SR, Ramirez L, Kim H, Gamelli RL, Kovacs EJ. Early pulmonary immune hyporesponsiveness is associated with mortality after burn and smoke inhalation injury. J Burn Care Res. 2012;33(1):26-35. doi: 10.1097/BCR.0b013e318234d903. PubMed PMID: 21979852; PMCID: PMC3253958.

5. Liu T, Qian WJ, Gritsenko MA, Xiao W, Moldawer LL, Kaushal A, Monroe ME, Varnum SM, Moore RJ, Purvine SO, Maier RV, Davis RW, Tompkins RG, Camp DG, 2nd, Smith RD, Inflammation, the Host Response to Injury Large Scale Collaborative Research P. High dynamic range characterization of the trauma patient plasma proteome. Mol Cell Proteomics. 2006;5(10):1899-913. doi: 10.1074/mcp.M600068-MCP200. PubMed PMID: 16684767; PMCID: PMC1783978.

6. Sweeney TE, Shidham A, Wong HR, Khatri P. A comprehensive time-course-based multicohort analysis of sepsis and sterile inflammation reveals a robust diagnostic gene set. Sci Transl Med. 2015;7(287):287ra71. doi: 10.1126/scitranslmed.aaa5993. PubMed PMID: 25972003; PMCID: PMC4734362.

7. Mayhall CG. The epidemiology of burn wound infections: then and now. Clin Infect Dis. 2003;37(4):543-50. doi: 10.1086/376993. PubMed PMID: 12905139.

8. Wurtz R, Karajovic M, Dacumos E, Jovanovic B, Hanumadass M. Nosocomial infections in a burn intensive care unit. Burns. 1995;21(3):181-4. PubMed PMID: 7794498.

9. Jeschke MG, Gauglitz GG, Kulp GA, Finnerty CC, Williams FN, Kraft R, Suman OE, Mlcak RP, Herndon DN. Long-term persistance of the pathophysiologic response to severe burn injury. PLoS One. 2011;6(7):e21245. doi: 10.1371/journal.pone.0021245. PubMed PMID: 21789167; PMCID: PMC3138751.

10. Branski LK, Herndon DN, Barrow RE, Kulp GA, Klein GL, Suman OE, Przkora R, Meyer W, 3rd, Huang T, Lee JO, Chinkes DL, Mlcak RP, Jeschke MG. Randomized controlled trial to determine the efficacy of long-term growth hormone treatment in severely burned children. Ann Surg. 2009;250(4):514-23. doi: 10.1097/SLA.0b013e3181b8f9ca. PubMed PMID: 19734776; PMCID: PMC3970433.

11. Williams FN, Jeschke MG, Chinkes DL, Suman OE, Branski LK, Herndon DN. Modulation of the hypermetabolic response to trauma: temperature, nutrition, and drugs. J Am Coll Surg. 2009;208(4):489-502. doi: 10.1016/j.jamcollsurg.2009.01.022. PubMed PMID: 19476781; PMCID: PMC3775552.

12. Maile R, Jones S, Pan Y, Zhou H, Jaspers I, Peden DB, Cairns BA, Noah TL. Association between early airway damage-associated molecular patterns and subsequent bacterial infection in patients with inhalational and burn injury. Am J Physiol Lung Cell Mol Physiol. 2015;308(9):L855-60. doi: 10.1152/ajplung.00321.2014. PubMed PMID: 25770180; PMCID: PMC4421787.

13. Zhang Q, Raoof M, Chen Y, Sumi Y, Sursal T, Junger W, Brohi K, Itagaki K, Hauser CJ. Circulating mitochondrial DAMPs cause inflammatory responses to injury. Nature. 2010;464(7285):104-7. doi: 10.1038/nature08780. PubMed PMID: 20203610; PMCID: PMC2843437.

14. Onarheim H, Reed RK, Laurent TC. Elevated hyaluronan blood concentrations in severely burned patients. Scand J Clin Lab Invest. 1991;51(8):693-7. PubMed PMID: 1806984.

15. Simmons JD, Lee YL, Mulekar S, Kuck JL, Brevard SB, Gonzalez RP, Gillespie MN, Richards WO. Elevated levels of plasma mitochondrial DNA DAMPs are linked to clinical outcome in severely injured human subjects. Ann Surg. 2013;258(4):591-6; discussion 6-8. doi: 10.1097/SLA.0b013e3182a4ea46. PubMed PMID: 23979273; PMCID: PMC3935616.

16. Hultman CS, Cairns BA, deSerres S, Frelinger JA, Meyer AA. Early, complete burn wound excision partially restores cytotoxic T lymphocyte function. Surgery. 1995;118(2):421-9; discussion 9-30. PubMed PMID: 7638760.

17. Ipaktchi K, Mattar A, Niederbichler AD, Hoesel LM, Vollmannshauser S, Hemmila MR, Su GL, Remick DG, Wang SC, Arbabi S. Attenuating burn wound inflammatory signaling reduces systemic inflammation and acute lung injury. J Immunol. 2006;177(11):8065-71. PubMed PMID: 17114480.

18. Till GO, Beauchamp C, Menapace D, Tourtellotte W, Jr., Kunkel R, Johnson KJ, Ward PA. Oxygen radical dependent lung damage following thermal injury of rat skin. J Trauma. 1983;23(4):269-77. PubMed PMID: 6842628.

19. Schmid E, Piccolo MT, Friedl HP, Warner RL, Mulligan MS, Hugli TE, Till GO, Ward PA. Requirement for C5a in lung vascular injury following thermal trauma to rat skin. Shock. 1997;8(2):119-24. PubMed PMID: 9261902.

20. Jones SW, Zhou H, Ortiz-Pujols SM, Maile R, Herbst M, Joyner BL, Jr., Zhang H, Kesic M, Jaspers I, Short KA, Meyer AA, Peden DB, Cairns BA, Noah TL. Bronchoscopy-derived correlates of lung injury following inhalational injuries: a prospective observational study. PLoS One.

2013;8(5):e64250. doi: 10.1371/journal.pone.0064250. PubMed PMID: 23691180; PMCID: PMC3656836.

21. Neely CJ, Kartchner LB, Mendoza AE, Linz BM, Frelinger JA, Wolfgang MC, Maile R, Cairns BA. Flagellin treatment prevents increased susceptibility to systemic bacterial infection after injury by inhibiting anti-inflammatory IL-10+ IL-12- neutrophil polarization. PLoS One. 2014;9(1):e85623. doi: 10.1371/journal.pone.0085623. PubMed PMID: 24454904; PMCID: PMC3893295.

22. Tompkins RG, Hilton JF, Burke JF, Schoenfeld DA, Hegarty MT, Bondoc CC, Quinby WC, Jr., Behringer GE, Ackroyd FW. Increased survival after massive thermal injuries in adults: preliminary report using artificial skin. Crit Care Med. 1989;17(8):734-40. PubMed PMID: 2546715.

23. Ryan CM, Schoenfeld DA, Thorpe WP, Sheridan RL, Cassem EH, Tompkins RG. Objective estimates of the probability of death from burn injuries. N Engl J Med. 1998;338(6):362-6. doi: 10.1056/NEJM199802053380604. PubMed PMID: 9449729.

24. Rehberg S, Maybauer MO, Enkhbaatar P, Maybauer DM, Yamamoto Y, Traber DL. Pathophysiology, management and treatment of smoke inhalation injury. Expert Rev Respir Med. 2009;3(3):283-97. doi: 10.1586/ERS.09.21. PubMed PMID: 20161170; PMCID: PMC2722076.

25. Johnson ER, Matthay MA. Acute lung injury: epidemiology, pathogenesis, and treatment. J Aerosol Med Pulm Drug Deliv. 2010;23(4):243-52. doi: 10.1089/jamp.2009.0775. PubMed PMID: 20073554; PMCID: PMC3133560.

26. Aeffner F, Davis IC. Respiratory syncytial virus reverses airway hyperresponsiveness to methacholine in ovalbumin-sensitized mice. PLoS One. 2012;7(10):e46660. doi: 10.1371/journal.pone.0046660. PubMed PMID: 23056391; PMCID: PMC3462783.

27. Driscoll JA, Brody SL, Kollef MH. The epidemiology, pathogenesis and treatment of Pseudomonas aeruginosa infections. Drugs. 2007;67(3):351-68. PubMed PMID: 17335295.

28. Matthay MA, Ware LB, Zimmerman GA. The acute respiratory distress syndrome. J Clin Invest. 2012;122(8):2731-40. doi: 10.1172/JCI60331. PubMed PMID: 22850883; PMCID: PMC3408735.

29. Matute-Bello G, Downey G, Moore BB, Groshong SD, Matthay MA, Slutsky AS, Kuebler WM, Acute Lung Injury in Animals Study G. An official American Thoracic Society workshop report: features and measurements of experimental acute lung injury in animals. Am J Respir Cell Mol Biol. 2011;44(5):725-38. doi: 10.1165/rcmb.2009-0210ST. PubMed PMID: 21531958.

30. Liu F, Li W, Pauluhn J, Trubel H, Wang C. Rat models of acute lung injury: exhaled nitric oxide as a sensitive, noninvasive real-time biomarker of prognosis and efficacy of intervention. Toxicology. 2013;310:104-14. doi: 10.1016/j.tox.2013.05.016. PubMed PMID: 23770417.

31. Reiss LK, Uhlig U, Uhlig S. Models and mechanisms of acute lung injury caused by direct insults. Eur J Cell Biol. 2012;91(6-7):590-601. doi: 10.1016/j.ejcb.2011.11.004. PubMed PMID: 22284832.

32. Ahn CS, Maitz PK. The true cost of burn. Burns. 2012;38(7):967-74. doi: 10.1016/j.burns.2012.05.016. PubMed PMID: 22795515.

33. Mosier MJ, Pham TN, Park DR, Simmons J, Klein MB, Gibran NS. Predictive value of bronchoscopy in assessing the severity of inhalation injury. J Burn Care Res. 2012;33(1):65-73. doi: 10.1097/BCR.0b013e318234d92f. PubMed PMID: 21941194.

34. Walker J. Diagnosis and management of patients with hypercalcaemia. Nurs Older People. 2015;27(4):22-6. doi: 10.7748/nop.27.4.22.e685. PubMed PMID: 25924757.

35. MacLoughlin RJ, Higgins BD, Devaney J, O'Toole D, Laffey JG, O'Brien T. Aerosol-mediated delivery of AAV2/6-IkappaBalpha attenuates lipopolysaccharide-induced acute lung injury in rats. Hum Gene Ther. 2015;26(1):36-46. doi: 10.1089/hum.2014.053. PubMed PMID: 25382145; PMCID: PMC4302961.

36. Lange M, Szabo C, Traber DL, Horvath E, Hamahata A, Nakano Y, Traber LD, Cox RA, Schmalstieg FC, Herndon DN, Enkhbaatar P. Time profile of oxidative stress and neutrophil activation in ovine acute lung injury and sepsis. Shock. 2012;37(5):468-72. doi: 10.1097/SHK.0b013e31824b1793. PubMed PMID: 22266977; PMCID: PMC4646062.

37. Esechie A, Kiss L, Olah G, Horvath EM, Hawkins H, Szabo C, Traber DL. Protective effect of hydrogen sulfide in a murine model of acute lung injury induced by combined burn and smoke inhalation. Clin Sci (Lond). 2008;115(3):91-7. doi: 10.1042/CS20080021. PubMed PMID: 18315525.

38. Imai Y, Kuba K, Neely GG, Yaghubian-Malhami R, Perkmann T, van Loo G, Ermolaeva M, Veldhuizen R, Leung YH, Wang H, Liu H, Sun Y, Pasparakis M, Kopf M, Mech C, Bavari S, Peiris JS, Slutsky AS, Akira S, Hultqvist M, Holmdahl R, Nicholls J, Jiang C, Binder CJ, Penninger JM. Identification of oxidative stress and Toll-like receptor 4 signaling as a key pathway of acute lung injury. Cell. 2008;133(2):235-49. doi: 10.1016/j.cell.2008.02.043. PubMed PMID: 18423196.

39. Liu B, Luo XJ, Yang ZB, Zhang JJ, Li TB, Zhang XJ, Ma QL, Zhang GG, Hu CP, Peng J. Inhibition of NOX/VPO1 pathway and inflammatory reaction by trimethoxystilbene in prevention of cardiovascular remodeling in hypoxia-induced pulmonary hypertensive rats. J Cardiovasc Pharmacol. 2014;63(6):567-76. doi: 10.1097/FJC.0000000000000082. PubMed PMID: 24492474.

40. Mizutani A, Enkhbaatar P, Esechie A, Traber LD, Cox RA, Hawkins HK, Deyo DJ, Murakami K, Noguchi T, Traber DL. Pulmonary changes in a mouse model of combined burn and smoke inhalation-induced injury. J Appl Physiol (1985). 2008;105(2):678-84. doi: 10.1152/japplphysiol.00232.2007. PubMed PMID: 18436699.

41. Soejima K, Traber LD, Schmalstieg FC, Hawkins H, Jodoin JM, Szabo C, Szabo E, Virag L, Salzman A, Traber DL. Role of nitric oxide in vascular permeability after combined burns and smoke inhalation injury. Am J Respir Crit Care Med. 2001;163(3 Pt 1):745-52. doi: 10.1164/ajrccm.163.3.9912052. PubMed PMID: 11254534.

42. Faure K, Sawa T, Ajayi T, Fujimoto J, Moriyama K, Shime N, Wiener-Kronish JP. TLR4 signaling is essential for survival in acute lung injury induced by virulent Pseudomonas aeruginosa secreting

type III secretory toxins. Respir Res. 2004;5:1. doi: 10.1186/1465-9921-5-1. PubMed PMID: 15040820; PMCID: PMC389879.

43. Aggarwal NR, Tsushima K, Eto Y, Tripathi A, Mandke P, Mock JR, Garibaldi BT, Singer BD, Sidhaye VK, Horton MR, King LS, D'Alessio FR. Immunological priming requires regulatory T cells and IL-10-producing macrophages to accelerate resolution from severe lung inflammation. J Immunol. 2014;192(9):4453-64. doi: 10.4049/jimmunol.1400146. PubMed PMID: 24688024; PMCID: PMC4001810.

44. Belperio JA, Keane MP, Burdick MD, Londhe V, Xue YY, Li K, Phillips RJ, Strieter RM. Critical role for CXCR2 and CXCR2 ligands during the pathogenesis of ventilator-induced lung injury. J Clin Invest. 2002;110(11):1703-16. doi: 10.1172/JCI15849. PubMed PMID: 12464676; PMCID: PMC151632.

45. Lange M, Hamahata A, Traber DL, Connelly R, Nakano Y, Traber LD, Schmalstieg FC, Herndon DN, Enkhbaatar P. Pulmonary microvascular hyperpermeability and expression of vascular endothelial growth factor in smoke inhalation- and pneumonia-induced acute lung injury. Burns. 2012;38(7):1072-8. doi: 10.1016/j.burns.2012.02.019. PubMed PMID: 22647495; PMCID: PMC3893691.

46. Bogdan C. Nitric oxide and the immune response. Nat Immunol. 2001;2(10):907-16. doi: 10.1038/ni1001-907. PubMed PMID: 11577346.

47. Odegaard JI, Ricardo-Gonzalez RR, Goforth MH, Morel CR, Subramanian V, Mukundan L, Red Eagle A, Vats D, Brombacher F, Ferrante AW, Chawla A. Macrophage-specific PPARgamma controls alternative activation and improves insulin resistance. Nature. 2007;447(7148):1116-20. doi: 10.1038/nature05894. PubMed PMID: 17515919; PMCID: PMC2587297.

48. Trifilieff A, Bench A, Hanley M, Bayley D, Campbell E, Whittaker P. PPAR-alpha and -gamma but not -delta agonists inhibit airway inflammation in a murine model of asthma: in vitro evidence for an NF-kappaB-independent effect. Br J Pharmacol. 2003;139(1):163-71. doi: 10.1038/sj.bjp.0705232. PubMed PMID: 12746235; PMCID: PMC1573830.

49. Albaiceta GM, Gutierrez-Fernandez A, Garcia-Prieto E, Puente XS, Parra D, Astudillo A, Campestre C, Cabrera S, Gonzalez-Lopez A, Fueyo A, Taboada F, Lopez-Otin C. Absence or inhibition of matrix metalloproteinase-8 decreases ventilator-induced lung injury. Am J Respir Cell Mol Biol. 2010;43(5):555-63. doi: 10.1165/rcmb.2009-0034OC. PubMed PMID: 19995943.

50. Chai JK, Cai JH, Deng HP, Zou XF, Liu W, Hu QG, Shen CA, Yin HN, Zhang XB, Chi YF, Ma L, Feng R. Role of neutrophil elastase in lung injury induced by burn-blast combined injury in rats. Burns. 2013;39(4):745-53. doi: 10.1016/j.burns.2012.08.005. PubMed PMID: 22999209.

51. Dubois B, Starckx S, Pagenstecher A, Oord J, Arnold B, Opdenakker G. Gelatinase B deficiency protects against endotoxin shock. Eur J Immunol. 2002;32(8):2163-71. doi: 10.1002/1521-4141(200208)32:8<2163::AID-IMMU2163>3.0.CO;2-Q. PubMed PMID: 12209628.

52. Panday A, Sahoo MK, Osorio D, Batra S. NADPH oxidases: an overview from structure to innate immunity-associated pathologies. Cell Mol Immunol. 2015;12(1):5-23. doi: 10.1038/cmi.2014.89. PubMed PMID: 25263488; PMCID: PMC4654378.

53. Armstrong R. The physiological role and pharmacological potential of nitric oxide in neutrophil activation. Int Immunopharmacol. 2001;1(8):1501-12. PubMed PMID: 11515815.

54. Sumimoto H, Minakami S. Oxidation of 20-hydroxyleukotriene B4 to 20-carboxyleukotriene B4 by human neutrophil microsomes. Role of aldehyde dehydrogenase and leukotriene B4 omega-hydroxylase (cytochrome P-450LTB omega) in leukotriene B4 omega-oxidation. J Biol Chem. 1990;265(8):4348-53. PubMed PMID: 2155225.

55. Frasch SC, Fernandez-Boyanapalli RF, Berry KA, Murphy RC, Leslie CC, Nick JA, Henson PM, Bratton DL. Neutrophils regulate tissue Neutrophilia in inflammation via the oxidant-modified lipid lysophosphatidylserine. J Biol Chem. 2013;288(7):4583-93. doi: 10.1074/jbc.M112.438507. PubMed PMID: 23293064; PMCID: PMC3576064.

56. Campbell EL, Bruyninckx WJ, Kelly CJ, Glover LE, McNamee EN, Bowers BE, Bayless AJ, Scully M, Saeedi BJ, Golden-Mason L, Ehrentraut SF, Curtis VF, Burgess A, Garvey JF, Sorensen A, Nemenoff R, Jedlicka P, Taylor CT, Kominsky DJ, Colgan SP. Transmigrating neutrophils shape the mucosal microenvironment through localized oxygen depletion to influence resolution of inflammation. Immunity. 2014;40(1):66-77. doi: 10.1016/j.immuni.2013.11.020. PubMed PMID: 24412613; PMCID: PMC3951457.

57. Speyer CL, Neff TA, Warner RL, Guo RF, Sarma JV, Riedemann NC, Murphy ME, Murphy HS, Ward PA. Regulatory effects of iNOS on acute lung inflammatory responses in mice. Am J Pathol. 2003;163(6):2319-28. doi: 10.1016/S0002-9440(10)63588-2. PubMed PMID: 14633605; PMCID: PMC1892362.

58. Trifilieff A, Fujitani Y, Mentz F, Dugas B, Fuentes M, Bertrand C. Inducible Nitric Oxide Synthase Inhibitors Suppress Airway Inflammation in Mice Through Down-Regulation of Chemokine Expression. The Journal of Immunology. 2000;165(3):1526-33. doi: 10.4049/jimmunol.165.3.1526.

59. Bosca L, Zeini M, Traves PG, Hortelano S. Nitric oxide and cell viability in inflammatory cells: a role for NO in macrophage function and fate. Toxicology. 2005;208(2):249-58. doi: 10.1016/j.tox.2004.11.035. PubMed PMID: 15691589.

60. Dunn JL, Hunter RA, Gast K, Maile R, Cairns BA, Schoenfisch MH. Direct detection of blood nitric oxide reveals a burn-dependent decrease of nitric oxide in response to Pseudomonas aeruginosa infection. Burns. 2016;42(7):1522-7. doi: 10.1016/j.burns.2016.05.005. PubMed PMID: 27268107; PMCID: PMC5056119.

61. Carraway MS, Piantadosi CA, Jenkinson CP, Huang Y-CT. Differential Expression of Arginase and iNOS in the Lung in Sepsis. Experimental Lung Research. 2009;24(3):253-68. doi: 10.3109/01902149809041533.

62. Hollenberg SM, Broussard M, Osman J, Parrillo JE. Increased microvascular reactivity and improved mortality in septic mice lacking inducible nitric oxide synthase. Circ Res. 2000;86(7):774-8. PubMed PMID: 10764411.

63. Hoshino K, Takeuchi O, Kawai T, Sanjo H, Ogawa T, Takeda Y, Takeda K, Akira S. Cutting edge: Toll-like receptor 4 (TLR4)-deficient mice are hyporesponsive to lipopolysaccharide: evidence for TLR4 as the Lps gene product. J Immunol. 1999;162(7):3749-52. PubMed PMID: 10201887.

64. Black KE, Collins SL, Hagan RS, Hamblin MJ, Chan-Li Y, Hallowell RW, Powell JD, Horton MR. Hyaluronan fragments induce IFNbeta via a novel TLR4-TRIF-TBK1-IRF3-dependent pathway. J Inflamm (Lond). 2013;10(1):23. doi: 10.1186/1476-9255-10-23. PubMed PMID: 23721397; PMCID: PMC3682892.

65. Cairns B, Maile R, Barnes CM, Frelinger JA, Meyer AA. Increased Toll-like receptor 4 expression on T cells may be a mechanism for enhanced T cell response late after burn injury. J Trauma. 2006;61(2):293-8; discussion 8-9. doi: 10.1097/01.ta.0000228969.46633.bb. PubMed PMID: 16917441.

66. Cairns BA, Barnes CM, Mlot S, Meyer AA, Maile R. Toll-like receptor 2 and 4 ligation results in complex altered cytokine profiles early and late after burn injury. J Trauma. 2008;64(4):1069-77; discussion 77-8. doi: 10.1097/TA.0b013e318166b7d9. PubMed PMID: 18404077.

67. Hayashi F, Smith KD, Ozinsky A, Hawn TR, Yi EC, Goodlett DR, Eng JK, Akira S, Underhill DM, Aderem A. The innate immune response to bacterial flagellin is mediated by Toll-like receptor 5. Nature. 2001;410(6832):1099-103. doi: 10.1038/35074106. PubMed PMID: 11323673.

68. Zahs A, Bird MD, Ramirez L, Choudhry MA, Kovacs EJ. Anti-IL-6 antibody treatment but not IL-6 knockout improves intestinal barrier function and reduces inflammation after binge ethanol exposure and burn injury. Shock. 2013;39(4):373-9. doi: 10.1097/SHK.0b013e318289d6c6. PubMed PMID: 23376955; PMCID: PMC3602394.

69. Faunce DE, Gregory MS, Kovacs EJ. Acute ethanol exposure prior to thermal injury results in decreased T-cell responses mediated in part by increased production of IL-6. Shock. 1998;10(2):135-40. PubMed PMID: 9721981.

70. Fontanilla CV, Faunce DE, Gregory MS, Messingham KA, Durbin EA, Duffner LA, Kovacs EJ. Anti-interleukin-6 antibody treatment restores cell-mediated immune function in mice with acute ethanol exposure before burn trauma. Alcohol Clin Exp Res. 2000;24(9):1392-9. PubMed PMID: 11003205.

71. Fielding CA, Jones GW, McLoughlin RM, McLeod L, Hammond VJ, Uceda J, Williams AS, Lambie M, Foster TL, Liao CT, Rice CM, Greenhill CJ, Colmont CS, Hams E, Coles B, Kift-Morgan A, Newton Z, Craig KJ, Williams JD, Williams GT, Davies SJ, Humphreys IR, O'Donnell VB, Taylor PR, Jenkins BJ, Topley N, Jones SA. Interleukin-6 signaling drives fibrosis in unresolved inflammation. Immunity. 2014;40(1):40-50. doi: 10.1016/j.immuni.2013.10.022. PubMed PMID: 24412616; PMCID: PMC3919204.

72. Vindenes H, Ulvestad E, Bjerknes R. Increased levels of circulating interleukin-8 in patients with large burns: relation to burn size and sepsis. J Trauma. 1995;39(4):635-40. PubMed PMID: 7473946.

73. Vindenes H, Bjerknes R. Microbial colonization of large wounds. Burns. 1995;21(8):575-9. PubMed PMID: 8747728.

74. Zheng H, Chen XL, Han ZX, Zhang Z, Wang SY, Xu QL. Ligustrazine attenuates acute lung injury after burn trauma. Burns. 2005;31(4):453-8. doi: 10.1016/j.burns.2004.10.023. PubMed PMID: 15896507.

75. Kim J, Natarajan S, Vaickus LJ, Bouchard JC, Beal D, Cruikshank WW, Remick DG. Diesel exhaust particulates exacerbate asthma-like inflammation by increasing CXC chemokines. Am J Pathol. 2011;179(6):2730-9. doi: 10.1016/j.ajpath.2011.08.008. PubMed PMID: 21967814; PMCID: PMC3260803.

76. Shallo H, Plackett TP, Heinrich SA, Kovacs EJ. Monocyte chemoattractant protein-1 (MCP-1) and macrophage infiltration into the skin after burn injury in aged mice. Burns. 2003;29(7):641-7. PubMed PMID: 14556721.

77. Furukawa K, Kobayashi M, Herndon DN, Pollard RB, Suzuki F. Appearance of monocyte chemoattractant protein 1 (MCP-1) early after thermal injury: role in the subsequent development of burn-associated type 2 T-cell responses. Ann Surg. 2002;236(1):112-9. PubMed PMID: 12131093; PMCID: PMC1422556.

78. Baker TA, Davis CS, Bach HHt, Romero J, Burnham EL, Kovacs EJ, Gamelli RL, Majetschak M. Ubiquitin and stromal cell-derived factor-1alpha in bronchoalveolar lavage fluid after burn and inhalation injury. J Burn Care Res. 2012;33(1):57-64. doi: 10.1097/BCR.0b013e31823dc559. PubMed PMID: 22105097; PMCID: PMC3626094.

79. Copeland S, Warren HS, Lowry SF, Calvano SE, Remick D, Inflammation, the Host Response to Injury I. Acute inflammatory response to endotoxin in mice and humans. Clin Diagn Lab Immunol. 2005;12(1):60-7. doi: 10.1128/CDLI.12.1.60-67.2005. PubMed PMID: 15642986; PMCID: PMC540200.

80. Zawacki BE, Jung RC, Joyce J, Rincon E. Smoke, burns, and the natural history of inhalation injury in fire victims: a correlation of experimental and clinical data. Ann Surg. 1977;185(1):100-10. PubMed PMID: 831629; PMCID: PMC1396243.

81. Matthew E, Warden G, Dedman J. A murine model of smoke inhalation. Am J Physiol Lung Cell Mol Physiol. 2001;280(4):L716-23. PubMed PMID: 11238012.

CHAPTER 2: DIRECT DETECTION OF BLOOD NITRIC OXIDE REVEALS A BURN-DEPENDENT DECREASE OF NITRIC OXIDE IN RESPONSE TO *PSEUDOMONAS AERUGINOSA* INFECTION[1][2]

Summary

Purpose: Burn injury is associated with severe immune dysfunction, including an anti-inflammatory state that occurs late after burn injury. While increased nitric oxide (NO) production is associated with severe infection and sepsis, the effect of burn trauma on these levels during a non-lethal infection remains unknown. We hypothesized that in a mouse model, 1) NO levels would be increased after nonlethal infection without trauma and 2) burn injury would lead to decreased NO production even during infection. Methods: Mice were infected via intra-tracheal inoculation with *Pseudomonas aeruginosa* 14 d following a 20% total body surface area contact burn. At 48 h following infection, blood was drawn to quantify NO concentrations using a microfluidic electrochemical sensor. Significant findings: In uninjured mice, infection caused a significant increase in blood NO levels. Increases in NO occurred in a dose-dependent response to the bacterial inoculum. Following burn injury, an identical infection did not elicit increases in NO. Conclusions: While increases in NO are expected over the course of an infection without prior trauma, burn injury and subsequent immune suppression decreases NO levels even in the presence of infection.

[1] Adapted for this dissertation from Dunn JLM, Hunter RA, Gast K, Maile R, Cairns BA, and Schoenfish MH. Direct detection of blood nitric oxide reveals a burn-dependent decrease of nitric oxide in response to *Pseudomonas aeruginosa* infection. 2016. Burns 42(7):1522-1527.

[2] Attribution: Julia Dunn performed all of the experiments including mouse injury and infection as well as collection of blood and tissue. Rebecca Hunter conducted measurement and analysis of NO in blood. Julia Dunn and Rebecca Hunter co-first authored the manuscript. Karli Gast assisted in tissue collections.

Introduction

Physical trauma such as burn injury causes severe immune dysfunction, often resulting in infection, sepsis, multiple organ dysfunction, and death (1). Historically, this immune response has been characterized by an initial pro-inflammatory period and a subsequent anti-inflammatory phase (1, 2). These periods have been referred to as the systemic inflammatory response syndrome (SIRS), during which pro-inflammatory mediators (e.g., tumor necrosis factor, interleukin-6, interleukin-1β) are released, and a compensatory anti-inflammatory response syndrome (CARS) thought to limit damage due to chronic inflammation (1-6). More recent studies have illustrated a more complex scenario, wherein pro- and anti-inflammatory cytokines may be secreted simultaneously, suggesting that the SIRS/CARS paradigm may be insufficient to characterize the immune response to trauma (3-5). Despite this paradigm shift, it remains true that late after trauma patients exhibit elevated susceptibility to nosocomial infection (6-8). Burn patients are especially prone to ventilator-associated pneumonia and wound infections (6, 9), and the leading cause of death following burn injury is related to infection and sepsis (6, 10). In particular, pulmonary infections by Gram-negative *Pseudomonas aeruginosa* are quite common (7). Novel methods are needed that will enable healthcare providers and researchers to monitor the immune response in real-time during trauma and infection.

Nitric oxide (NO) is a free radical species that is intricately involved with the innate immune response (11-26), and as such, *in vivo* levels will likely reflect the immune status of an individual. Indeed, the up-regulation of inducible nitric oxide synthase (iNOS) early after trauma has been observed, in addition to accumulation of NO byproducts in blood and tissue (7, 12, 17, 27-31). Until recently, direct detection of NO in whole blood was not feasible, requiring either the measurement of its byproducts (i.e., nitrate and nitrate) or the use of complex instrumentation (i.e., electron paramagnetic resonance spectroscopy) (32). Studies measuring NO byproducts in sheep have found that serum NO is increased in sheep after burn and smoke inhalation, and that this increase can be blocked with iNOS inhibitors (33).

Direct measurement of NO is likely to rapidly and sensitively detect changes in patient status; therefore, such measurements should be incorporated into clinically relevant models. Because of the availability of genetically modified mice, confirming the usefulness of NO as a readout in mouse models of trauma will enable elucidation of disease mechanisms that impact NO production. Recently, a microfluidic amperometric sensor was developed and used to directly measure increases in NO levels during a lethal murine model of sepsis (28).

We expect that NO levels may be decreased during an infection following burn injury. Because patients demonstrate susceptibility to infection late after trauma, we focused on NO levels in a nonlethal infection model at 14 days after burn injury. Quantifying changes in NO concentration may allow for the elucidation of immune dysfunction, indicated by either elevated levels during systemic infection or decreased levels during immune suppression.

Methods

Murine model of burn injury and infection. Nine week-old female C57BL/6 mice weighing 18-20 g underwent a 20% total body surface area (TBSA) burn injury as previously described (34). Briefly, mice were anesthetized with gaseous isofluorane, their dorsal flanks were shaved, and they received a subcutaneous injection of morphine sulphate prior to receiving a full-thickness burn with 4 applications of a copper rod heated in boiling water. Following burn injury, mice were resuscitated via an intraperitoneal injection of lactated Ringer's solution. Throughout the experiment, mice were monitored and received morphine in their drinking water (0.02 mg mL^{-1}; 4 mg kg^{-1} body weight per day) *ad libitum*. Sham (0% TBSA) mice also underwent these treatments, except the application of the copper rod.

At 14 d following burn injury, pneumonia was induced via the intratracheal administration of 50 μL *Pseudomonas aeruginosa* (PAK strain) following sedation with Avertin. Uninfected groups were administered 50 μL PBS with 1% protease peptone in the same manner. At 48 h following infection, ~300 μL blood was drawn into EDTA-coated microcentrifuge tubes via submandibular puncture. This blood

was immediately injected into the microfluidic device and analyzed amperometrically to determine NO concentrations.

Microfluidic amperometric sensor for nitric oxide measurement. Devices were fabricated as previously described (28). Working electrodes were 100 µm wide and consisted of 150 nm thick platinum with a 10 nm titanium seed layer, coated with a selective film (adhesion layer of 1% v/v (3-aminopropyl)triethoxysilane and a fluoroalkoxysilane xerogel) to impart selectivity to NO. The fluoroalkoxysilane membrane solution was prepared via the acid catalyzed hydrolysis and condensation of (heptadecafluoro-1,1,2,2-tetrahydrodecyl)trimethoxysilane and methyltrimethoxysilane as reported previously (35, 36). Reference electrodes consisted of a 10 nm titanium adhesion layer followed by a ~1 µm silver layer, chemically oxidized by reaction with 50 mM ferric chloride for 10 s to create a silver/silver chloride pseudo-reference/counter electrode. The ~90 µm microfluidic channel was formed using Kapton® tape.

The working and reference/counter electrodes of the microfluidic device were connected to a CH Instruments 1030A 8-channel potentiostat (Austin, TX). Prior to sample analysis, the device was polarized at +800 mV vs. the Ag/AgCl pseudo-reference/counter electrode for at least to 1 h in PBS. To calibrate the device, a saturated NO standard solution (prepared by purging deaerated PBS with NO gas for ~10 min to yield a 1.9 mM solution of NO) was diluted with PBS and introduced into the inlet reservoir.

Statistical analysis. Where appropriate, either an unpaired, two-tailed Student's t-test or two-way ANOVA with Bonfennori post-test was used to determine statistical significance between groups, with $p < 0.05$ considered to be significant.

Results

Nitric oxide levels are increased during pneumonia without prior burn injury. Blood samples were drawn 48 h following infection with 1 x 10^6 CFU of *P. aeruginosa* and immediately analyzed using

the microfluidic sensor (Figure 2.1). As shown in Figure 2.2A, blood NO levels were significantly increased in the infected versus uninfected mice at this time point (810 ± 180 nM and 370 ± 40 nM, respectively). As expected, these data suggest that activation of the immune response following infection leads to increased production of NO.

Increased infectious dose corresponds with elevated serum NO. Blood samples were drawn 24 h and 72 h following infection with either 5×10^5 or 5×10^6 CFU of *P. aeruginosa*. As indicated in Figure 1B, blood NO levels were higher in uninjured mice exposed to a higher infectious dose at 24 h (3.0 ± 0.2 μM vs. 6.2 ± 0.7 μM) and 72 h (7.0 ± 1.4 μM vs. 15.2 ± 4.7 μM) following infection. At both high- and low-dose inocula, blood NO concentrations were higher at 72 h than at 24 h. We also harvested lungs and quantified bacterial load in these mice at 72 hours after infection. There was a significant difference in bacterial load between mice with high and low dose bacterial inoculum, with a corresponding significant difference in plasma NO levels (Figure 2.2B).

Burn injury inhibits nitric oxide release following infection. Blood samples from infected (5×10^6 CFU) and uninfected mice 14 d after burn injury were analyzed using the electrochemical sensor. Concentrations of NO in blood of infected burned mice were not significantly elevated compared to uninfected burn mice (290 ± 80 nM vs. 410 ± 110 nM) (Figure 2). We also harvested lungs and quantified bacterial load in these mice at 72 hours after infection, and observed a significant reduction in pulmonary bacterial clearance in burn mice compared to sham mice and corresponding reduction in NO (Figure 2.3). These data indicate a late-stage effect of burn injury on immune function and NO production during an infection. Also of note, the NO concentrations observed in uninfected burn mice were equivalent to those in the uninfected sham mice.

We measured blood NO levels at 24 h and 72 h following a low-dose (5×10^5 CFU) infection with *P. aeruginosa*, and observed that NO concentrations were lower in burn infected mice compared to unburned infected mice at both 24 h (1.1 ± 0.4 vs. 3.0 ± 0.2 μM) and 72 h (6.0 ± 0.6 vs. 7.0 ± 1.4 μM)

following the infection (Figure 2.4A). Following inoculation with a high-dose (5 x 10^6 CFU) of *P. aeruginosa*, we observed elevated blood NO in burned mice compared to unburned mice at 24 h (7.5 ± 0.7 μM vs. 6.2 ± 0.7 μM), however while blood NO continued to rise in unburned mice, NO was not increased in burned mice at 72 h (4.2 ± 2.0 μM vs. 15.2 ± 4.7 μM) post infection (Figure 2.4B).

Discussion

In this study, we evaluated the effect of infection and burn injury on endogenous NO levels in a murine model. It is well understood that NO, along with other reactive oxygen and nitrogen species (ROS and RNS), are produced at higher levels during infection. Until recently, direct detection of NO has not been possible and analysis of its byproducts (nitrate and nitrite) has been required to estimate NO production. The microfluidic electrochemical sensor utilized herein allows for the immediate and direct detection of NO in a small (~250 μL) volume of whole blood, without the addition of external reagents. During an infection with no previous trauma, NO levels were increased relative to control mice. This result is not surprising, as NO is known for its antibacterial activity (37) and has been previously demonstrated to increase during systemic infection (28). We therefore conclude that our novel monitor sensitively detects changes in endogenous NO during nonlethal infection in mice.

However, this trend was not observed or was attenuated during infection that occurred 14 d following burn injury. Indeed, NO concentrations in infected burn mice were equivalent to those of uninfected burn and sham mice, suggesting immune suppression as a result of the burn injury. Even following high dose infection, when at 24 h NO concentrations were higher in burn than unburned mice, the injured mice were unable to sustain a robust response and NO concentrations diminished by 72 h compared with unburned mice.

The dysfunctional immune response following burn injury has been well documented (2). Cairns *et al.* demonstrated that while expression of TLR2 and TLR4 by macrophages is increased early (3 d) following burn injury, these levels are significantly decreased at 14 d (38). Numerous immune defense

systems are linked to TLR, including the induction of iNOS (39). Other studies have linked TLR with the induction of iNOS and concomitant release of NO by innate immune cells (e.g., macrophages) (40-42). For example, TLR is directly involved in microbe recognition by innate immune cells (TLR2 for Gram-positive peptidoglycan and TLR4 for Gram-negative lipopolysaccharide) and thus mediates subsequent inflammatory signals, including NO (39). Future studies should determine whether TLR signaling is directly linked to endogenous NO following infection.

While increased levels of endogenous NO may indicate development of a severe infection in otherwise healthy animals, the immune dysfunction that occurs late after trauma (e.g., burn injury) significantly alters NO production. As such, monitoring *in vivo* NO production in real time may provide insight into emerging infection as well as immune dysfunction. Reduction in NO production by innate immune cells, along with other aspects of immune suppression (e.g., shifts in T cell phenotype (43), altered cytokine profiles (44)), contribute to the increased infection susceptibility of burn patients. The clinical utility of NO measurement can be further evaluated by monitoring concentration changes throughout the course of infection/sepsis and throughout the dynamic immune response following trauma. In murine models, differences in NO concentration caused by infection with more virulent strains and during antibiotic treatment must also be evaluated.

FIGURES

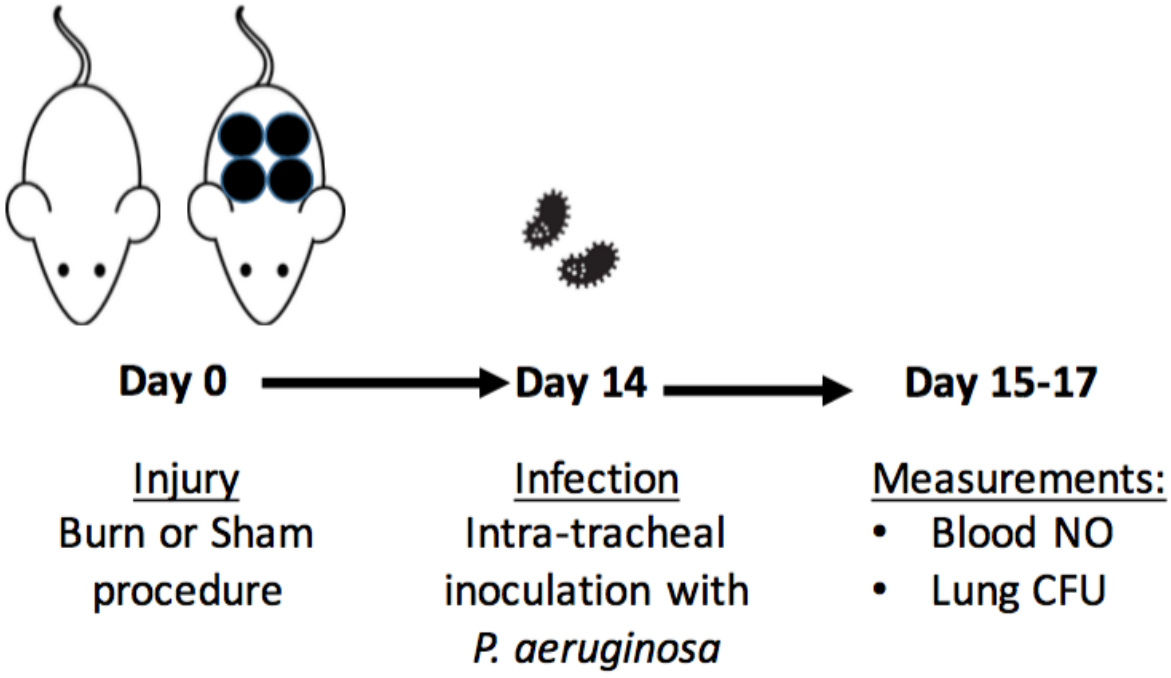

Figure 2.1: Experimental design for burn injury, infection, and blood NO analysis. 14 days after burn or sham procedure, mice were infected via intra-tracheal inoculation with *P. aeruginosa* and blood NO and bacterial burden in the lung was quantified at 24-72h after infection.

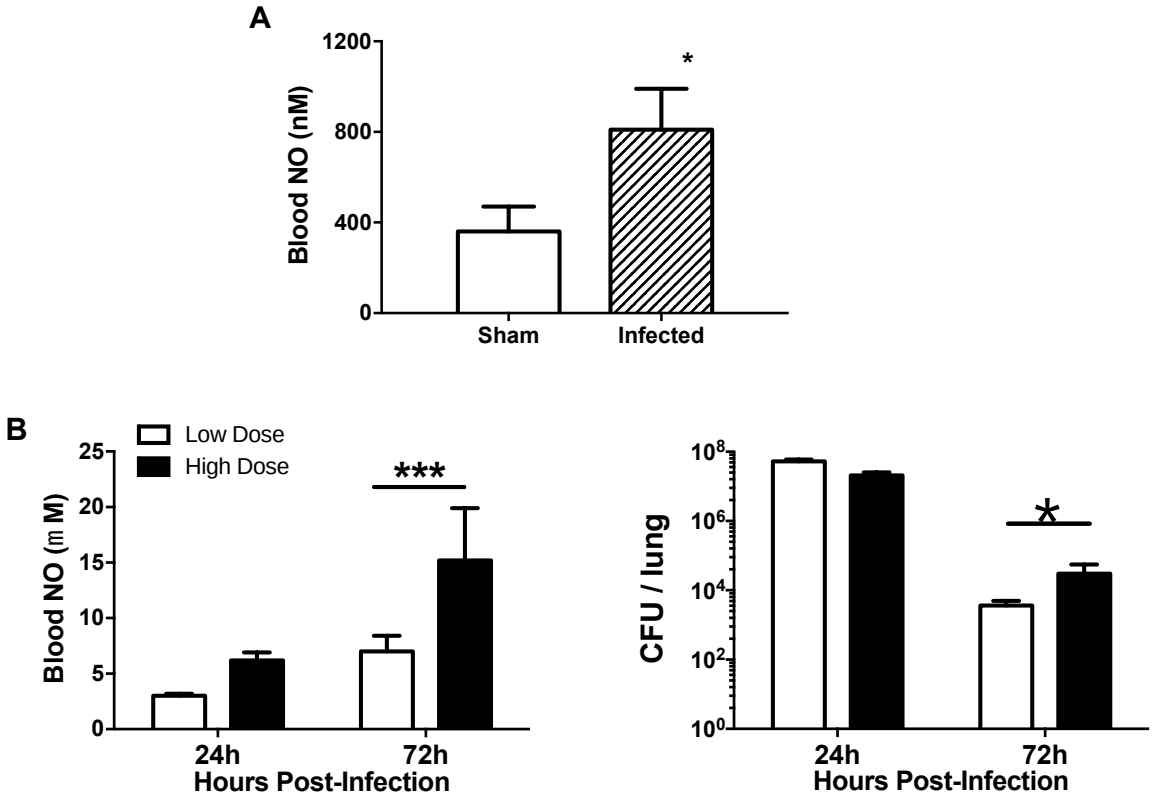

Figure 2.2: Nitric Oxide (NO) levels are elevated following infection without prior injury in a dose-dependent fashion. Mice (n=4) were infected with of *P. aeruginosa* and blood NO analyzed. A) NO levels were significantly increased 48 h following infection with1 x 10^6 CFU compared to uninfected counterparts. Statistical significance is indicated by *, $p < 0.05$ by a Student's *t* test. B) NO levels in blood and bacterial recovery from lungs were higher in mice inoculated with 5 x 10^5 CFU vs. 5 x 10^6 CFU at 72 hours post infection. Statistical significance is indicated by *, $p<0.05$ and ***, $p < 0.001$ by Two-way ANOVA with Bonfennori post-test. Data are given as mean ± standard deviation.

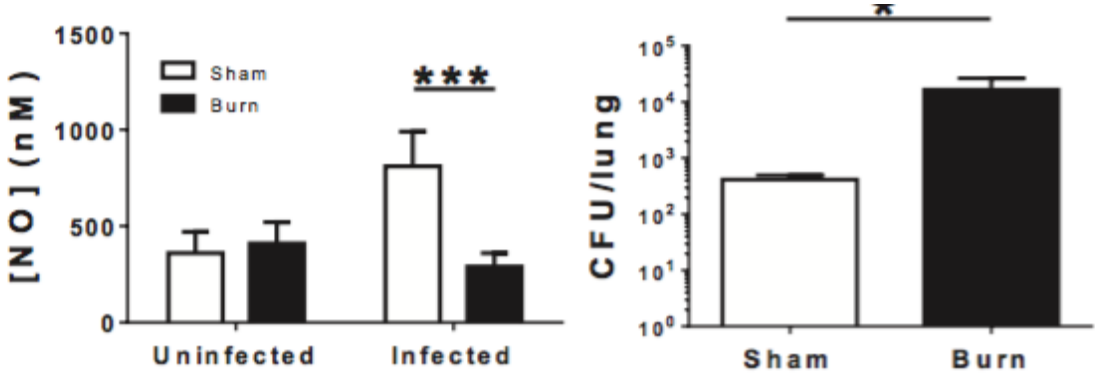

Figure 2.3: Relative to sham mice, burn injury causes decreased blood NO concentrations and increased pulmonary bacterial load following a 14 d post-burn infection. Mice (n=4) were infected with 5 x 10^6 CFU of *P. aeruginosa* 14 d after injury and blood NO analyzed 72 h after infection. Statistical significance is indicated by *, $p<0.05$ and ***, $p < 0.001$ by a Two-way ANOVA followed by Bonfennori post-test (A) and Student's t-test (B). Data are given as mean ± standard deviation.

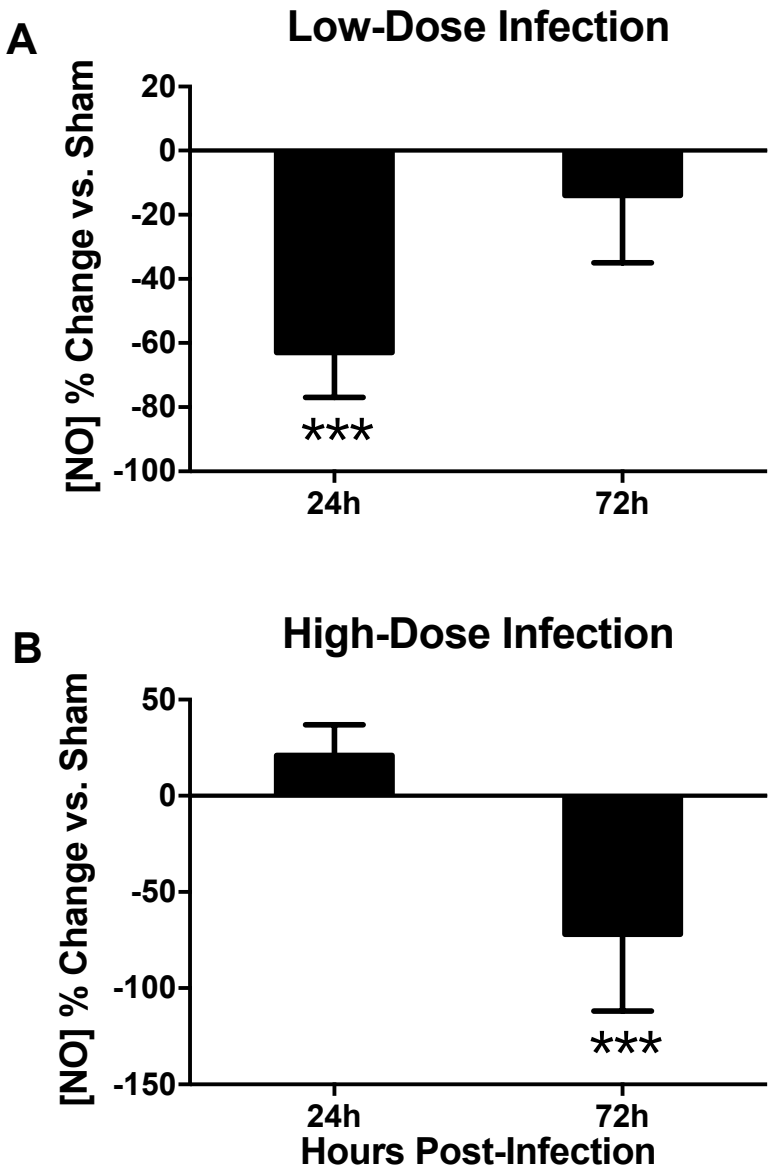

Figure 2.4: Inoculation dose impacts blood NO concentration in burn mice following infection. Mice (n=3-4) were infected with A) 5 x 10^5 or B) 5 x 10^6 CFU of *P. aeruginosa* and blood NO analyzed after 24 h or 72 h. Statistical significance is indicated by ***, $p < 0.001$ by a Two-way ANOVA followed by Bonfennori post-test. Data are given as mean ± standard deviation.

REFERENCES

1. Mannick JA, Rodrick ML, Lederer JA. The immunologic response to injury. Journal of the American College of Surgeons. 2001;193(3):237-44. doi: http://dx.doi.org/10.1016/S1072-7515(01)01011-0.

2. Hotchkiss RS, Coopersmith CM, McDunn JE, Ferguson TA. The sepsis seesaw: tilting toward immunosuppression. Nature Medicine. 2009;15(5):496-7.

3. Liu T, Qian WJ, Gritsenko MA, Xiao W, Moldawer LL, Kaushal A, Monroe ME, Varnum SM, Moore RJ, Purvine SO, Maier RV, Davis RW, Tompkins RG, Camp DG, 2nd, Smith RD, Inflammation, the Host Response to Injury Large Scale Collaborative Research P. High dynamic range characterization of the trauma patient plasma proteome. Molecular & cellular proteomics : MCP. 2006;5(10):1899-913. doi: 10.1074/mcp.M600068-MCP200. PubMed PMID: 16684767; PMCID: 1783978.

4. Finnerty CC, Jeschke MG, Herndon DN, Gamelli R, Gibran N, Klein M, Silver G, Arnoldo B, Remick D, Tompkins RG, Investigators of the I, the Host Response Glue G. Temporal cytokine profiles in severely burned patients: a comparison of adults and children. Molecular medicine. 2008;14(9-10):553-60. doi: 10.2119/2007-00132.Finnerty. PubMed PMID: 18548133; PMCID: 2424320.

5. Xiao W, Mindrinos MN, Seok J, Cuschieri J, Cuenca AG, Gao H, Hayden DL, Hennessy L, Moore EE, Minei JP, Bankey PE, Johnson JL, Sperry J, Nathens AB, Billiar TR, West MA, Brownstein BH, Mason PH, Baker HV, Finnerty CC, Jeschke MG, Lopez MC, Klein MB, Gamelli RL, Gibran NS, Arnoldo B, Xu W, Zhang Y, Calvano SE, McDonald-Smith GP, Schoenfeld DA, Storey JD, Cobb JP, Warren HS, Moldawer LL, Herndon DN, Lowry SF, Maier RV, Davis RW, Tompkins RG, Inflammation, Host Response to Injury Large-Scale Collaborative Research P. A genomic storm in critically injured humans. The Journal of experimental medicine. 2011;208(13):2581-90. doi: 10.1084/jem.20111354. PubMed PMID: 22110166; PMCID: 3244029.

6. Weinstein RA, Mayhall CG. The Epidemiology of Burn Wound Infections: Then and Now. Clinical Infectious Diseases. 2003;37(4):543-50. doi: 10.1086/376993.

7. Driscoll J, Brody S, Kollef M. The Epidemiology, Pathogenesis and Treatment of Pseudomonas aeruginosa Infections. Drugs. 2007;67(3):351-68. doi: 10.2165/00003495-200767030-00003.

8. Adib-Conquy M, Cavaillon J-M. Compensatory anti-inflammatory response syndrome. Thrombosis and Haemostasis. 2009;101(1):36-47. doi: 10.1160/TH08-07-0421.

9. Wurtz R, Karajovic M, Dacumos E, Jovanovic B, Hanumadass M. Nosocomial infections in a burn intensive care unit. Burns. 1995;21(3):181-4. PubMed PMID: 7794498.

10. Cioffi WG. What's new in burns and metabolism. Journal of the American College of Surgeons. 2001;192(2):241-54.

11. Armstrong R. The physiological role and pharmacological potential of nitric oxide in neutrophil activation. International immunopharmacology. 2001;1(8):1501-12.

12. Assreuy J, Barja-Fidalgo C, Tavares-Murta BM. Inflammatory and Vascular Alterations in Sepsis: The Role of Nitric Oxide-Dependent Mechanisms. Anti-Inflammatory & Anti-Allergy Agents in Medicinal Chemistry (Formerly Cu. 2006;5(1):35-44.

13. Beckman JS, Koppenol WH. Nitric oxide, superoxide, and peroxynitrite: The good, the bad, and the ugly. Am J Physiol-Cell Physiol. 1996;271(5):C1424-C37. PubMed PMID: WOS:A1996VT08800002.

14. Bogdan C. Nitric oxide and the immune response. Nat Immunol. 2001;2(10):907-16.

15. Boscá L, Zeini M, Través PG, Hortelano S. Nitric oxide and cell viability in inflammatory cells: a role for NO in macrophage function and fate. Toxicology. 2005;208(2):249-58. doi: http://dx.doi.org/10.1016/j.tox.2004.11.035.

16. Coleman JW. Nitric oxide in immunity and inflammation. International Immunopharmacology. 2001;1(8):1397-406. doi: http://dx.doi.org/10.1016/S1567-5769(01)00086-8.

17. Fortin CF, McDonald PP, Fülöp T, Lesur O. Sepsis, leukocytes, and nitric oxide (NO): an intricate affair. Shock. 2010;33(4):344-52.

18. Frances R, Munoz C, Zapater P, Uceda F, Gascon I, Pascual S, Perez-Mateo M, Such J. Bacterial DNA activates cell mediated immune response and nitric oxide overproduction in peritoneal macrophages from patients with cirrhosis and ascites. Gut. 2004;53(6):860-4.

19. Hierholzer C, Kalff JC, Billiar TR, Bauer AJ, Tweardy DJ, Harbrecht BG. Induced nitric oxide promotes intestinal inflammation following hemorrhagic shock. American Journal of Physiology-Gastrointestinal and Liver Physiology. 2004;286(2):G225-G33.

20. Hollenberg SM, Broussard M, Osman J, Parrillo JE. Increased microvascular reactivity and improved mortality in septic mice lacking inducible nitric oxide synthase. Circulation research. 2000;86(7):774-8.

21. Kirkebøen KA, Strand ØA. The role of nitric oxide in sepsis – an overview. Acta Anaesthesiologica Scandinavica. 1999;43(3):275-88. doi: 10.1034/j.1399-6576.1999.430307.x.

22. Knight J. Review: Free radicals, antioxidants, and the immune system. Annals of Clinical & Laboratory Science. 2000;30(2):145-58.

23. Lowenstein CJ, Dinerman JL, Snyder SH. Nitric Oxide: A Physiologic Messenger. Annals of Internal Medicine. 1994;120(3):227-37.

24. MacMicking J, Xie QW, Nathan C. Nitric oxide and macrophage function. Annu Rev Immunol. 1997;15:323-50. PubMed PMID: ISI:A1997WT66900013.

25. Snyder SH, Bredt DS. Biological roles of nitric oxide. Scientific American. 1992;266(5):74-7.

26. Vincent J-L, Zhang H, Szabo C, Preiser J-C. Effects of Nitric Oxide in Septic Shock. American Journal of Respiratory and Critical Care Medicine. 2000;161(6):1781-5. doi: 10.1164/ajrccm.161.6.9812004.

27. Carraway MS, Piantadosi CA, Jenkinson CP, Huang Y-CT. Differential expression of arginase and iNOS in the lung in sepsis. Experimental lung research. 1998;24(3):253-68.

28. Hunter RA, Privett BJ, Henley WH, Breed ER, Liang Z, Mittal R, Yoseph BP, McDunn JE, Burd EM, Coopersmith CM, Ramsey JM, Schoenfisch MH. Microfluidic amperometric sensor for analysis of nitric oxide in whole blood. Analytical Chemistry. 2013;85(12):6066-72. doi: 10.1021/ac400932s.

29. Carcillo JA. Nitric oxide production in neonatal and pediatric sepsis. Critical care medicine. 1999;27(6):1063-5.

30. Dhillon SS, Mahadevan K, Bandi V, Zheng Z, Smith CW, Rumbaut RE. Neutrophils, nitric oxide, and microvascular permeability in severe sepsis. CHEST Journal. 2005;128(3):1706-12.

31. Kao CC, Bandi V, Guntupalli KK, Wu M, Castillo L, Jahoor F. Arginine, citrulline and nitric oxide metabolism in sepsis Clin Sci. 2009;117(1):23-30.

32. Hetrick EM, Schoenfisch MH. Analytical Chemistry of Nitric Oxide. Annual Review of Analytical Chemistry. 2009;2(1):409-33. doi: 10.1146/annurev-anchem-060908-155146.

33. Soejima K, Schmalstieg FC, Traber LD, Szabo C, Salzman A, Traber DL. Role of nitric oxide in myocardial dysfunction after combined burn and smoke inhalation injury. Burns. 2001;27(8):809-15. PubMed PMID: 11718983.

34. Hultman CS, Cairns BA, deSerres S, Frelinger JA, Meyer AA. Early, complete burn wound excision partially restores cytotoxic T lymphocyte function. Surgery. 1995;118(2):421-30. doi: http://dx.doi.org/10.1016/S0039-6060(05)80354-X.

35. Shin JH, Weinman SW, Schoenfisch MH. Sol-gel derived amperometric nitric oxide microsensor. Analytical Chemistry. 2005;77(11):3494-501. doi: 10.1021/ac048153i. PubMed PMID: ISI:000229561800019.

36. Shin JH, Privett BJ, Kita JM, Wightman RM, Schoenfisch MH. Fluorinated xerogel-derived microelectrodes for amperometric nitric oxide sensing. Analytical Chemistry. 2008;80(18):6850-9. doi: 10.1021/ac800185x. PubMed PMID: ISI:000259199400003.

37. Carpenter AW, Schoenfisch MH. Nitric oxide release: Part II. Therapeutic applications. Chemical Society Reviews. 2012;41(10):3742-52. doi: 10.1039/C2CS15273H.

38. Cairns BA, Barnes CM, Mlot S, Meyer AA, Maile R. Toll-like Receptor 2 and 4 Ligation Results in Complex Altered Cytokine Profiles Early and Late After Burn Injury. Journal of Trauma and Acute Care Surgery. 2008;64(4):1069-78.

39. Underhill DM, Ozinsky A. Toll-like receptors: key mediators of microbe detection. Current opinion in immunology. 2002;14(1):103-10.

40. Baumgarten G, Knuefermann P, Schuhmacher G, Vervölgyi V, von Rappard J, Dreiner U, Fink K, Djoufack C, Hoeft A, Grohé C. Toll-like receptor 4, nitric oxide, and myocardial depression in endotoxemia. Shock. 2006;25(1):43-9.

41. Hoshino K, Takeuchi O, Kawai T, Sanjo H, Ogawa T, Takeda Y, Takeda K, Akira S. Cutting edge: Toll-like receptor 4 (TLR4)-deficient mice are hyporesponsive to lipopolysaccharide: evidence for TLR4 as the Lps gene product. The Journal of Immunology. 1999;162(7):3749-52.

42. Brightbill HD, Libraty DH, Krutzik SR, Yang R-B, Belisle JT, Bleharski JR, Maitland M, Norgard MV, Plevy SE, Smale ST. Host defense mechanisms triggered by microbial lipoproteins through toll-like receptors. Science. 1999;285(5428):732-6.

43. Daniel T, Alexander M, Hubbard WJ, Chaudry IH, Choudhry MA, Schwacha MG. Nitric oxide contributes to the development of a post-injury Th2 T-cell phenotype and immune dysfunction. Journal of Cellular Physiology. 2006;208(2):418-27.

44. Ulloa L, Tracey KJ. The 'cytokine profile': a code for sepsis. Trends in molecular medicine. 2005;11(2):56-63.

CHAPTER 3: MAMMALIAN TARGET OF RAPAMYCIN REGULATES A HYPER-RESPONSIVE STATE IN PULMONARY NEUTROPHILS LATE AFTER BURN INJURY.[1]

Summary

Bacterial pneumonia is a leading cause of death in burn patients, highlighting the severe immune dysfunction that follows traumatic injury. Metabolism is also perturbed in burn patients; we therefore examined the interplay between metabolism and innate immunity in the context of burn injury by suppressing the mammalian target of rapamycin (mTOR) in a murine model of burn injury. Following burn injury, we observe recruitment of neutrophils to the lungs, accompanied by increased *ex vivo* reactive oxygen and nitrogen species (RONS) production by neutrophils. Elevated RONS production correlates with improved clearance of *Pseudomonas aeruginosa*, despite burn-dependent downregulation of TLR2 and TLR4 expression on granulocytes. mTOR inhibition prevented the enhanced bacterial clearance in injured mice, and caused overwhelming mortality in burn mice after high-dose infection. Rapamycin treatment did not alter neutrophil recruitment to the lung in either injured or infected animals; however, oxidative burst was decreased by rapamycin treatment. Our results indicate the importance of RONS activity following burn injury, and illustrate that neutrophil activity within the lung tissue is more important than recruitment for infection clearance following cutaneous burn injury.

Introduction

In 2015 almost 500,000 patients sought medical care for a burn injury in the United States, resulting in approximately 40,000 Intensive Care Unit admissions and over 3,000 fatalities. Severe burns

[1] Attribution: Julia Dunn designed and carried out experiments, analyzed data, created figures, and wrote manuscript. Karli Gast, Marci Sessions, and Rebecca Hunger analyzed data and created figures. Lance Thurlow administered rapamycin and carried out associated experiments.

often require several weeks of hospitalization, during which patients require careful monitoring to prevent and treat infections (1, 2). Burn injury leads to immune perturbations that render patients highly susceptible to opportunistic bacterial infections during recovery. Indeed, patients without apparent lung damage at admission often develop bacterial pneumonia during hospitalization, most often due to *Pseudomonas aeruginosa*. Improved understanding of the complex immune response to burn injury may illuminate treatments to minimize complications, decrease recovery times, and improve long-term prognosis.

The immune response to burn injury is complex and dynamic. For years it was believed that in burns, as in sepsis, patients experience an initial Systemic Inflammatory Response Syndrome (SIRS) marked by pro-inflammatory cytokines and other inflammatory mediators. In sepsis, SIRS is followed by a later, Compensatory Anti-Inflammatory Response Syndrome (CARS) where immunosuppression renders the patient vulnerable to infection. Recent studies indicate that the SIRS/CARS paradigm may not accurately represent the complex immune response in burn patients because pro- and anti-inflammatory mediators are often detected simultaneously (1-6). Several animal models of burn injury have been described, including scalds, contact burns, and flame burns in pigs, rats, and mice (7-10). While the preponderance of animal studies has focused on the early immune response following injury, animal studies focused on the late immune response have been infrequent and do not show clear immunosuppression.

Following traumatic injury, patients experience severe metabolic dysregulation, characterized by elevated basal metabolic rate and a paradoxical comingling of hyperglycemia and hyperinsulinemia (2, 9, 11, 12). Several studies have demonstrated altered metabolism in animal models of burn injury (13-15). The relationship between metabolism and immunity has been focus of much recent research activity (16, 17). Insulin receptor signaling suppresses Toll-like Receptor (TLR) expression in human granulocytes (18) and hyperglycemia perturbs both cytokine secretion and TLR signaling in myeloid cells (19-22). Insulin receptor signaling leads to mTOR activation, allowing cells to interpret nutrient availability to

support translational and metabolic processes that lie downstream of mTOR (23). mTOR responds to signaling via TLR and chemokine receptors on innate immune cells (24), however the importance of mTOR signaling in antimicrobial activity by neutrophils has not been clearly elucidated.

We hypothesize that mTOR activity promotes innate immune cell function late after a cutaneous burn injury. Using systemic administration of rapamycin in a murine model of contact burn, we observed an mTOR-dependent decrease in neutrophil function in the lung following injury. These changes resulted in decreased bacterial clearance and survival following a pulmonary *P. aeruginosa* infection.

Methods

Burn injury and rapamycin treatment. Nine week old Female C57/BL6 mice (Taconic Farms; Hudson, NY) were housed in a specific pathogen free environment. All procedures were carried out in accordance with guidelines from the National Institutes of Health regarding use of vertebrate animals in research. Protocols were approved by the University of North Carolina at Chapel Hill's Institutional Animal Care and Use Committee. Based on previous studies and IACUC recommendations to limit animal numbers, 3-4 sham and 4-5 burn animals were used for experiments without infection; for infections studies 4-5 sham and 5-6 burn mice were used per group. Experiments were repeated to confirm findings and representative data are shown.

The 20% total body surface area full-thickness contact burn procedure was carried out under isofluorane sedation as previously described, including prophylactic subcutaneous morphine prior to injury and oral morphine *ad libitum* in drinking water following injury (25). Rapamycin was administered (4 mg/kg/d) daily starting 7 d before the burn injury via an intraperitoneal injection.

Infection and sample collection. Pseudomonas aeruginosa strain PAK was grown until mid-log phase in LB broth. Bacteria were pelleted, washed, and suspended with ice cold protease-peptone in phosphate buffered saline (1% by weight; PP-PBS). Mice were sedated with tribromoethanol (475mg/kg body weight. Sigma-Aldrich; St. Louis, MO), sedation was confirmed by toe-pinch, and mice were

mounted on an intubation platform. A MicroSprayer® Aerosolizer Model 1A-1C and FMJ-250 High-Pressure Syringe (Penn Century, Inc.; Wyndmoor, PA) nozzle was inserted into the trachea and 50μL of aerosolized inoculum or vehicle control (1% PP-PBS) was instilled into the airway.

Levels of nitric oxide (NO) were measured directly in blood as previously described (26). To determine bacterial burden, lung and liver tissue were collected at time of sacrifice and serial dilutions of tissue homogenate in PBS were plated on LB-agar plates and grown overnight at 37˚C.

To prepare tissue for histology, lungs were inflated with paraformaldehyde (4% by weight in PBS) to a constant pressure and fixed overnight. Lungs were embedded in paraffin, sectioned, and hematoxylin and eosin (H&E) stained at the Lineberger Comprehensive Cancer Center Animal Histopathology Core. Images were taken with an Olympus BX61 Upright Wide Field Microscope at the UNC Microscopy Services Laboratory.

Flow cytometric analysis. Lung tissue was minced and digested with collagenase I (4.5 mg) and DNAse (2 ug) with shaking for 1 h at 37˚C. Filtered samples were subjected to ACK lysis and treated with a blocking immunoglobulin against CD16/CD32 (eBioscience; San Diego, CA) prior to staining with fluorescently conjugated antibodies against CD45, CD11b, CD11c, Ly6C, Ly6G, and F4/80 (BD Biosciences; San Jose, CA). To quantify RONS production, stained cells were incubated with 0.75 mg Dihydrorhodamine 123 (DHR; Thermo-Fischer; Waltham, MA). Duplicate samples were either stimulated with 62.5 ng phorbol 12-myristate 13-acetate (PMA) or left unstimulated. After 30 min, reactions were quenched with a fixation buffer containing 1% paraformaldehyde and mean fluorescence intensity (MFI) was measured. Samples were analyzed at the UNC Flow Cytometry Core Facility on a CyAn and Summit 5.3 software was used to analyze data (Beckmann-Coulter; Indianapolis, IN). Neutrophils were defined as $CD45^{+}CD11b^{+}CD11c^{-}Ly6G^{+}$ and macrophages were defined as $CD45^{+}CD11c^{+}Ly6C^{+}F4/80^{+}Ly6G^{-}$.

Statistical analysis. GraphPad Prism Version 5.0 for Windows was used to analyze data by Student's t-Test, One-Way Analysis of Variance (ANOVA) with Tukey post-test, or Two-Way ANOVA with Bonferroni post-test, as appropriate. Data are represented as mean +/- standard error of the mean (SEM).

Results and Discussion

Burn injury leads to sustained recruitment of neutrophils to the pulmonary vasculature. The most common cause of mortality amongst burn patients late after injury is bacterial pneumonia. In order to characterize the immune environment of the lung, we performed cutaneous burn or sham injury on wildtype C57BL/6 mice. Using flow cytometry, we observed that neutrophils are recruited to the lung within hours of the injury (Figure 3.1A), and absolute numbers remain high for two weeks (Figure 3.1B). Figure 1C shows a representative flow plot of $Ly6g^{-}Ly6C^{+}F4/80^{+}$ macrophages and $Ly6g^{+}Ly6C^{-}F4/80^{-}$ neutrophils after gating on $CD45^{+}$ and excluding $CD11b^{-}CD11c^{-}$ cells. The gates were used to calculate the frequency of neutrophils, which increased approximately five-fold in the lung compared to sham injured mice at 14 days post injury (dpi). We did not observe an increase in macrophage numbers or frequency in the lung following burn injury (Figure 3.1D). Histology revealed that the neutrophils are sequestered in the lung vasculature, with no appearance of neutrophils, edema, or other damage in the airway or alveolar space (Figure 3.1E).

Neutrophils that accumulate in the pulmonary vasculature after burn have greater oxidative activity ex vivo. In order to determine whether burn injury alters the function of innate immune cells in the lung, we quantified reactive oxygen and nitrogen species (RONS) production by cells isolated from whole lung 14 d after cutaneous burn injury. We utilized Dihydrorhodamine-123 (DHR) to detect the production of both reactive nitrogen and oxygen species in cells (27). In burned mice compared to sham we observed a significant increase in the ability of neutrophils to oxidize DHR without further stimulation *ex vivo* (Figure 3.2A). Stimulation with PMA revealed that the maximal RONS production was equivalent in burn and sham neutrophils, resulting in a significantly reduced stimulation index (stimulated

MFI/unstimulated MFI; Figure 3.2B). Neither resting nor maximal RONS production was altered in lung macrophages after burn injury. These data suggest that pulmonary neutrophils, which accumulate late after burn injury, likely have hyper-responsive oxidative activity *in vivo*.

Burn mice clear bacterial infection more effectively than sham injured mice despite reduced TLR expression. We hypothesized that the increased oxidative capacity of neutrophils late after injury accounts for the ability of burned mice to clear a pulmonary bacterial infection. We inoculated burn or sham injured mice 14 d after injury with aerosolized *Pseudomonas aeruginosa* (strain PAK), a clinically relevant opportunistic pathogen that frequently causes fatal pneumonia in burn patients. We observed a significant increase in the clearance of PAK in burn mice compared to sham mice, despite comparable increases in neutrophil numbers in the airway (Figure 3.3A). On examination of the innate cell activity in the lung, we found that both burn injury alone and burn injury plus infection resulted in elevated RONS production by pulmonary neutrophils *ex vivo*; however, we did not observe an infection-dependent increase in neutrophil RONS production in either burn or sham animals (Figure 3.3B). In contrast, only bacterial infection significantly increased RONS by pulmonary macrophages. These findings suggest that the increased oxidative capacity of neutrophils late after injury is maintained during bacterial infection.

Toll-like receptor (TLR) signaling is an important sensing mechanism for antimicrobial responses. We have previously described reduced TLR expression by innate cells late after burn injury (8). Other studies have shown that TLR2 and TLR4 signaling impact neutrophil chemotaxis, activation, and lifespan, with the latter effects being especially important for prolonged responses to stimulus as in the case of our model (28). Herein, using flow cytometry, we observe significantly reduced TLR2 and TLR4 expression in burn mice compared to sham at 14 d after injury (Figure 3.3C). These changes in TLR expression occurred with and without infection. The ability of burn mice to clear pulmonary bacteria therefore appears more tightly correlated with oxidative burst than TLR expression.

Inhibition of mTOR reverses burn injury-induced innate immune hyper-responsiveness in the lung. It has been proposed that mTOR activity impacts neutrophil recruitment, RONS production and TLR signaling (24). mTOR can act downstream of the insulin receptor, making it a target of hyperinsulinemia observed in burn patients (29). Furthermore, processes downstream of mTOR activation, such as oxidative burst and protein translation, are enhanced by hyperglycemia (30-32). Because of the importance of mTOR and its signaling partners in insulin signaling and immune regulation, we hypothesize that mTOR promotes granulocyte hyper-responsiveness following trauma and infection by boosting TLR sensitivity and RONS production. To test this hypothesis, we inhibited mTOR activity with systemic administration of rapamycin and measured bacterial clearance as well as TLR expression and RONS production by pulmonary granulocytes following injury (Figure 3.4).

We observed increased bacterial burden in rapamycin treated burn mice compared to rapamycin treated sham mice (Figure 3.5A). At a high infectious dose, we observed significant mortality within 72 h of infection only in burn injury and rapamycin treated mice (Figure 3.5B). We have previously reported that increased blood nitric oxide (NO) marks a robust innate response to bacterial infection (26). Using a novel microfluidics based electrode to rapidly detect blood NO, we found that sham injured mice were able to mount a significantly increased NO response after PAK infection. In contrast, burn mice infected 14 d after injury had a significant reduction in the concentration of blood NO compared to infected sham mice. mTOR inhibition suppressed systemic NO production following infection in both sham and burn mice (Figure 3.5C).

We explored the cellular mechanism of the decreased bacterial control and increased mortality following burn plus rapamycin treatment. Rapamycin did not impact neutrophil or macrophage recruitment to the lungs in any treatment group (data not shown). Neutrophil and macrophage TLR expression was reduced by rapamycin treatment in both sham and burn injured mice (Figure 3.6A). Future studies should determine whether signal transduction downstream of TLR ligation is similarly impaired by rapamycin treatment. We found that in neutrophils (Figure 3.6B) and macrophages (Figure

3.6C), increased RONS production after burn and infection was dependent on mTOR; however, there was a further burn-dependent decrease of RONS production by neutrophils, evidenced by a reduced stimulation index, which was independent of mTOR activity (Figure 3.6B).

In conclusion, we report substantial neutrophil accumulation in the lung following burn injury, accompanied by increased RONS production and minimal extravasation into the airway. In contrast, macrophages are not "primed" by burn injury in this way. When challenged with a pulmonary bacterial infection, we observe enhanced bacterial clearance in burn mice compared to uninjured controls, accompanied by increased RONS production by both lung neutrophils and macrophages even in the face of reduced TLR expression. Augmented RONS production, but not granulocyte recruitment, was abolished by mTOR inhibition after burn injury. The absence of the innate "priming" effect of burn injury in rapamycin-treated mice led to increased bacterial susceptibility in burn mice compared to uninjured controls. After burn injury, reduced TLR expression and mTOR-inhibition suppresses the burn-dependent increase in RONS production by innate cells. We hypothesize that after burn injury, accelerated metabolism increases mTOR signaling, priming innate immune activity to protect the airway from infection by driving up innate cell RONS production. In this study oxidative burst appears to be more important for bacterial clearance than granulocyte recruitment because mTOR suppression led to increased bacterial burden. It may be more therapeutically beneficial to target innate immune effector function rather than recruitment in trauma patients. Future studies will determine whether systemic agonists of AMPK and HIF1α, which act up- and downstream of mTOR, respectively (23, 24), are effective in offsetting pneumonia after burn injury in mice. Additional studies are underway to quantify factors that impact mTOR signaling in trauma patients.

FIGURES

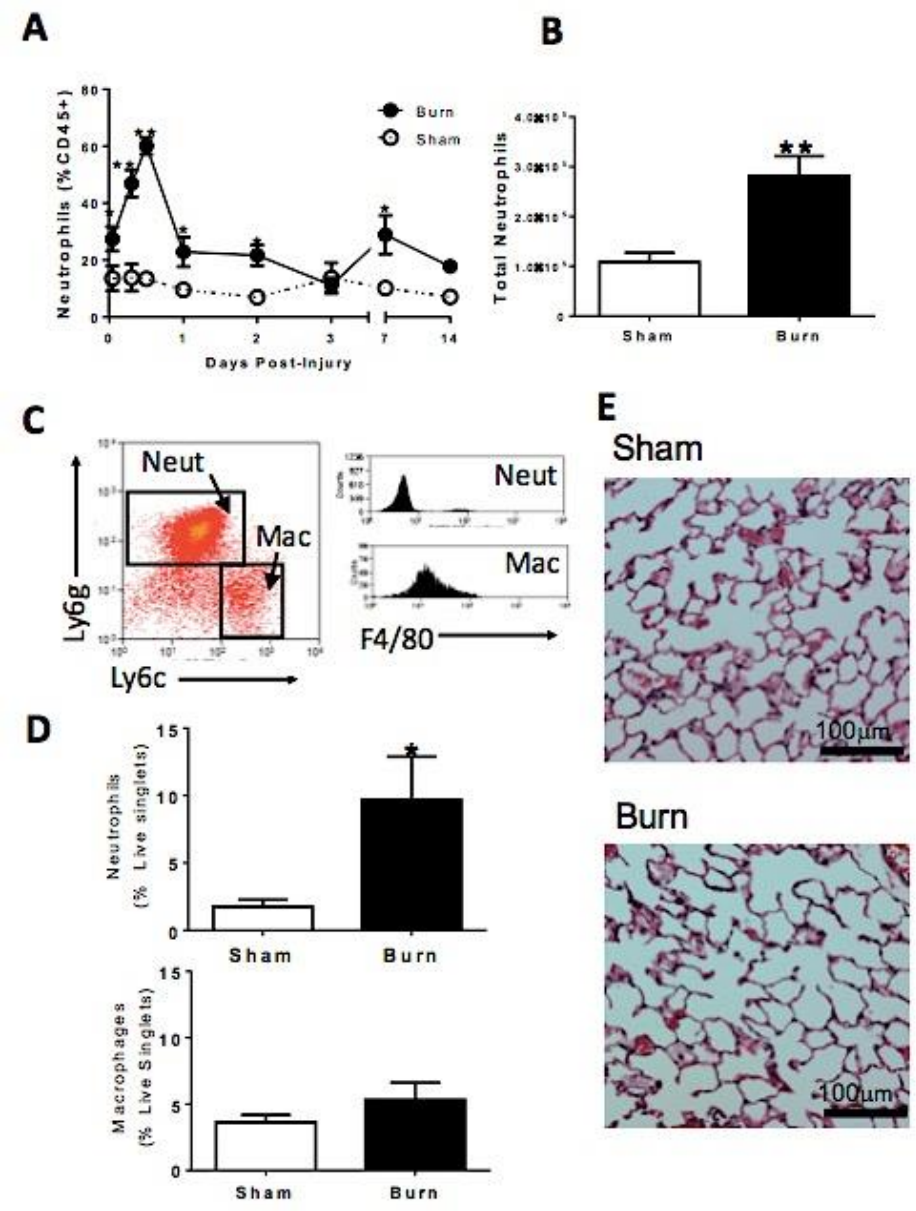

Figure 3.1: Neutrophils are recruited to the lung following burn injury. A) Neutrophils are shown as a percentage of $CD45^+$ cells from whole lung tissue as measured by flow cytometry. B) Total number of neutrophils in the lung is determined as (%neutrophils as live cells x live cells counted at harvest). C) Representative $Ly6g^-Ly6C^+F4/80^+$ macrophages and $Ly6g^+Ly6C^-F4/80^-$ neutrophils flow plots after gating on $CD45^+$ and excluding $CD11b^-CD11c^-$ cells. D) Neutrophils and macrophages are shown as a fraction of live cells as measured by flow cytometry. E) Representative specimens of H&E stained distal airway are shown from sham and burn mice at 12 h after treatment. Data shown are +/-SEM. Samples were analyzed by Student's t-test and significance indicated by *$p<0.05$, **$p<0.01$.

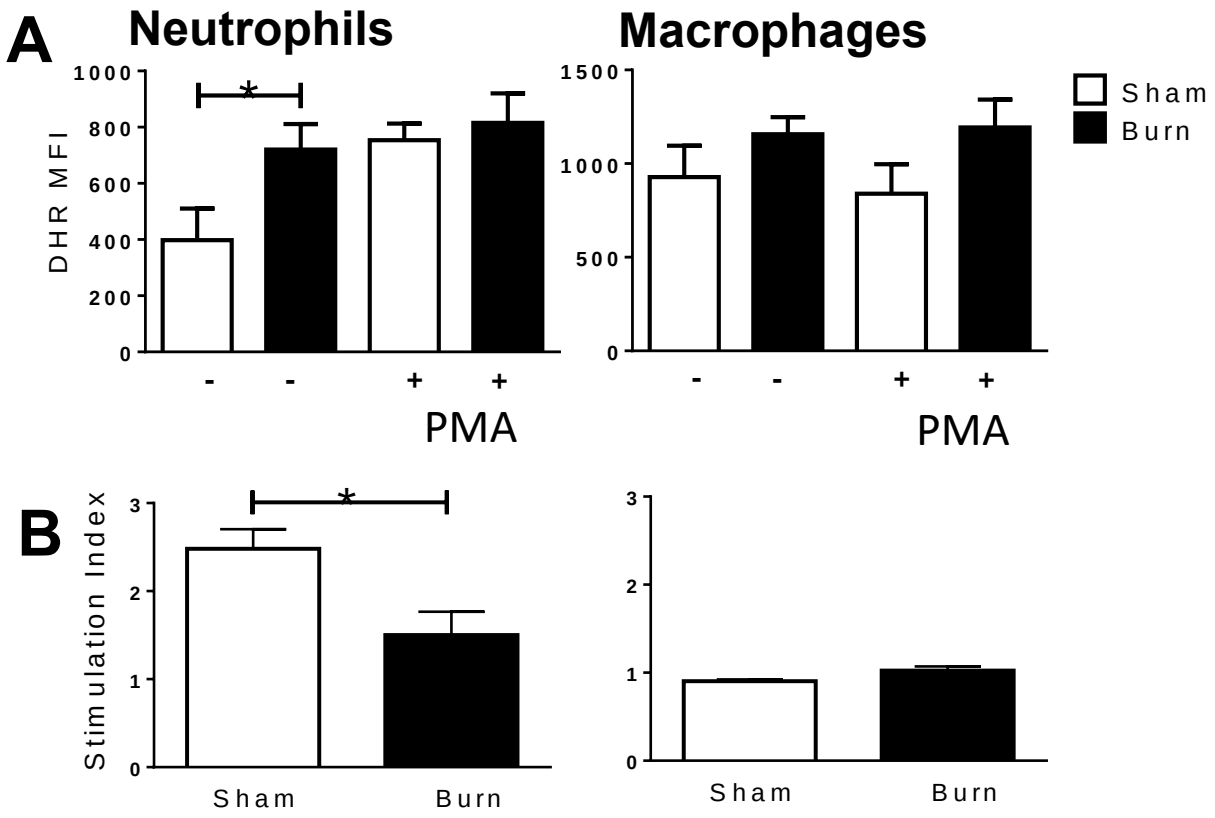

Figure 3.2: Burn injury impacts reactive oxygen and nitrogen species (RONS) production in neutrophils. Cells from whole lung tissue were collected at 14 d post-injury and analyzed by flow cytometry. A) DHR MFI of gated neutrophils or macrophages was measured in unstimulated samples. B) DHR MFI was measured in gated neutrophils and macrophages from paired stimulated and unstimulated samples. Stimulation index was calculated by dividing the DHR MFI of stimulated samples by that of unstimulated samples. Data shown are +/-SEM. Data were analyzed by Two-way ANOVA with Bonferroni post-test (A) or Student's t-test (B) and significance denoted as *$p<0.05$.

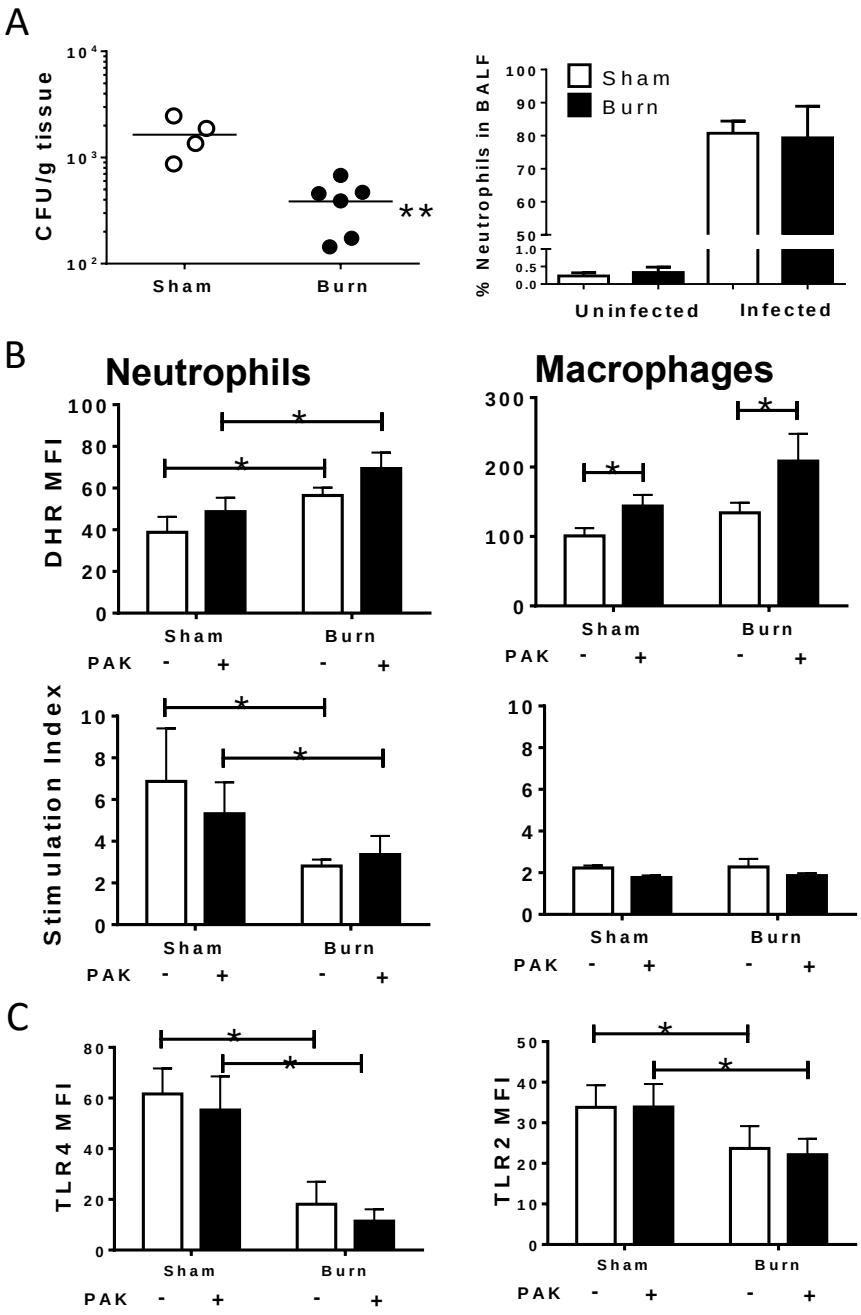

Figure 3.3: Changes in immune function, but not recruitment, lead to improved bacterial clearance in the lung following burn injury. Mice were infected intratracheally with 1×10^6 CFU of PAK at 14 dpi and samples were collected 48 h later. A) Bacterial burden in whole lung homogenate was observed in burn mice compared with sham mice. B) DHR MFI of gated pulmonary neutrophils or macrophages from both stimulated and unstimulated samples was measured by flow cytometry. Unstimulated values are shown, as well as the stimulation index (DHR MFI stimulated / DHR MFI unstimulated) C) MFI of PE-labeled TLR4 on gated neutrophils and TLR2 on gated macrophages was determined by flow cytometry in samples from lung. Data shown are +/-SEM. Data were analyzed by Two-way ANOVA with Bonferroni post-test or Student's t-test and significance indicated as *$p<0.05$, **$p<0.01$.

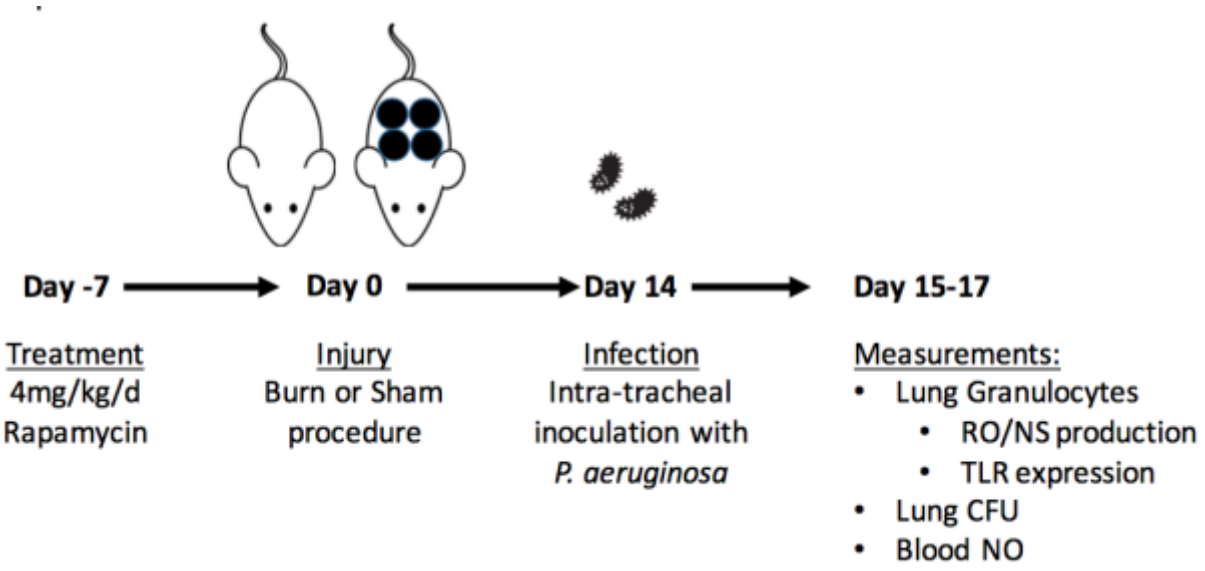

Figure 3.4: Experimental design for rapamycin administration, burn injury, infection, and analysis. Rapamycin was administered via intraperitoneal injection (4mg/kg/d) starting 1 week prior to burn or sham procedure. Mice were infected with *P. aeruginosa* via intratracheal inoculation 2 weeks following injury, and tissues were harvested for analysis between 24 and 72h later.

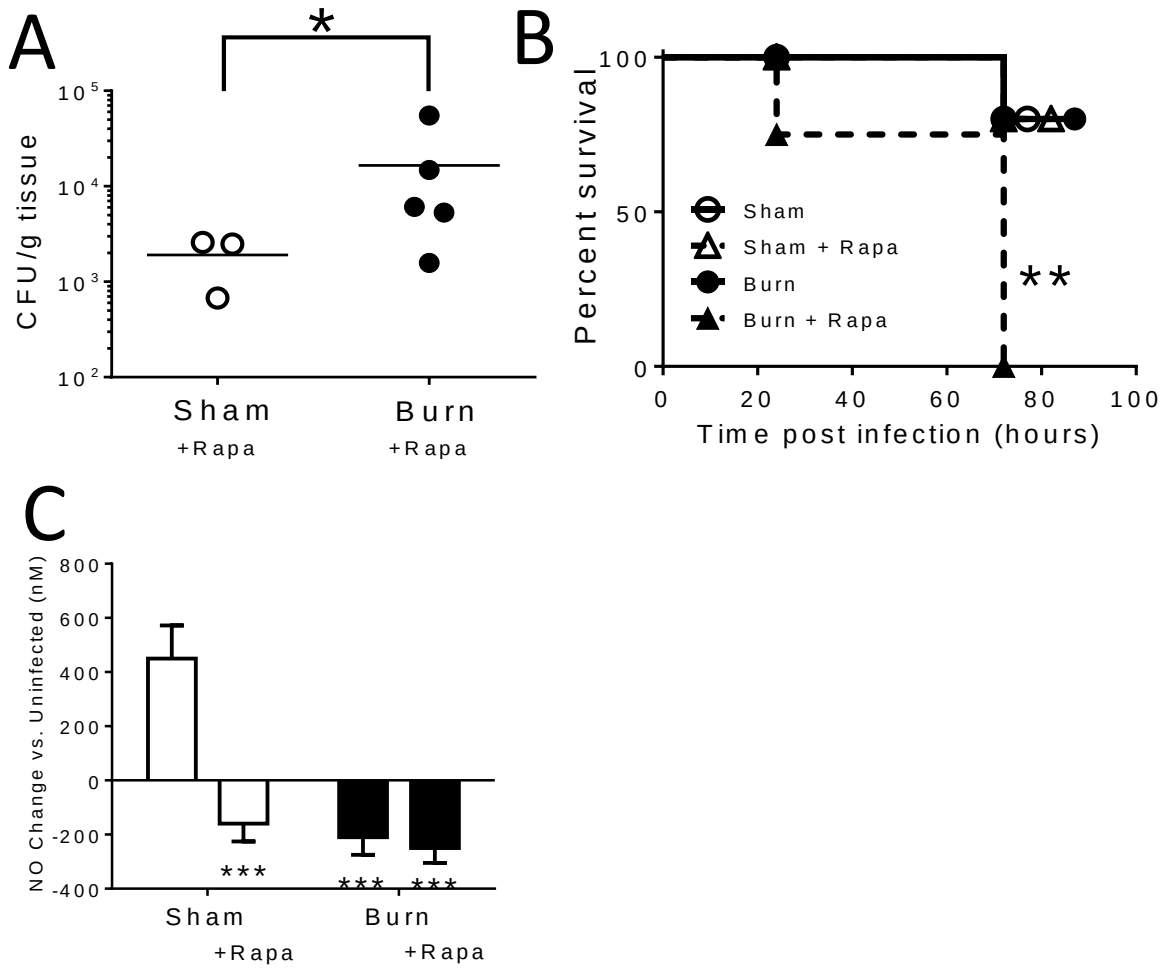

Figure 3.5: mTOR activity is required for survival and efficient bacterial clearance in burned mice following infection. Mice underwent an intra-tracheal inoculation with PAK at 14 dpi. A) 48 hours following infection with 1×10^6 CFU of PAK, bacterial burden was determined in whole lung homogenate. B) Following infection with 5×10^6 CFU of PAK, mice were monitored for morbidity for 72h, and moribund or deceased animals were recorded. C) Blood from the submandibular vein was collected and NO levels were directly measured. Data were analyzed by Student's T-test or two-way ANOVA with Bonferroni post-test and are represented as mean +/-SEM. *p<0.05, **p<0.01, *** p < 0.001.

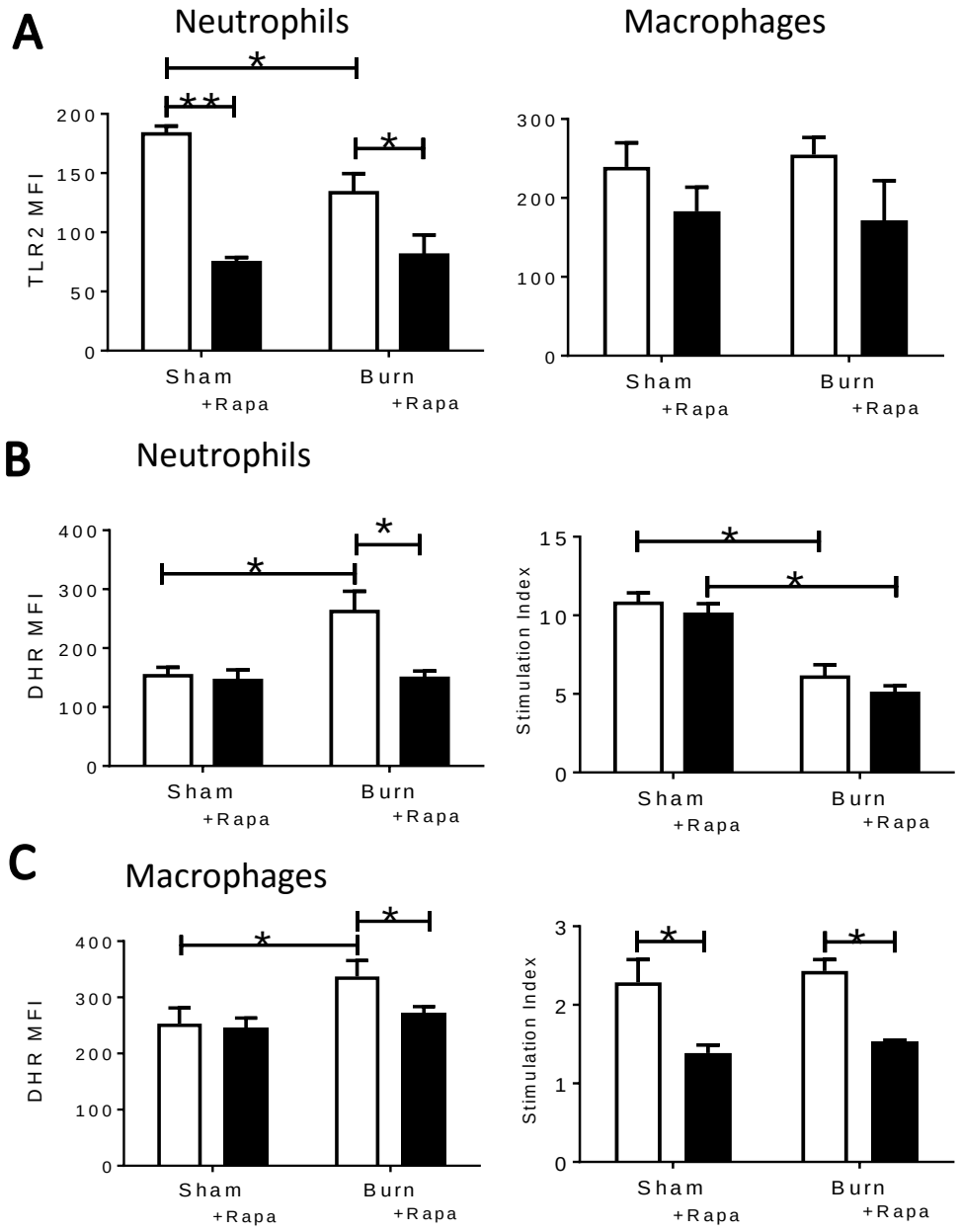

Figure 3.6: mTOR inhibition impacts innate immune function following burn injury and infection. Mice underwent an intra-tracheal inoculation with 1×10^6 CFU PAK at 14 dpi., with or without Rapamycin treatment. A) MFI of PE-labeled TLR2 on neutrophils and macrophages from whole lung cell suspensions was determined by flow cytometry. B-C), DHR MFI of gated pulmonary B) neutrophils and C) macrophages from both stimulated and unstimulated samples was measured by flow cytometry. Unstimulated values are shown, as well as the stimulation index (DHR MFI stimulated / DHR MFI unstimulated). Data were analyzed by two-way ANOVA with Bonferroni post-test and are represented as mean +/-SEM. *$p<0.05$, **$p<0.01$.

REFERENCES

1. Finnerty CC, Jeschke MG, Herndon DN, Gamelli R, Gibran N, Klein M, Silver G, Arnoldo B, Remick D, Tompkins RG, Investigators of the I, the Host Response Glue G. Temporal cytokine profiles in severely burned patients: a comparison of adults and children. Molecular medicine. 2008;14(9-10):553-60. doi: 10.2119/2007-00132.Finnerty. PubMed PMID: 18548133; PMCID: 2424320.

2. Jeschke MG, Gauglitz GG, Kulp GA, Finnerty CC, Williams FN, Kraft R, Suman OE, Mlcak RP, Herndon DN. Long-term persistance of the pathophysiologic response to severe burn injury. PLoS One. 2011;6(7):e21245. doi: 10.1371/journal.pone.0021245. PubMed PMID: 21789167; PMCID: PMC3138751.

3. Jones SW, Zhou H, Ortiz-Pujols SM, Maile R, Herbst M, Joyner BL, Jr., Zhang H, Kesic M, Jaspers I, Short KA, Meyer AA, Peden DB, Cairns BA, Noah TL. Bronchoscopy-derived correlates of lung injury following inhalational injuries: a prospective observational study. PLoS One. 2013;8(5):e64250. doi: 10.1371/journal.pone.0064250. PubMed PMID: 23691180; PMCID: PMC3656836.

4. Maile R, Jones S, Pan Y, Zhou H, Jaspers I, Peden DB, Cairns BA, Noah TL. Association between early airway damage-associated molecular patterns and subsequent bacterial infection in patients with inhalational and burn injury. Am J Physiol Lung Cell Mol Physiol. 2015;308(9):L855-60. doi: 10.1152/ajplung.00321.2014. PubMed PMID: 25770180; PMCID: PMC4421787.

5. Mendoza AE, Maile LA, Cairns BA, Maile R. Burn injury induces high levels of phosphorylated insulin-like growth factor binding protein-1. International journal of burns and trauma. 2013;3(4):180-9. PubMed PMID: 24273693; PMCID: 3828739.

6. Xiao W, Mindrinos MN, Seok J, Cuschieri J, Cuenca AG, Gao H, Hayden DL, Hennessy L, Moore EE, Minei JP, Bankey PE, Johnson JL, Sperry J, Nathens AB, Billiar TR, West MA, Brownstein BH, Mason PH, Baker HV, Finnerty CC, Jeschke MG, Lopez MC, Klein MB, Gamelli RL, Gibran NS, Arnoldo B, Xu W, Zhang Y, Calvano SE, McDonald-Smith GP, Schoenfeld DA, Storey JD, Cobb JP, Warren HS, Moldawer LL, Herndon DN, Lowry SF, Maier RV, Davis RW, Tompkins RG, Inflammation, Host Response to Injury Large-Scale Collaborative Research P. A genomic storm in critically injured humans. The Journal of experimental medicine. 2011;208(13):2581-90. doi: 10.1084/jem.20111354. PubMed PMID: 22110166; PMCID: 3244029.

7. Abdullahi A, Amini-Nik S, Jeschke MG. Animal models in burn research. Cellular and molecular life sciences : CMLS. 2014;71(17):3241-55. doi: 10.1007/s00018-014-1612-5. PubMed PMID: 24714880; PMCID: 4134422.

8. Cairns BA, Barnes CM, Mlot S, Meyer AA, Maile R. Toll-like Receptor 2 and 4 Ligation Results in Complex Altered Cytokine Profiles Early and Late After Burn Injury. Journal of Trauma and Acute Care Surgery. 2008;64(4):1069-78.

9. Gauglitz GG, Song J, Herndon DN, Finnerty CC, Boehning D, Barral JM, Jeschke MG. Characterization of the inflammatory response during acute and post-acute phases after severe

burn. Shock. 2008;30(5):503-7. doi: 10.1097/SHK.0b013e31816e3373. PubMed PMID: 18391855.

10. Neely CJ, Kartchner LB, Mendoza AE, Linz BM, Frelinger JA, Wolfgang MC, Maile R, Cairns BA. Flagellin treatment prevents increased susceptibility to systemic bacterial infection after injury by inhibiting anti-inflammatory IL-10+ IL-12- neutrophil polarization. PLoS One. 2014;9(1):e85623. doi: 10.1371/journal.pone.0085623. PubMed PMID: 24454904; PMCID: PMC3893295.

11. Williams FN, Jeschke MG, Chinkes DL, Suman OE, Branski LK, Herndon DN. Modulation of the hypermetabolic response to trauma: temperature, nutrition, and drugs. J Am Coll Surg. 2009;208(4):489-502. doi: 10.1016/j.jamcollsurg.2009.01.022. PubMed PMID: 19476781; PMCID: 3775552.

12. Mecott GA, Al-Mousawi AM, Gauglitz GG, Herndon DN, Jeschke MG. The role of hyperglycemia in burned patients: evidence-based studies. Shock. 2010;33(1):5-13. doi: 10.1097/SHK.0b013e3181af0494. PubMed PMID: 19503020; PMCID: 3878072.

13. Sugita H, Kaneki M, Sugita M, Yasukawa T, Yasuhara S, Martyn JA. Burn injury impairs insulin-stimulated Akt/PKB activation in skeletal muscle. American journal of physiology Endocrinology and metabolism. 2005;288(3):E585-91. doi: 10.1152/ajpendo.00321.2004. PubMed PMID: 15536206.

14. Carter EA, Paul KW, Barrow SA, Fischman AJ, Tompkins RG. Previous burn injury predisposes mice to lipopolysaccharide-induced changes in glucose metabolism. Journal of burn care & research : official publication of the American Burn Association. 2012;33(5):683-9. doi: 10.1097/BCR.0b013e31825d6a86. PubMed PMID: 22961012; PMCID: 3441057.

15. Xu H, Yu YM, Ma H, Carter EA, Fagan S, Tompkins RG, Fischman AJ. Glucose metabolism during the early "flow phase" after burn injury. The Journal of surgical research. 2013;179(1):e83-90. doi: 10.1016/j.jss.2012.02.037. PubMed PMID: 22459295; PMCID: 4074901.

16. Keating R, McGargill MA. mTOR Regulation of Lymphoid Cells in Immunity to Pathogens. Front Immunol. 2016;7:180. doi: 10.3389/fimmu.2016.00180. PubMed PMID: 27242787; PMCID: PMC4862984.

17. Tsalikis J, Croitoru DO, Philpott DJ, Girardin SE. Nutrient sensing and metabolic stress pathways in innate immunity. Cell Microbiol. 2013;15(10):1632-41. doi: 10.1111/cmi.12165. PubMed PMID: 23834352.

18. Ghanim H, Mohanty P, Deopurkar R, Sia CL, Korzeniewski K, Abuaysheh S, Chaudhuri A, Dandona P. Acute modulation of toll-like receptors by insulin. Diabetes care. 2008;31(9):1827-31. doi: 10.2337/dc08-0561. PubMed PMID: 18556339; PMCID: 2518353.

19. Devaraj S, Venugopal SK, Singh U, Jialal I. Hyperglycemia induces monocytic release of interleukin-6 via induction of protein kinase c-{alpha} and -{beta}. Diabetes. 2005;54(1):85-91. PubMed PMID: 15616014.

20. Devaraj S, Jialal I. Increased secretion of IP-10 from monocytes under hyperglycemia is via the TLR2 and TLR4 pathway. Cytokine. 2009;47(1):6-10. doi: 10.1016/j.cyto.2009.02.004. PubMed PMID: 19447045; PMCID: 2771557.

21. Shanmugam N, Reddy MA, Guha M, Natarajan R. High glucose-induced expression of proinflammatory cytokine and chemokine genes in monocytic cells. Diabetes. 2003;52(5):1256-64. PubMed PMID: 12716761.

22. Shanmugam N, Gaw Gonzalo IT, Natarajan R. Molecular mechanisms of high glucose-induced cyclooxygenase-2 expression in monocytes. Diabetes. 2004;53(3):795-802. PubMed PMID: 14988266.

23. Hay N, Sonenberg N. Upstream and downstream of mTOR. Genes Dev. 2004;18(16):1926-45. doi: 10.1101/gad.1212704. PubMed PMID: 15314020.

24. Weichhart T, Hengstschlager M, Linke M. Regulation of innate immune cell function by mTOR. Nat Rev Immunol. 2015;15(10):599-614. doi: 10.1038/nri3901. PubMed PMID: 26403194.

25. Dunn JL, Hunter RA, Gast K, Maile R, Cairns BA, Schoenfisch MH. Direct detection of blood nitric oxide reveals a burn-dependent decrease of nitric oxide in response to Pseudomonas aeruginosa infection. Burns. 2016;42(7):1522-7. doi: 10.1016/j.burns.2016.05.005. PubMed PMID: 27268107; PMCID: PMC5056119.

26. Dunn JL, Hunter RA, Gast K, Maile R, Cairns BA, Schoenfisch MH. Direct detection of blood nitric oxide reveals a burn-dependent decrease of nitric oxide in response to Pseudomonas aeruginosa infection. Burns. 2016. doi: 10.1016/j.burns.2016.05.005. PubMed PMID: 27268107.

27. Crow JP. Dichlorodihydrofluorescein and dihydrorhodamine 123 are sensitive indicators of peroxynitrite in vitro: implications for intracellular measurement of reactive nitrogen and oxygen species. Nitric Oxide. 1997;1(2):145-57. doi: 10.1006/niox.1996.0113. PubMed PMID: 9701053.

28. Sabroe I, Dower SK, Whyte MK. The role of Toll-like receptors in the regulation of neutrophil migration, activation, and apoptosis. Clinical infectious diseases : an official publication of the Infectious Diseases Society of America. 2005;41 Suppl 7:S421-6. doi: 10.1086/431992. PubMed PMID: 16237641.

29. Xin-Long C, Zhao-Fan X, Dao-Feng B, Wei D. mTOR partly mediates insulin resistance by phosphorylation of insulin receptor substrate-1 on serine(307) residues after burn. Burns. 2011;37(1):86-93. doi: 10.1016/j.burns.2010.04.005. PubMed PMID: 20594757.

30. Fejfarova V, Jirkovska A, Lupinkova J, Kovar J, Kalanin J, Striz I, Skibova J, Boucek P, Pelikanova . Effect of acute hyperglycemia and/or hyperinsulinemia on polymorphonuclear functions in healthy subjects. Metabolism. 2006;55(6):811-8. doi: 10.1016/j.metabol.2006.02.007. PubMed PMID: 16713442.

31. Stegenga ME, van der Crabben SN, Dessing MC, Pater JM, van den Pangaart PS, de Vos AF, Tanck MW, Roos D, Sauerwein HP, van der Poll T. Effect of acute hyperglycaemia and/or hyperinsulinaemia on proinflammatory gene expression, cytokine production and neutrophil function in humans. Diabet Med. 2008;25(2):157-64. doi: 10.1111/j.1464-5491.2007.02348.x. PubMed PMID: 18290856; PMCID: PMC2268957.

32. Hand WL, Hand DL, Vasquez Y. Increased polymorphonuclear leukocyte respiratory burst function in type 2 diabetes. Diabetes Res Clin Pract. 2007;76(1):44-50. doi: 10.1016/j.diabres.2006.07.015. PubMed PMID: 16959366.

CHAPTER 4: DAMPS IN CIRCULATION FOLLOWING TRAUMA PROMOTE INFLAMMATION IN THE LUNG

Summary

Acute lung injury (ALI) in patients who have experienced severe trauma with no direct lung insult is thought to be caused by release of damage associated molecular patterns (DAMPs) from injured tissue into circulation. Existing murine models of ALI rely on either a pathogenic signal or direct injury to the lung and have therefore failed to accurately model patients developing ALI after burns without smoke inhalation. To test the hypothesis that DAMP release precipitates ALI and optimize a murine model of ALI that is driven by systemic DAMPs, we intravenously administered components of the extracellular matrix or mitochondrial fragments and quantified accumulation of protein and live cells in the airway. A 20% total body surface area burn injury, alone, did not cause significant airway inflammation, nor did administration of DAMPs to unburned mice. When administered following a burn injury, however, mitochondrial homogenate (MTD) and hyaluronic acid (HA) led to increased cells and protein in the BALF. Purified mitochondrial DNA, alone, did not amplify inflammation in burned mice, however it increased cellular recruitment to the airway when co-administered with HA. Collectively, these results indicate that sufficient damage patterns in circulation can not only promote neutrophil accumulation in the pulmonary microvasculature but can ultimately lead to extravasation of neutrophils into the lung. Future studies using this model will determine the molecular mechanisms that sense DAMPs and the downstream effects of this detection on cytokine and chemokine production and leukocyte function.

Introduction

Traumatic injury results in destruction of cells and tissue and the release of molecular signals that are recognized as signals of damage and are therefore known as damage-associated molecular patterns (DAMPs). For example, genetic material is normally sequestered inside cells, however lytic cell death and some forms of programmed cell death cause DNA to be released from the cell –the presence of extracellular DNA is therefore a signal of tissue stress or damage, acting on Toll-like receptor 9 to trigger activation of MyD88 and induction of IL-6 and IL-10 (1, 2). In addition to intracellular molecules that can act as DAMPs, extracellular molecules can be modified to signal tissue damage. Hyaluronic Acid (HA) is the main component of the extra-cellular matrix and exists in a high molecular weight (HMW) form under physiological circumstances. HA is subject to degradation by proteases, reactive oxygen species, and mechanical stress resulting in medium molecular weight (MMW) fragments (3-5). MMW HA is recognized by Toll-like receptor 4 (TLR4) and has a potent effect on granulocyte function, especially phagocytosis, at a wide range of concentrations in both blood and tissue (5, 6). Changes in leukocyte function, including adhesion, extravasation, and activation, that occur in response to DAMP signaling may account for systematic damage following localized injuries.

Several studies have identified DAMPs in patient biofluids after severe injuries. Hyaluronic acid (HA) is elevated in trauma patient serum within the first three days of the injury, returning to normal levels at the end of two weeks (7). Both HA and dsDNA are elevated in BALF of patients with inhalational injury, especially those who have, or who go on to develop, bacterial pneumonia (8). It is unknown whether dsDNA in this study was derived from mtDNA released by stressed cells or nuclear DNA released by necrotic cells. Mitochondrial DAMPs were observed in serum following large bone fractures and mtDNA concentrations in serum after trauma have been correlated with adverse patient outcomes (9, 10). Collectively, these studies indicate that DAMP concentration is positively correlated with injury severity.

Patients who experience severe trauma without direct insult to the lungs are at significant risk of developing ALI, marked by impaired oxygen exchange and the presence of pulmonary infiltrates (11, 12). Injuries such as these may include severe burns affecting greater than 30% of the total body surface area (TBSA) or compounded injuries (i.e. burn + bone fractures or blunt force trauma) (13, 14). Attempts to generate murine models of ALI in injuries such as these, which result from systemic damage, have struggled because of the technical challenge of ethically conducting mouse burns greater than 20% TBSA, since these injuries require extensive pain control and supportive care. Although a 20% TBSA burn in mice leads to accumulation of neutrophils in pulmonary microvasculature, it does not lead to perturbation of the alveolar/capillary barrier (15). A murine model would enable deeper understanding of the cellular and molecular determinants of disease and represent a powerful tool for developing therapeutic interventions.

Recently it was shown that systemic administration of mitochondrial DAMPs (MTD) consisting of homogenized mitochondria resulted in ALI in a mouse model (9). In the same report, MTD were shown to stimulate neutrophil degranulation, cytokine production, and migration in vitro (9). Because MTD contains dsDNA in the form of mtDNA, we sought to determine whether MTD or mtDNA could act as DAMPs in our model (Figure 4.1). We also investigated the ability of MMW HA to induce an inflammatory response, alone and in combination with mtDNA (Figure 4.1). Our results indicate that neither DAMP administration nor burn injury, alone, are sufficient to disrupt the alveolar/capillary barrier; however, combined insults significantly increased protein concentration and live cell numbers in BALF. These data confirm the feasibility of modeling ALI in mice without a direct lung insult or microbial signal.

Methods

Mouse housing and burn injury. Female C57/B6 mice purchased from Taconic farms were housed in a specific pathogen-free facility. Burn and sham procedure were carried out as previously described (16). Briefly, mice were anesthetized with gaseous isofluorane and their dorsums were shaved

prior to subcutaneous administration of morphine. A copper rod heated in a boiling water bath was used to administer a full-thickness 20% total body surface area contact burn and mice were resuscitated with an intraperitoneal injection of lactated Ringer's solution. Sham mice were not exposed to the copper rod; all mice received morphine in their drinking water ad libitum.

DAMP preparation and administration. Medium molecular weight (MMW) HA was purchased from Fischer Scientific (Cat no: GLR004) and resuspended to 1 mg/mL in PBS. Dilutions were prepared in PBS prior to administration. Intranasal administration was accomplished in 50uL volumes and intravenous doses were 200uL.

Mitochondria were isolated from liver tissue using a Mitochondrial Isolation Kit purchased from Fischer Scientific (Cat no: PI89801) per the manufacturer's instructions. To prepare MTD, mitochondria were suspended in 1mL PBS and sonicated ten times for 30 s. Large debris was removed by centrifugation, and protein content was determined by Bradford assay. Average protein concentration per homogenized liver was calculated in order to calculate a dose equivalent to 5% of the liver (9). mtDNA was isolated from mitochondria using a QIAGEN DNA extraction kit, resuspended in PBS, and quantified using a nanodrop. mtDNA was sonicated at 2 second intervals for a total of 10 seconds, and the efficiency of degradation was confirmed by running samples through an agarose gel. Intravenous dosages were prepared in 200uL volumes.

Sample collection and analysis. Mice were euthanized with gaseous isofluorane and BAL was collected with 3 washes of PBS containing 0.6 mM EDTA. Protein concentration was measured in supernatants from the first wash using a Bradford assay. Cell pellets from all 3 washes were combined and suspended in PBS with 10% FBS. Live cells were counted using a hemacytometer and trypan blue stain.

To enumerate neutrophils, cells were analyzed by flow cytometry. Following incubation with Fc block (eBiosciences), cells were stained with antibodies against CD45, CD11b, CD11c, and Ly6G (BD

Biosciences; San Jose, CA). Samples were analyzed at the UNC Flow Cytometry Core Facility on a CyAn and Summit 5.3 software was used to analyze data (Beckmann-Coulter; Indianapolis, IN). Neutrophils were defined as $CD45^{+}CD11b^{+}CD11c^{-}Ly6G^{+}$.

To quantify IL-6 in serum, blood was collected from the submandibular vein into EDTA-coated tubes prior to euthanasia. Samples were centrifuged and serum was removed and frozen prior to analysis. 1:1 dilutions of serum in PBS were analyzed via IL-6 ELISA (eBiosciences) per the manufacturer's protocol.

Statistical analysis. GraphPad Prism Version 5.0 for Windows was used to analyze data by Student's t-Test, One-Way Analysis of Variance (ANOVA) with Tukey post-test, or Two-Way ANOVA with Bonferroni post-test, as appropriate. Data are represented as mean +/- standard error of the mean (SEM).

Results

Hyaluronic acid. In order to measure the incidence of ALI, live cell count and protein concentration in BALF were measured in mice treated with vehicle or 2 ug MMW HA. Intravenous administration of 2ug MMW HA in sham mice did not lead to a significant increase in either protein accumulation or cellularity in the airway at 12 h (Figure 4.2 A-B). In contrast, administration of 1ug HA in burn mice causes a significant increase in protein concentration in the airway at 12h (Figure 4.2 C). Similarly, we observed an increase in live cell count in BALF 12h after burn and HA treatment (Figure 4.2 D).

To determine whether the route of administration would impact the inflammatory response to HA, intravenous administration was compared with intranasal administration in burn-treated mice. No difference was observed in either protein concentration or neutrophil recruitment to the airway when mice were treated with intranasal HA compared with intravenous HA (Figure 4.2 E-F).

Mitochondrial DAMPs. It has been reported that intravenous administration of MTD causes ALI in a rodent model; we therefore sought to confirm this finding and to determine whether it is amplified by concomitant burn injury (9). In sham-treated mice, intravenous MTD administration caused an accumulation of live cells in the airway that did not achieve statistical significance (Figure 4.3 A). Burn and MTD treatment led to significantly more live cells in the BALF with the majority of those cells identified as neutrophils at 48h (Figure 4.3 A-B). Increased cellularity in burn and MTD treated mice was sustained from 24-48h and was accompanied by an increase in protein concentration that did not achieve statistical significance (Figure 4.3 C-D). We observed an acute (3-24h) increase in serum IL-6 in burn and MTD treated mice compared to shams (Figure 4.3 F).

Several DAMPs may be present in mitochondrial lysate, including mtDNA, cytochrome C, and N-formylmethioline, therefore we set out to characterize the role of a specific DAMP in the inflammatory response. Previous studies have reported a link between concentrations of mtDNA in serum and outcomes in trauma patients (10). Because mtDNA is a part of the mitochondrial lysate that makes up MTD, we designed experiments to determine whether purified mtDNA rather than bulk mitochondrial homogenate could cause ALI. Administration of 750 ng mtDNA after burn injury caused an increase in neutrophils but not protein in the airway at 48h (Figure 4.4 A-B). Because mtDNA exists in a supercoiled form, mtDNA was sonicated to produce smaller fragments. Sonicated mtDNA did not increase protein leakage but induced slightly more live cell recruitment to the airway compared with unsonicated mtDNA (Figure 4.4 C-D).

Combined administration of mtDNA and HA. To determine whether there might be a synergistic effect of HA and mtDNA on development of ALI following injury, sonicated mtDNA and HA (MDH) were co-administered to burned mice. To titrate the appropriate amount of mtDNA to administer with HA, 150 ng/mL, 400 ng/mL, and 1000 ng/mL of mtDNA were administered along with HA in burned mice and results were compared with vehicle control in uninjured mice. Both medium and high dosages of mtDNA caused statistically significant increases in cellularity (Figure 4.5).

Discussion

Severe traumatic injury has been shown to induce acute lung injury (ALI), even in the absence of a direct insult to the lung. Injuries such as this include severe scalds, contact burns, or electrical burns where there was no smoke present at the time of injury. Pulmonary inflammation elevates patients' risk of contracting and succumbing to pulmonary infection. To improve outcomes for such patients will require improved understanding of the molecular and cellular mechanisms that drive ALI in the absence of a direct pulmonary insult or pathogen challenge. Existing studies have identified biomarkers of pathogenesis in animal models and human studies.

It is known that complement activation in the serum following thermal injury leads to changes in the vascular epithelium and consequently enhanced interactions with platelets and leukocytes (15). TLR4 ligation and signaling have also been shown to determine the onset and outcome of ALI (17, 18). These and other findings have failed to translate to the clinic because it has not been shown that they can be targeted without rendering patients severely immunocompromised.

A systematic analysis of ALI following severe trauma has been impeded by the lack of an effective mouse model that recapitulates pulmonary inflammation without either a direct pulmonary insult or systemic shock with sepsis or administration of endotoxin. Importantly, ALI without direct lung injury is seldom observed in patients who present with less than 30% TBSA, and it is impossible to study burns greater than 20% TBSA in mice because of the technical difficulty of creating a murine intensive care unit, which would be required to ethically care for mice subjected to a more extensive injury (13, 14). We hypothesized that ALI following large burn injuries results from release of a high concentration of damage associated molecular patterns (DAMPs) from injured tissue into circulation. We endeavored to test this hypothesis by administering DAMPs into circulation, alone or in concert with a thermal injury, in order to delineate the role of specific DAMPs on induction of pulmonary inflammation following trauma.

Although several studies have identified elevated DAMPs in patients and animals who develop ALI subsequent to trauma (8, 19), to our knowledge only one prior study has specifically tested whether intravenous DAMP administration could induce ALI (9). Mitochondrial homogenate (MTD) administration led to rapid increases in protein, IL-6, and live cells in BALF. Here we present data that indicates that combining burn injury and MTD administration amplifies accumulation of protein and neutrophils in the airway. Unlike burn injury alone, which leads to accumulation of neutrophils in the pulmonary microvasculature and interstitial space but not the airway, MTD administration promotes neutrophil extravasation. Although enriched mtDNA was not sufficient to reproduce the inflammatory phenotype observed with MTD, mtDNA in combination with HA led to similar increase in live cells in BALF samples. We propose that co-administration of sonicated mtDNA and HA (MDH) is preferable to MTD as a model for ALI because the relevant molecular signals are more clearly defined than in whole mitochondrial lysate.

The burn with MDH model presents an opportunity to address several important questions about the pathogenesis of ALI. To more fully characterize the immune state of the injury, it will be important to examine chemokine and cytokine expression in the lung to determine signals that draw neutrophils into the airway. Moreover, because HA and mtDNA are recognized by pattern recognition receptor (PRR) signaling, it will be important to evaluate the role of PRR ligation and signaling on leukocyte migration and cytokine production in this model. Finally, a chief characteristic of ALI in trauma patients is that it renders them susceptible to pulmonary infection. It will therefore be important in future studies to determine whether mice treated with burn and MDH are susceptible to infection in both acute and chronic phases after injury.

The results of this research point to an important question about the role of DNA DAMPs in human ALI. Although one report showed a positive correlation between serum mtDNA and injury severity, the authors did not examine the abundance of genomic DNA (10). Our studies have used fluorometric readouts to quantify double stranded DNA in patient serum that would not differentiate

between mtDNA and nuclear DNA, therefore it is unknown whether the dsDNA observed in patient serum results from stressed cells releasing mitochondrial contents or lytic cells releasing nuclear contents (8). One potential source of extracellular DNA is the production of neutrophil extracellular traps (NETs) which may contain either genomic DNA, mtDNA, or both (20). Moreover, different cellular signaling events drive the production of NETs enriched in genomic or mitochondrial DNA, therefore interfering with NETosis and, by extension, dsDNA enrichment in serum will benefit from understanding which pathways are at play. Animal models have the potential to clarify causal relationships that can only be guessed at in patient samples and to test methods to manipulate the release and detection of DAMPs after injury to improve clinical outcomes.

FIGURES

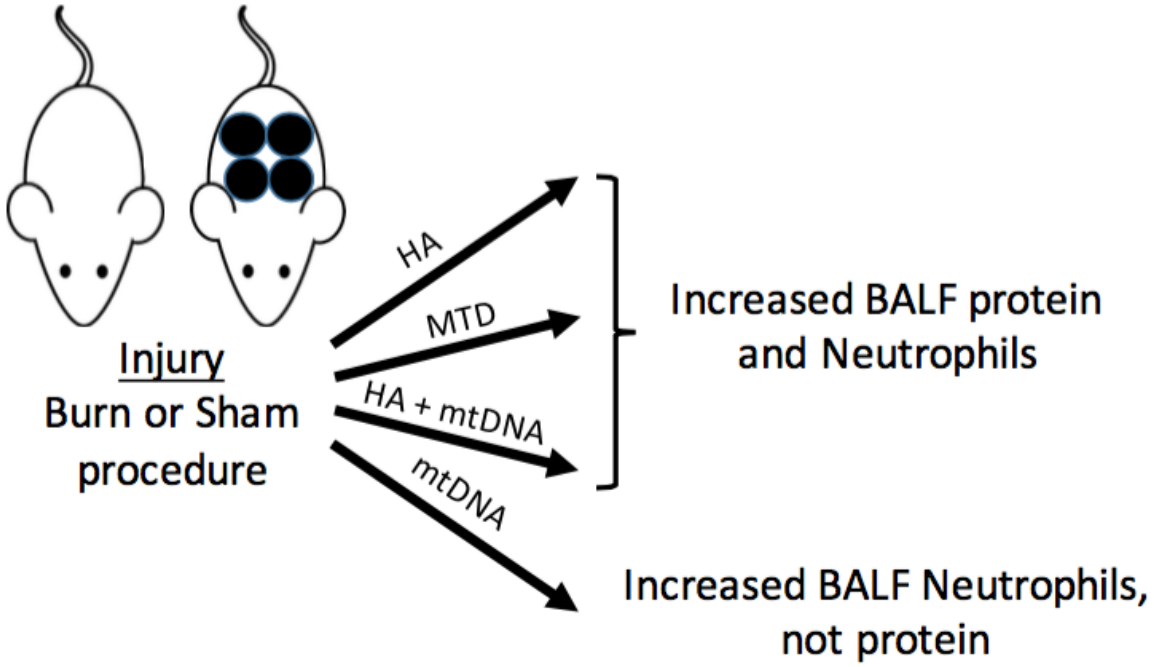

Figure 4.1: Experimental design for intravenous DAMP administration. After burn or sham injury, hyaluronic acid (HA), mitochondrial homogenate (MTD), and mitochondrial DNA (mtDNA) were administered via intravenous injection alone or in combination.

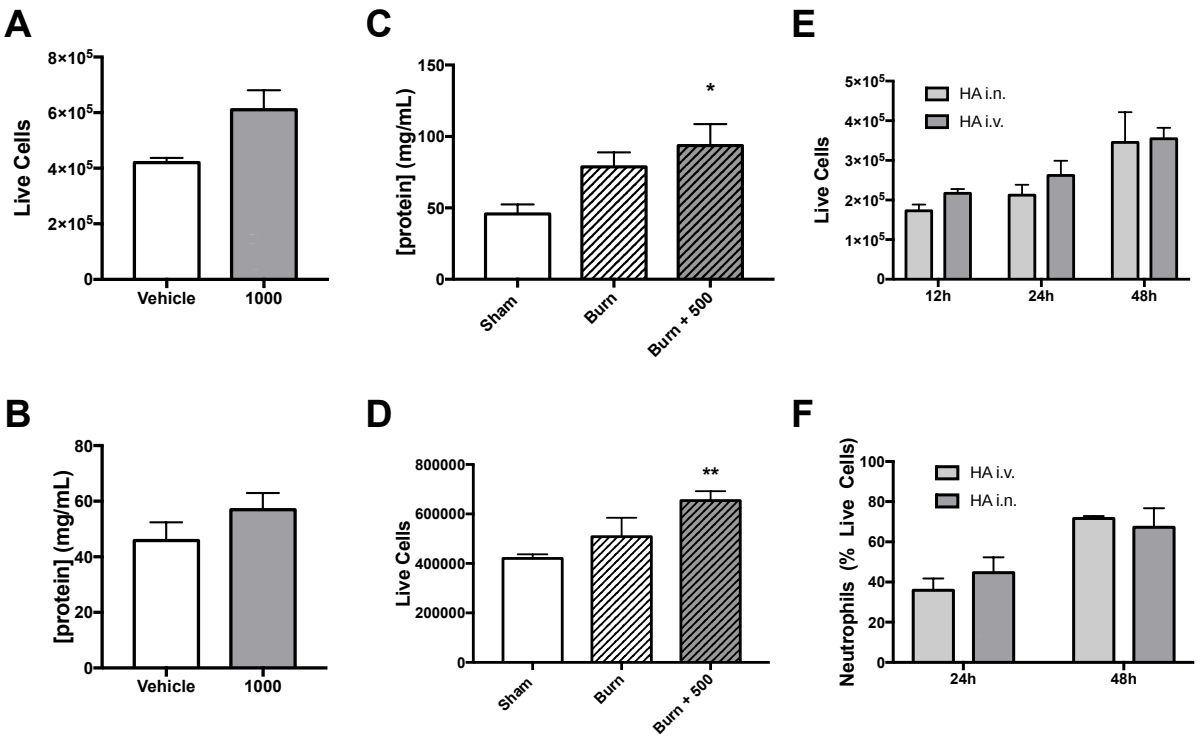

Figure 4.2: Hyaluronic acid administration leads to mild pulmonary inflammation after burn injury regardless of administration route. Live cells (A) and protein concentration (B) in the BALF of mice who received intravenous administration of either PBS or 2 mg HA. Live cells (C) and protein concentration (D) in BALF of uninjured mice treated with PBS (open bars), burned mice treated with PBS (hatched bars), and burned mice treated with 1 mg HA (shaded, hatched bars). (E) Live cells recovered from BALF of mice treated with HA via intravenous or intranasal exposure immediately after burn injury. (F) Live cells recovered from BALF of burned mice treated with either intravenous or intranasal HA were analyzed by flow cytometry. * $p<0.05$.

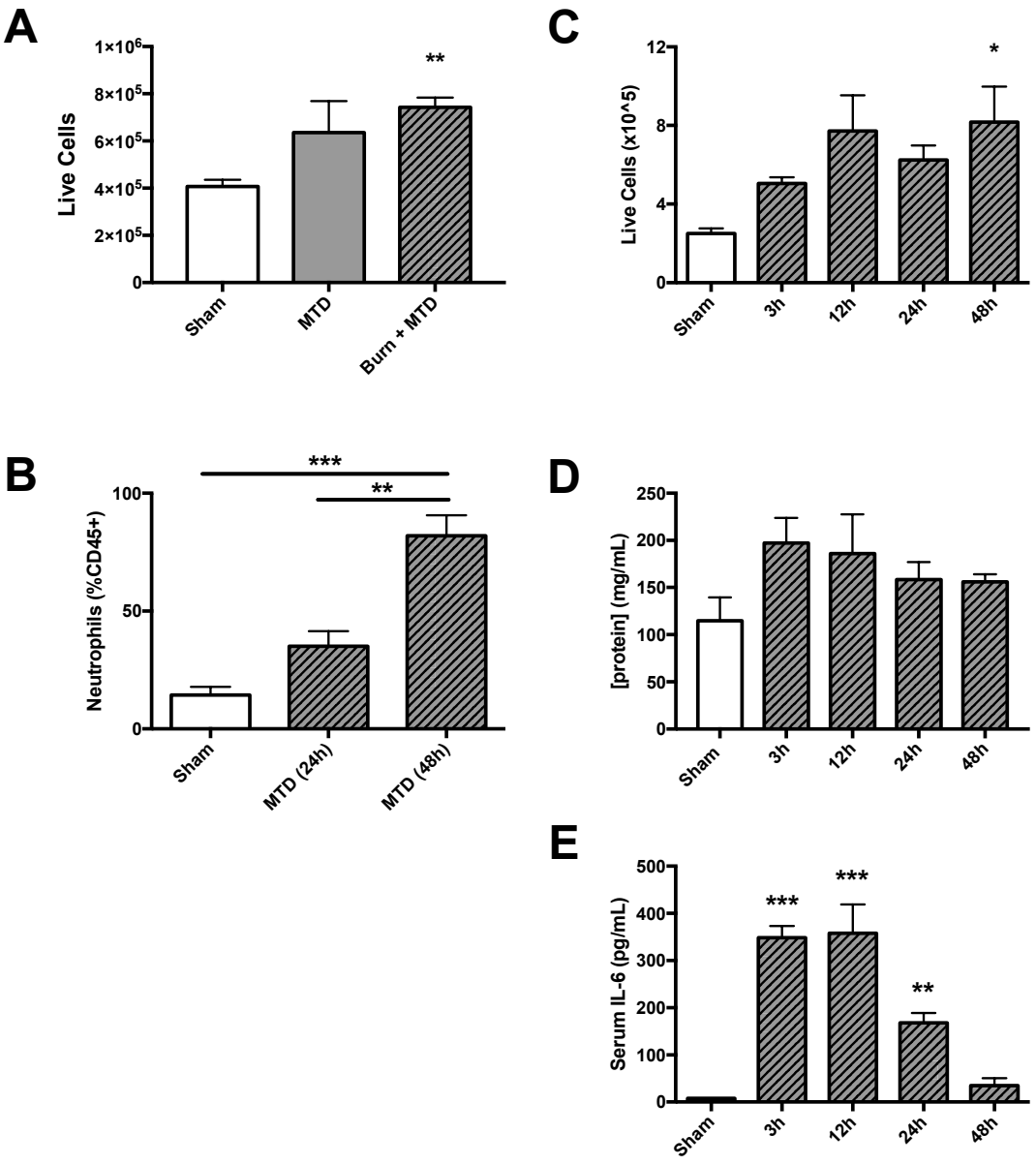

Figure 4.3: MTD administration after burn injury leads to pulmonary inflammation marked by neutrophil recruitment to the airway. (A) Live cells recovered from BALF of sham mice treated with PBS (open bars), sham mice treated with MTD (shaded bars), and burn mice treated with MTD (shaded, hatched bars). (B) Live cells recovered from BAL of sham mice treated with PBS (open bars) or burned mice treated with MTD (shaded, hatched bars) were analyzed by flow cytometry to quantify neutrophil numbers. (C) Protien concentration in BALF, (D) live cells in BALF, and (E) IL-6 in serum of sham mice treated with PBS (open bars) or burn mice treated with MTD (shaded, hatched bars). * $p < 0.05$, ** $p < 0.005$, *** $p < 0.001$.

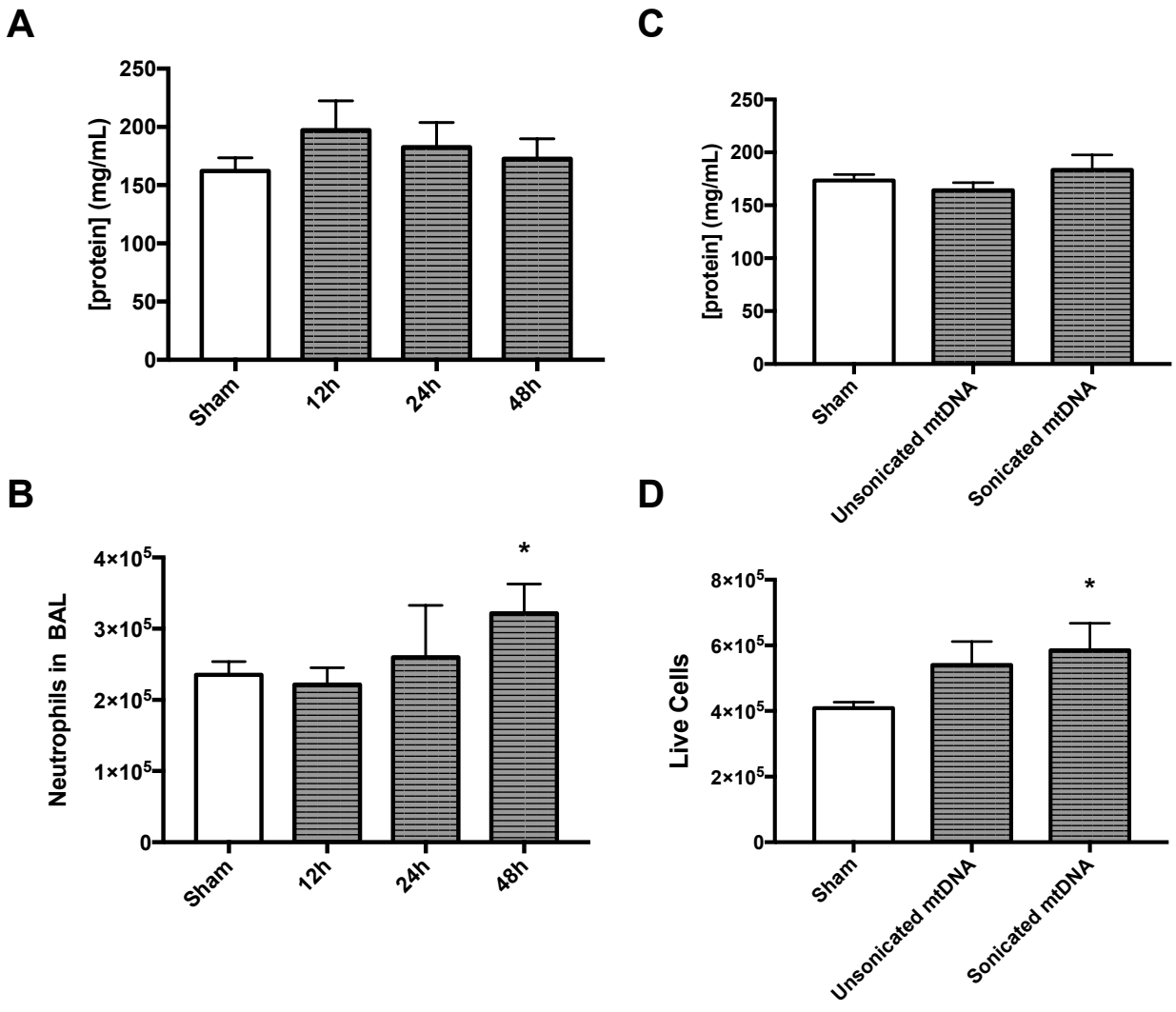

Figure 4.4: mtDNA administration after burn injury does not induce pulmonary inflammation. Protein concetration (A) and gated neutrophils (B) in BALF from sham mice treated with PBS (open bars) and burn mice treated with mtDNA (shaded, hatched bars). (A) Protein concentration and (B) live cells in BALF from sham mice treated with PBS (open bars) and burn mice treated with unsonicated mtDNA and sonicated mtDNA. * $p < 0.05$.

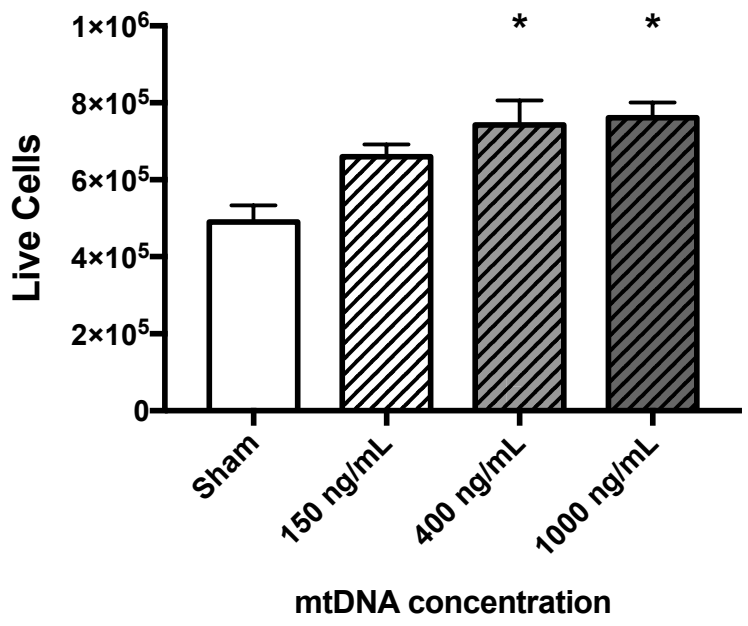

Figure 4.5: Coadministration of HA and mtDNA after burn injury leads to significant increase in cellular recruitment to the lung. Live cells recovered from the BALF of sham mice treated with PBS (open bar), burn mice treated with 500 ug/mL HA and 150 ng/mL sonicated mtDNA (hatched bars), 400 ng/mL sonicated mtDNA (light shaded hatched bars), or 1000 ng/mL sonicated mtDNA (dark shaded hatched bars). * $p<0.05$.

REFERENCES

1. Chen J, Hartono JR, John R, Bennett M, Zhou XJ, Wang Y, Wu Q, Winterberg PD, Nagami GT, Lu CY. Early interleukin 6 production by leukocytes during ischemic acute kidney injury is regulated by TLR4. Kidney Int. 2011;80(5):504-15. doi: 10.1038/ki.2011.140. PubMed PMID: 21633411; PMCID: PMC3394593.

2. Rao H, Zeng Q, Liang Y, Xiao C, Xie S, Xu X. Correlation between TLR9 Expression and Cytokine Secretion in the Clinical Diagnosis of Systemic Lupus Erythematosus. Mediators Inflamm. 2015;2015:710720. doi: 10.1155/2015/710720. PubMed PMID: 26457008; PMCID: PMC4589624.

3. Noble PW. Hyaluronan and its catabolic products in tissue injury and repair. Matrix Biol. 2002;21(1):25-9. PubMed PMID: 11827789.

4. Singleton PA, Lennon FE. Acute Lung Injury Regulation by Hyaluronan. J Allergy Ther. 2011;Suppl 4. doi: 10.4172/2155-6121.S4-003. PubMed PMID: 24244887; PMCID: PMC3828630.

5. Campo GM, Avenoso A, Campo S, D'Ascola A, Traina P, Rugolo CA, Calatroni A. Differential effect of molecular mass hyaluronan on lipopolysaccharide-induced damage in chondrocytes. Innate Immun. 2010;16(1):48-63. doi: 10.1177/1753425909340419. PubMed PMID: 19710088.

6. Hakansson L, Hallgren R, Venge P. Regulation of granulocyte function by hyaluronic acid. In vitro and in vivo effects on phagocytosis, locomotion, and metabolism. J Clin Invest. 1980;66(2):298-305. doi: 10.1172/JCI109857. PubMed PMID: 7400316; PMCID: PMC371711.

7. Onarheim H, Reed RK, Laurent TC. Elevated hyaluronan blood concentrations in severely burned patients. Scand J Clin Lab Invest. 1991;51(8):693-7. PubMed PMID: 1806984.

8. Maile R, Jones S, Pan Y, Zhou H, Jaspers I, Peden DB, Cairns BA, Noah TL. Association between early airway damage-associated molecular patterns and subsequent bacterial infection in patients with inhalational and burn injury. Am J Physiol Lung Cell Mol Physiol. 2015;308(9):L855-60. doi: 10.1152/ajplung.00321.2014. PubMed PMID: 25770180; PMCID: PMC4421787.

9. Zhang Q, Raoof M, Chen Y, Sumi Y, Sursal T, Junger W, Brohi K, Itagaki K, Hauser CJ. Circulating mitochondrial DAMPs cause inflammatory responses to injury. Nature. 2010;464(7285):104-7. doi: 10.1038/nature08780. PubMed PMID: 20203610; PMCID: PMC2843437.

10. Simmons JD, Lee YL, Mulekar S, Kuck JL, Brevard SB, Gonzalez RP, Gillespie MN, Richards WO. Elevated levels of plasma mitochondrial DNA DAMPs are linked to clinical outcome in severely injured human subjects. Ann Surg. 2013;258(4):591-6; discussion 6-8. doi: 10.1097/SLA.0b013e3182a4ea46. PubMed PMID: 23979273; PMCID: PMC3935616.

11. Johnson ER, Matthay MA. Acute lung injury: epidemiology, pathogenesis, and treatment. J Aerosol Med Pulm Drug Deliv. 2010;23(4):243-52. doi: 10.1089/jamp.2009.0775. PubMed PMID: 20073554; PMCID: PMC3133560.

12. Matthay MA, Ware LB, Zimmerman GA. The acute respiratory distress syndrome. J Clin Invest. 2012;122(8):2731-40. doi: 10.1172/JCI60331. PubMed PMID: 22850883; PMCID: PMC3408735.

13. Zheng H, Chen XL, Han ZX, Zhang Z, Wang SY, Xu QL. Ligustrazine attenuates acute lung injury after burn trauma. Burns. 2005;31(4):453-8. doi: 10.1016/j.burns.2004.10.023. PubMed PMID: 15896507.

14. Schmid E, Piccolo MT, Friedl HP, Warner RL, Mulligan MS, Hugli TE, Till GO, Ward PA. Requirement for C5a in lung vascular injury following thermal trauma to rat skin. Shock. 1997;8(2):119-24. PubMed PMID: 9261902.

15. Till GO, Beauchamp C, Menapace D, Tourtellotte W, Jr., Kunkel R, Johnson KJ, Ward PA. Oxygen radical dependent lung damage following thermal injury of rat skin. J Trauma. 1983;23(4):269-77. PubMed PMID: 6842628.

16. Dunn JL, Hunter RA, Gast K, Maile R, Cairns BA, Schoenfisch MH. Direct detection of blood nitric oxide reveals a burn-dependent decrease of nitric oxide in response to Pseudomonas aeruginosa infection. Burns. 2016;42(7):1522-7. doi: 10.1016/j.burns.2016.05.005. PubMed PMID: 27268107; PMCID: PMC5056119.

17. Imai Y, Kuba K, Neely GG, Yaghubian-Malhami R, Perkmann T, van Loo G, Ermolaeva M, Veldhuizen R, Leung YH, Wang H, Liu H, Sun Y, Pasparakis M, Kopf M, Mech C, Bavari S, Peiris JS, Slutsky AS, Akira S, Hultqvist M, Holmdahl R, Nicholls J, Jiang C, Binder CJ, Penninger JM. Identification of oxidative stress and Toll-like receptor 4 signaling as a key pathway of acute lung injury. Cell. 2008;133(2):235-49. doi: 10.1016/j.cell.2008.02.043. PubMed PMID: 18423196.

18. Faure K, Sawa T, Ajayi T, Fujimoto J, Moriyama K, Shime N, Wiener-Kronish JP. TLR4 signaling is essential for survival in acute lung injury induced by virulent Pseudomonas aeruginosa secreting type III secretory toxins. Respir Res. 2004;5:1. doi: 10.1186/1465-9921-5-1. PubMed PMID: 15040820; PMCID: PMC389879.

19. Onarheim H, Missavage AE, Gunther RA, Kramer GC, Reed RK, Laurent TC. Marked increase of plasma hyaluronan after major thermal injury and infusion therapy. J Surg Res. 1991;50(3):259-65. PubMed PMID: 1999915.

20. Lood C, Blanco LP, Purmalek MM, Carmona-Rivera C, De Ravin SS, Smith CK, Malech HL, Ledbetter JA, Elkon KB, Kaplan MJ. Neutrophil extracellular traps enriched in oxidized mitochondrial DNA are interferogenic and contribute to lupus-like disease. Nat Med. 2016;22(2):146-53. doi: 10.1038/nm.4027. PubMed PMID: 26779811; PMCID: PMC4742415.

CHAPTER 5: CXCL1 DRIVES NEUTROPHIL RECRUITMENT AND ONSET OF ALI FOLLOWING ACUTE WOOD SMOKE INHALATION[1]

Summary

Inhalational injury associated with structural fires, wildfires, or explosions leads to acute lung injury (ALI) and acute respiratory distress syndrome, for which innovative and faithful animal models are needed to develop effective therapeutics. We have previously reported that damage associated molecular patterns (DAMPs) and anti-inflammatory cytokines are correlated with infectious complications in patients diagnosed with inhalational injury. In this report we describe a novel murine model of acute inhalational injury that precipitates ALI characterized by an accumulation of protein and neutrophils in the airway as well as histological evidence of tissue damage. This model recapitulates clinically relevant phenotypes including susceptibility to opportunistic infection with *Pseudomonas aeruginosa*, abundance of the DAMPs hyaluronic acid and dsDNA, and polarization towards IL-10 early after injury. Using iNOS-/- mice, we found that iNOS is required for increases in IL-10, MCP1, and HA following injury but not for protein accumulation, CXCL1 expression and neutrophilia, dsDNA, or infection susceptibility. In agreement with previous studies that established the importance of CXCR2 signaling in inflammation following ventilator-induced lung injury, we demonstrated that inhibition of CXCL1 attenuated neutrophil recruitment, decreased histopathology scores, and improved bacterial clearance in our model of smoke inhalation. Together these data highlight the importance of differentiating between physiological and pathological inflammation after acute smoke exposure and suggest that future studies in patients

[1] Attribution: Julia Dunn designed and carried out experiments, analyzed data, created figures, and wrote manuscript. Laurel Kartchner designed and carried out experiments. Wesley Stepp, Lindsey Glenn and Madison Malfitano carried out experiments and analyzed data.

should explore the potential therapeutic benefit of attenuating neutrophil recruitment in the first 24h after injury.

Introduction

Acute smoke inhalation presents a clinical challenge. Acute smoke inhalation resulting from structural fires or, increasingly across the western United States, proximity to wildfires, results in severe and complex damage to the lung. Inhalational injuries are associated with lengthy and expensive hospitalizations, especially when they occur concomitantly with cutaneous burn injury (1). Smoke inhalation is often accompanied by cutaneous burns, lacerations, or fractures; in such cases inhalational injury is treated last, as it is dwarfed by the immediacy of other traumatic injuries (2).

The physiological imbalances that result from acute smoke inhalation are not completely understood, in large part because a systematic analysis of patient outcomes is complicated by several variables that are difficult to control for during outcome analysis. This patient population spans all ages, ethnicities, and comorbidities. Moreover, the severity of inhalational injury depends on the smoke source, which varies from structure to structure, as well as concentration and duration of exposure. Because synthetic materials often burn faster and release more toxics than wood, the types of lung injuries treated at trauma centers changes as common construction materials change (2). Different strategies have been proposed to diagnose the severity of inhalational injury, ranging from quantification of serum factors to measurements of lung function (3-5). Mosier et al emphasize the importance of bronchoscopic analysis (visual assessment of the airway) for predicting outcomes; however, these strategies also have significant drawbacks and do not uniformly predict outcomes (3).

A leading cause of mortality following inhalational injury is bacterial pneumonia, which is thought to be the result of poor mucociliary clearance combined with impaired immunological surveillance(6). Some studies have examined patient bronchoaveolar lavage fluid (BALF) in order to characterize the inflammatory state, identify patients at risk for developing pneumonia, and initiate antibacterial prophylaxis in high-risk patients. Two damage-associated molecular patterns (DAMPs),

dsDNA and hyaluronic acid (HA), are elevated in patients with inhalational injury, especially those who subsequently develop bacterial pneumonia (7). Our group has previously shown that IL-10 was elevated in patients who develop pulmonary or peripheral bacterial infections and others have observed elevated IL-10 in patients who do not survive inhalational injury (5, 8). The prevailing opinion is that trauma leads to release of DAMPs that promote an anti-inflammatory phenotype in the lung and contribute to patients' inability to fight opportunistic bacterial infections; however, we have not observed a direct correlation between DAMP levels and IL-10 levels in patients. We therefore sough to develop a mouse model of inhalational injury to further delineate the relationship between DAMPS and cytokine release.

Wood smoke inhalation elicits a clinically relevant injury model. A reliable small animal model of disease is an invaluable resource for the development of therapeutic interventions. Despite differences in magnitude, innate immune responses to stress are largely similar in humans and mice, including cytokine and chemokine production as well as leukocyte activation (9). Several studies have utilized small (mice, rats) and large (sheep, pigs) animal models to address trauma and acute smoke inhalation, primarily using cotton as a source of smoke (10-16). Neutrophil accumulation and activation are associated with oxidative tissue damage in an ovine model of cotton smoke inhalation and bacterial infection (15). Inhibiting protein oxidation in a mouse model of cotton smoke inhalation with burn injury resulted in elevated IL-10 as well as an improvement in lung structure (12). Despite these insights, it is necessary to study inhalational injury in a more clinically relevant background due to significant disagreement between human clinical findings and results of animal studies (2, 12). We propose that these differences are due, in part, to reliance on cotton smoke, because there are differences between injury induced by cotton smoke, wood smoke, and plastic smoke (11).

This study addresses the hypothesis that immune activation early after smoke inhalation leads to inflammation and damage to the tissue architecture, which renders the lung vulnerable to bacterial challenge. In this study, we describe a novel murine model of acute exposure to smoke derived from plywood, a common building material comprised of wood and adhesives. This model recapitulates many

phenotypes previously described in patients diagnosed with an inhalational injury as well as key traits of murine acute lung injury. Additionally, we demonstrate the importance of neutrophil recruitment and activity as a key determinant of pathology in smoke inhalation and further establish the utility of this model for testing interventions that counteract the negative physiological consequences of smoke inhalation.

In this study, we report that exposure to wood smoke leads to the neutrophil accumulation in the airway, elevated protein levels of IL-10, MCP-1, and CXCL1/KC, as well as accumulation of DAMPs (HA and dsDNA) in the airways and alveoli. Furthermore, mechanistic studies demonstrate that iNOS expression is necessary for elevations in IL-10, MCP-1, and HA but not for changes in CXCL1, neutrophil recruitment or the susceptibility to bacterial challenge. In contrast, CXCL1 neutralization results in an approximate 50% decrease in neutrophil recruitment to the airway following injury and improved bacterial clearance. Thus, this study establishes the utility of this model in establishing molecular mechanisms that drive this complex injury and highlights its suitability for testing interventions that counteract the negative physiological consequences of smoke inhalation.

Methods

Mouse housing and care. Female C57BL/6 mice aged 8-10 weeks were purchased from Taconic Farms and housed in specific pathogen free facilities. All protocols were approved by the University of North Carolina at Chapel Hill's Institutional Animal Care and Use Committee and were verified to follow guidelines from the National Institute of Health concerning use of vertebrate animals in research.

Smoke inhalation. Mice were anesthetized using tribromoethanol (475mg/kg body weight; Sigma-Aldrich) and their dorsum shaved (Fisher NC0854145) prior to injection of subcutaneous morphine sulphate (3mg/kg body weight; Westward). Mice were then placed on an intubation platform (Penn Century). A catheter (22G x 1", Exel) was placed in the trachea after visualization with a laryngoscope. Mice were then secured to a platform in a supine position and placed in an animal induction chamber (Stoelting NC9296517). Plywood sectioned into strips (2.5cm x 8cm, Lowe's Item

#12206 Model # 776391100000) was placed in a side-arm flask on a heat block set to 500°C, causing the board to smolder and produce smoke. ~50g of wood was used at the start of experiments, with additional strips added as needed. Air pumped through the flask forced smoke into the induction chamber for three exposures of 2 minutes with a 1 minute break between exposures. Clear walls of the induction chamber allow visual assessment of smoke density –air pressure was kept constant, and the chamber was vented or kept sealed in order to maintain smoke density that resulted in visual obstruction at 1-1.5 inches. The heat plate, flask, and induction chamber were set up in a dedicated fume hood. Mice were resuscitated with an intraperitoneal injection of lactated Ringer's solution (1mL/kg body weight; Baxter Healthcare Incorporated), and were given morphine in their drinking water ad libitum for the duration of the experiment. Sham mice were treated identically except that air was pumped into the induction chamber rather than smoke. Prior to tissue collection, mice were euthanized with gaseous isofluorane.

Bacterial infection. Pseudomonas aeruginosa (strain PA01) was grown in Luria-Bertani (LB) broth at 37°C with shaking to reach mid-log phase growth. Bacterial pellets were washed and resuspended with cold PBS with 1% Protease Peptone (PP-PBS) and diluted to 5×10^6 CFU/mL. Serial dilutions of inoculum were plated on LB agar to confirm bacterial dosage. 200 uL of inoculum was administered to mice via tail vein injection –mock-infected mice received 200uL PP-PBS. Bacterial burden in the airway at time of harvest was determined by plating 100uL of broncho-alveolar lavage fluid (BALF) in duplicate on LB agar. Bacterial burdens in liver and spleen were determined by plating serial dilutions of organ homogenate in PP-PBS on LB agar plates.

Broncho-alveolar lavage sample acquisition and processing. To collect broncho-alveolar lavage fluid (BALF), a catheter (22G x 1", Exel) was inserted into the trachea and connected to a syringe containing 1mL 0.6mM EDTA in PBS. 0.6mL was instilled into the lungs and then withdrawn three times to obtain a primary wash. Typical recovery was 0.75 mL. Two subsequent washes were combined to obtain a secondary wash, for which typical recovery was 2 mL. Cell pellets from primary and secondary

washes were combined for analysis via flow cytometry or pelleted and stored at -80°C for subsequent analysis by qPCR.

Cell-free supernatant from primary wash was analyzed by Bradford assay and enzyme-linked immune-sorbent assay (ELISA) for IL-10, hyaluronic acid, CXCL1, CXCL2 (R&D), IL-12, and MCP-1 (eBioscience) according to manufacturer's instructions. Cell-free DNA was enriched from secondary BALF. Briefly, 500 µl of BALF supernatant was treated with 50 µl of Proteinase K solution and 125 µl of S&P Proteinase K Digestion Buffer (Zymo Research, Irvine, CA). Following proteinase K addition, samples were incubated for 30 minutes at 55ºC, then 2.7 volumes of S&P DNA binding buffer (Zymo Research) were added to each sample. Samples were then mixed and added to Zymo-Spin III-S columns for DNA isolation per the manufacturer's protocol. cfDNA was eluted from the column using 50 µl of pre-warmed DNA Elution Buffer (Zymo Research). Total cfDNA per mL of BAL input was determined using the Qubit 3.0 fluorimeter (Life Technologies) and the Qubit dsDNA high-sensitivity detection reagents (Life Technologies).

Lungs were removed from mice after BAL extraction. Minced lung tissue was digested in 4 mL PBS with 10% Fetal Bovine Serum (PBS-FBS) with 1500 u/mouse collagenase (Worthington) and 0.1 µg/mouse DNase and shaken at 250rpm at 37°C for 1 h. Samples were filtered through a 100 µm cell strainer. Red blood cells were removed with ACK Lysis Buffer and remaining cells were suspended in PBS-FBS prior to flow cytometric analysis. Live cells from lung digest and BALF were counted manually with a hemocytometer using 0.01% trypan blue cell viability dye (Life Technologies).

Flow cytometry. Following incubation with Fc Block (eBiosciences), cells were stained with labeled antibodies against CD45, CD11b, CD11c, and Ly6G (eBiosciences; BD Biosciences). Cells were fixed with 1% paraformaldehyde prior to analysis on a CyAn (Beckmann-Coulter). Samples were analyzed with Summit 5.1 software (Beckmann-Coulter). Neutrophils were defined as CD45+CD11b+CD11c-Ly6G+, and Macrophages were defined as CD45+CD11c+Ly6G-.

Isolation and analysis of gene expression by qRT-PCR. Total RNA was isolated using the RNeasy Mini-RNA extraction kit (Qiagen) for BAL cells and the RNeasy Mini-RNA Fibrous Tissue kit (Qiagen) for mouse whole lungs. Reverse transcription reactions were performed with the VILO Reverse Transcription master mix (Life Technologies) using 0.25 μg of total RNA. Real-time qRT-PCR was performed using the QuantStudio 6 (Life Technologies) machine and TaqMan Gene Expression master mix (Thermo-Fischer). Each reaction contained 1X TaqMan Gene Expression master mix, cDNA from 40 ng of RNA, and 1X of gene specific primer/probe combinations (Life Technologies Cat. #4331182; Gapdh Primer ID Mm99999915_g1, Tbp Primer ID Mm01277042_m1, IL-10 Primer ID Mm01288386_m1, IL-12b Primer ID Mm01288989_m1, MMP8 Primer ID Mm00439509_m1, MMP9 Primer ID Mm00442991_m1) in a total volume of 20 μl. PCR was performed in duplicate by cycling at 50ºC for 2 min, 95°C for 15 min, followed by 40 cycles of denaturation at 95°C for 10 s, and annealing and extension at 60°C for 30 s. Values were derived using the delta-delta cT method comparing sham mice to inhalation injury mice at each timepoint.

Histopathology. To prepare lung tissue for histology, lungs were inflated with 4% paraformaldehyde (PFA) in PBS to a constant pressure of 20cmH_2O. Inflated tissue was stored overnight in 4% PFA, then rinsed with 70% ethanol. Left lobes were embedded in paraffin and 4um sections of tissue containing large airway branches were taken and stained with hematoxylin and eosin (H&E) at the UNC Animal Histopathology Core Facility. Images of deidentified specimens were taken at the UNC Microscopy Services Laboratory using an Olympus BX61 light microscope. At least 10 non-overlapping sections of distal lung tissue (excluding major blood vessels and large airways) were taken per specimen using the UPlanFLN 40X/0.75 objective. The UPlanFLN 20X/0.50 objective was used to obtain sequential images of a large airway. Images of the distal lung tissue were scored on a scale of 0 (normal) to 2 (maximal) for neutrophil infiltration, proteinaceous debris, and congestion in microvasculature (17). Images of large airway sections were scored for the same traits in addition to cytoplasmic vacuolization and soughing of airway epithelial cells. Normalized tissue damage scores were obtained for each

specimen by obtaining a weighted value to averaged scores for distal and large airway sections, separately, according to the following formula: [(neutrophil score * .25) + (proteinaceous debris * .15) + (congestion * .3) + (sloughing + vacuolization * .3)] = Tissue Damage Score. Reported scores were obtained by a single blinded individual, and findings were confirmed by a second blinded individual.

Patient Samples. Patient BALF was obtained and analyzed as previously described (5). Briefly, patients were admitted to the North Carolina Jaycee Burn Center at the University of North Carolina and were intubated and on mechanical ventilation for treatment of burn and inhalation injury. Subjects were enrolled over a 2-year period and followed until discharge or death. Serial bronchial washings from clinically-indicated bronchoscopies were collected and analyzed for markers of tissue injury and inflammation. This study was approved by the UNC Biomedical Institutional Review Board. In this analysis we excluded patients who were not diagnosed with inhalational injury and patients for whom HA was only measured at days 0 and 1.

Statistical Analysis. GraphPad Prism Version 5.0 for Windows was used to analyze data by Student's t-Test, One-Way Analysis of Variance (ANOVA) with Tukey post-test, or Two-Way ANOVA with Bonferroni post-test, as appropriate. In cases where data are represented in relation to sham average, one-sample t-Test was used to compare values and means to a hypothetical value of 1. Data are represented as mean +/- standard error of the mean (SEM). Statistical significance is indicated as * $p < 0.05$, ** $p < 0.005$, *** $p < 0.001$.

Results

Smoke inhalation causes inflammation in the airway. In mouse models of ALI, an increase in the live cell count and protein concentration in the BALF are associated with inflammation and perturbation of the alveolar-capillary barrier (17). Therefore, we isolated BALF from sham mice and mice who were exposed to plywood smoke, enumerated live cells, and analyzed the total protein content in BALF supernatants. Quantification of live cells in the BALF revealed increased cellularity in the airway at 24h,

48h, 72h, and 96h following smoke inhalation compared to sham controls (Figure 5.1 A). In the BALF supernatants from mice exposed to smoke, we observed an increase in the total protein concentrations, especially at 24h and 96h (Figure 5.1 B). Using flow cytometry to characterize cells derived from the BALF, we observed an increase in the total number of neutrophils following smoke inhalation compared to sham-treated mice (Figure 5.1 C). By contrast, macrophage numbers in the airway were not significantly altered by smoke inhalation (Figure 5.1 E). Smoke inhalation did not cause a significant increase in the frequency of either neutrophils or macrophages in interstitial lung tissue at 24h, 48h, or 96h (Figure 5.1 C-D).

MMP8 (also known as neutrophil collagenase) and MMP9 are produced by activated neutrophils to break down connective tissue during leukocyte migration and to promote inflammation by proteolytically activating cytokines and chemokines. RNA expression of MMP8 and MMP9 was quantified in cells extracted from BALF by qRT-PCR. We observed an increase in the expression of MMP9 but not MMP8 in BALF cells at both 24h and 96h following smoke inhalation compared to sham-treated mice (Figure 5.1 G). By contrast, smoke inhalation did not cause a change in either MMP8 or MMP9 in interstitial lung tissue (data not shown). To further characterize the activation status of immune cells in the BALF, we quantified expression of NOS2 by qRT-PCR. We observe a 7.35-fold increase ($p=0.13$) in NOS2 expression in smoke-treated mice relative to sham at 24h (Figure 5.1H)

In order to thoroughly characterize damage to lung tissue, sections of fixed tissue were analyzed for five indicators of histopathology, which were normalized to calculate a tissue damage score for both distal lung tissue and large airway epithelium (Figure 5.2 A-B). Within 24h of smoke inhalation, we observed cytoplasmic vacuolization and sloughing in epithelial cells of the large airways of smoke mice (Figure 5.2 G) compared to sham (Figure 5.2 F) as well as hemorrhage and edema in distal lung tissue (Figure 5.2 C). Analysis of specimens taken 96h following smoke inhalation indicated an influx of neutrophils and macrophages to the distal lung tissue as well as increased congestion of the pulmonary microvasculature (Figure 5.2 E,H).

Anti-inflammatory cytokines precede HA in the airway. We have previously demonstrated that elevated IL-10, a skewed IL-10/IL-12 ratio, and elevations in dsDNA and HA are reliable predictors of patient outcomes (5, 7). In mice exposed to plywood smoke, IL-10 is significantly elevated in BALF at 24h compared to uninjured mice, however the increase is transient and was not significant at subsequent time points (Figure 5.3 A). No significant changes in IL-12 protein in BALF were observed at any time (data not shown). These data are supported by qRT-PCR, which illustrates an increase in IL10 mRNA in cells recovered from the BALF of injured animals normalized to sham average at 24h (Figure 5.3 B). This increase is followed by downregulation relative to sham-treated mice between 48h and 96h. By contrast, IL-12 mRNA expression was slightly downregulated in BAL cells at 24-48h post-injury and increased at 72h (data not shown). In interstitial lung tissue, no statistically significant changes in IL-10 gene expression were observed at either 24h or 96h. IL-12 gene expression was significantly downregulated in lung tissue at 96h following smoke inhalation compared to sham-treated controls (Figure 5.3 B).

Hyaluronic acid (HA) and cell-free double-stranded DNA (dsDNA) were measured in BALF following smoke inhalation or sham procedure. The sham procedure did not change levels of HA or dsDNA at any time (Figure 5.3 C-D). dsDNA was elevated in injured mice compared to shams at 12-24h before returning to baseline at all subsequent time points (Figure 5.3 C). By contrast, concentrations of HA increased over time and reached a peak at 72-96h (Figure 5.3 D). This time-dependent increase in HA in the mouse model of inhalational injury mirrors data obtained from patients diagnosed with inhalational injury (Figure 5.3 E).

Systemic infections manifest in the airway of injured mice. Patients diagnosed with inhalational injury frequently develop pneumonia following colonization by opportunistic bacteria, most frequently *Pseudomonas aeruginosa*. We therefore propose that any clinically relevant animal model should render mice susceptible to bacterial challenge that does not cause infection in uninjured mice. In this study, mice were exposed to an intravenous inoculation with *P. aeruginosa* (strain PA01) 48h following smoke exposure or sham treatment. We quantified bacterial recovery from BALF at 24h, 48h, and 96h following

infection (Figure 5.4 A). No bacteria were recovered from BALF of sham mice after intravenous inoculation with *P. aeruginoasa* strain PA01. When mice were inoculated with PA01 48h after smoke inhalation, bacteria were recovered from BALF at 24h, 48h, and 96h after inoculation. Bacterial recovery from liver and spleen tissue was sporadic and unaltered by injury status (data not shown). Infection augmented concentrations of protein and HA in the BALF of injured mice (Figure 5.4 B-C).

iNOS deficiency reverses cytokine and chemokine upregulation but not injury severity. iNOS upregulation in lung tissue has been observed in other models of acute smoke inhalation (13, 16), and iNOS activity is known to modulate neutrophil recruitment and activation as well as cytokine and chemokine production (18). We therefore designed a series of experiments to determine the impact of iNOS expression on inflammation following acute smoke inhalation. iNOS-/- mice on a C57BL/6 background were bred in-house alongside WT control mice. We did not observe a change in protein accumulation in the BALF of iNOS-/- mice following smoke inhalation at either 24h (data not shown) or 96h following smoke inhalation or sham procedure (Figure 5.5 A). Similarly, iNOS deficiency did not significantly alter neutrophil numbers in the BALF at 24h (data not shown) or 96h following injury (Figure 5.5 B).

While IL-10 and MCP-1 were elevated in BALF 24h following smoke inhalation in WT mice, a similar increase was absent in iNOS-/- animals (Figure 5.5 C-D). The smoke-dependent increase in HA concentration in BALF at 96h was also attenuated in iNOS-/- animals, however concentrations of dsDNA were not altered in iNOS-/- mice compared to WT controls (Figure 5.5 E-F). WT and iNOS-/- mice were inoculated via tail vein injection with 1x10^6 CFU PA01 at 48 h following injury or control procedure, and CFU recovery from BAL was measured 48h later. We did not observe an iNOS-dependent difference in bacterial clearance following an intravenous challenge (data not shown). *CXCL1 drives neutrophil recruitment to the airway following smoke exposure*. In order to delineate potential chemotactic signals responsible for neutrophil recruitment to the airway following smoke inhalation, we measured the neutrophil chemoattractants CXCL1 (also known as KC) and CXCL2 in BALF. At 24h post-injury we

observed an increase in CXCL1 in BALF; however, CXCL1 concentrations returned to baseline at all subsequent time points (Figure 5.6 A). We did not detect CXCL2 in injured mice at any time following injury (data not shown).

To determine whether CXCL1 was responsible for neutrophil recruitment to the airway following inhalational injury, we intravenously administered a neutralizing antibody against CXCL1 or isotype control immediately after smoke or sham procedure and at 24h. We observed a significant decrease in total neutrophil numbers in the airway at 24h, 48h and 72h compared to smoke-treated mice given an isotype control antibody (Figure 5.6 B). Increased concentration of neutralizing antibody did not alter neutrophil numbers (data not shown), suggesting that another chemotactic signal contributes to neutrophil recruitment, especially at 72-96h. We quantified histopathology at 24h in mice treated with neutralizing antibody or isotype control and observed a significant decrease in tissue damage scores in distal airway specimens (Figure 5.6 C). This decrease was primarily attributable to a decrease in congestion scores (0.93 ± 0.11 vs. 0.27 ± 0.28; $p<0.05$).

To test whether attenuated neutrophil recruitment impacted sensitivity to bacterial infection in the lung following intravenous inoculation, we infected anti-CXCL1 and isotype treated mice at 48h following injury with 1x10^6 CFU PA01 and quantified CFUs, protein, neutrophils, and HA in BAL at 48h following infection (Figure 5.7 A). Significantly less bacteria were recovered from the airway of mice treated with a neutralizing antibody prior to infection (Figure 5.7 D). Following infection, recruitment of neutrophils to the airway was unaltered by early administration of anti-CXCL1, however HA in the airway was decreased in these mice (Figure 5.7 C-D). Administration of neutralizing antibody did not alter protein recovery from the airway in either uninfected or infected mice (Figure 5.7 E).

Discussion

Inhalation of plywood smoke yields a clinically relevant phenotype. Acute smoke inhalation presents a significant clinical challenge for survivors of structural fires, inhabitants of regions at risk for wildfires, first responders, and members of the armed forces. Inhalational injury is among a spectrum of

stimuli that can precipitate acute lung injury (ALI) and acute respiratory distress syndrome (ARDS). Despite significant research into targeted therapies for ALI/ARDS, an effective pharmaceutical intervention does not currently exist (19). Inhalational injury and ALI are not uniform diseases –they are brought on by a multitude of stimuli and their outcomes are impacted by comorbidities from inflammatory disorders to smoker status (17, 19-21). It is therefore critical that future research into inhalational injury and ALI accounts for these complexities. Clinical research can make use of resources available through the Precision Medicine Initiative (PMI), and animal studies should be designed to replicate, as faithfully as possible, the etiology of human disease.

Herein we report the development of a mouse model of acute exposure to smoke derived from plywood, a common building material. This model recapitulates many of the phenotypes previously reported to predict outcomes in patients, including a predominance of neutrophils in the airway, polarization towards IL-10 production, and elevated dsDNA and HA within 72h of the injury (5, 7, 22). It has previously been reported that macrophage numbers in the airway do not change between the acute phase of ARDS and resolution; however, neutrophil numbers are subject to change based on disease state (22). We observed a similar phenotype in our model of acute exposure to plywood smoke. Specifically, we demonstrated that macrophage numbers in BALF are unaltered by the injury, while the number of neutrophils increases following smoke inhalation (Figure 1C-F).

Because pneumonia poses a significant challenge to patient recovery, it is critical that any animal model faithfully recapitulate susceptibility to opportunistic infection. In this injury model, mice exposed to smoke from plywood are susceptible to infection following a systemic bacterial challenge. Infection is restricted to the airway and is not detectable in the liver or the spleen.

Importantly, because of the challenges inherent in clinical research regarding the timing and frequency of sample acquisition, this model clarifies the dynamic relationship between DAMPs and anti-inflammatory cytokines in the injured lung. Prevailing wisdom is that tissue damage leads to DAMP release, and detection of DAMPs through scavenger receptors and other pattern recognition receptors

triggers an anti-inflammatory signaling cascade to limit further damage due to immunopathology. Data from this model echo published clinical data, which suggests that anti-inflammatory cytokine production occurs rapidly in the lung following injury in an attempt to minimize inflammation that would compromise gas exchange across the alveolar-capillary barrier.

iNOS drives inflammation but not outcomes after inhalational injury. It has been reported that a murine model of cotton smoke inhalation with and without burn injury led to an increase in iNOS expression and activity in the airway (13), and iNOS is expressed in macrophages and airway epithelial cells following sepsis (23). We interrogated the inflammatory response to acute smoke inhalation in mice deficient for iNOS and observed that, in the absence of iNOS, many relevant injury phenotypes are absent. Notably, iNOS deficiency prevents smoke-induced elevation of IL-10 and MCP-1 at 24h, as well as release of HA into the airway at 96h. These changes did not, however impact neutrophil recruitment or damage to the alveolar-capillary barrier. Moreover, in support of other studies which have demonstrated that iNOS expression and activity is dispensable for clearance of *P. aeruginosa* infection, we do not observe any change in bacterial clearance in injured mice deficient for iNOS (24).

This result is significant in that it illustrates the distinction between inflammation, immunopathology, and protective immunity. Until now, it has been impossible to differentiate between correlative and causative relationships. Previously, both IL-10 and dsDNA have been correlated with the onset of infection, however data using iNOS-/- mice alongside WT counterparts indicate that dsDNA can be elevated without a concomitant increase in IL-10 and that these changes do not alter the outcomes following bacterial challenge. These data indicate that it may be possible, using translationally relevant models, to uncouple clinical phenotypes from outcomes and therefore identify the most effective intervention strategies.

CXCL1 signaling drives outcomes after smoke inhalation. Significant clinical data exists suggesting that expression of the potent neutrophil chemoattractant IL-8 is elevated following trauma and that its activity is a key determinant of outcomes (8, 25). A spike in IL-8 is observed in patient serum

following burn injury in the absence of sepsis (25). In a study of inhalational injury, IL-8 was elevated in survivors compared to those who succumbed to the injury (8).

In an animal model, inhibition of the murine IL-8 homologue CXCL1 (also known as KC) secretion into the serum following burn correlated with a decrease in several markers of lung injury (26). Here we show that intravenous administration of a neutralizing antibody against CXCL1 attenuates neutrophil recruitment to the airway. Although this did not significantly impact the injury phenotype as assessed by concentration of protein and HA in BALF, it did render the mice less susceptible to infection. Following infection, neutrophil recruitment to the airway was equivalent in mice treated with neutralizing antibody compared to isotype control, indicating that mice maintained the ability to mount a protective immune response. This result highlights an important objective in modulating the immune response to trauma; specifically, to reduce pathogenic inflammation without paralyzing the immune response and increasing vulnerability to infection.

Future studies to determine how inhalation becomes inflammation. Because inhibition of CXCL1 signaling did not completely deter neutrophil recruitment and CXCL2 was not detectable after smoke inhalation, it would be beneficial to characterize the role of LTB4 in neutrophil recruitment. Furthermore, we hypothesize that airway epithelial cells produce CXCL1 following smoke exposure, and studies are underway to test this hypothesis and to determine the molecular signals that trigger release of CXCL1.

Changes in expression of TLR on immune cells following burn injury have been described previously (27-29). TLR signaling is upregulated in trauma patients (30) and is critical for survival in *Pseudomonas*-induced ALI (31). Signaling via TLR-TRIF-NFkB in myeloid cells promotes ALI in an acid aspiration model by promoting pathogenic inflammation following detection of oxidized lipids (32). Future studies in our model of acute exposure to plywood smoke will therefore be focused on determining the effect of smoke inhalation on TLR4 expression and the role of TLR4 signaling in inflammation following injury and susceptibility to pneumonia.

FIGURES

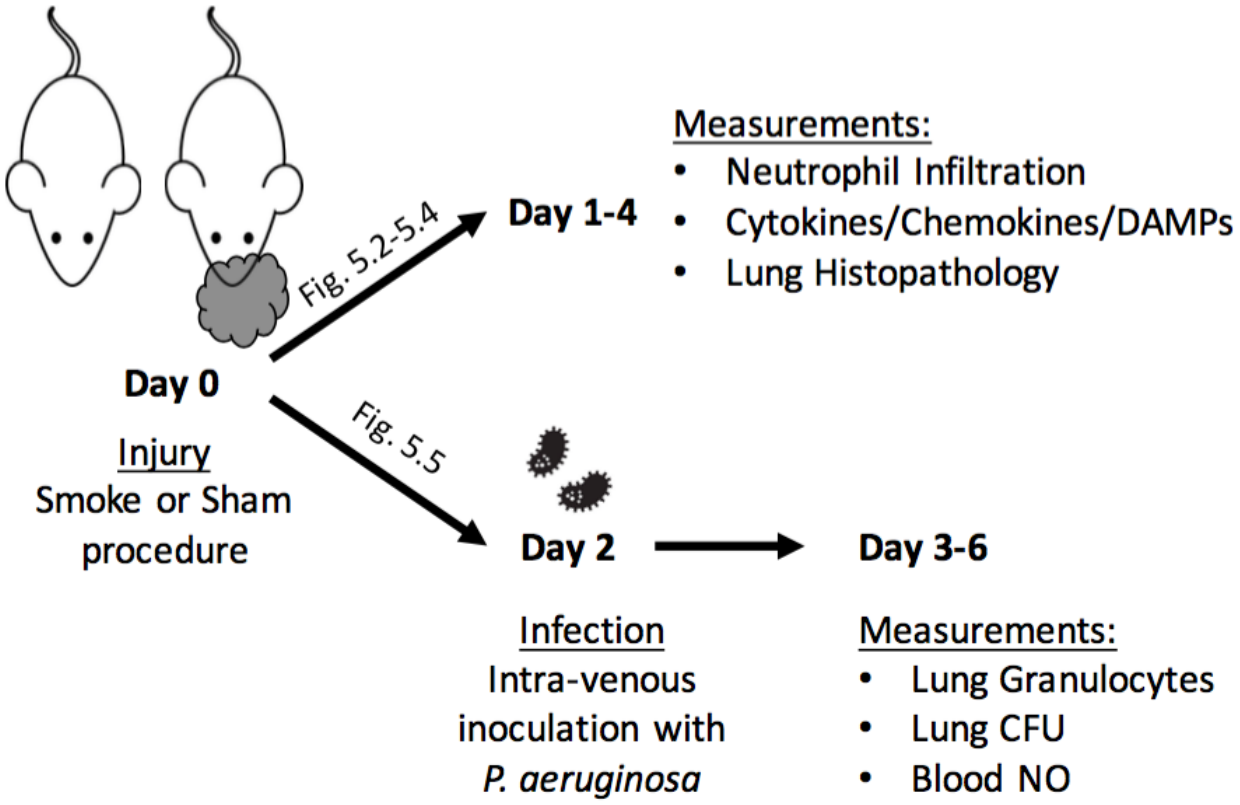

Figure 5.1: Experimental model of smoke exposure. Mice exposed to smoke from particle board were analyzed for evidence of acute lung injury (ALI) and for bacterial control after systemic inoculation.

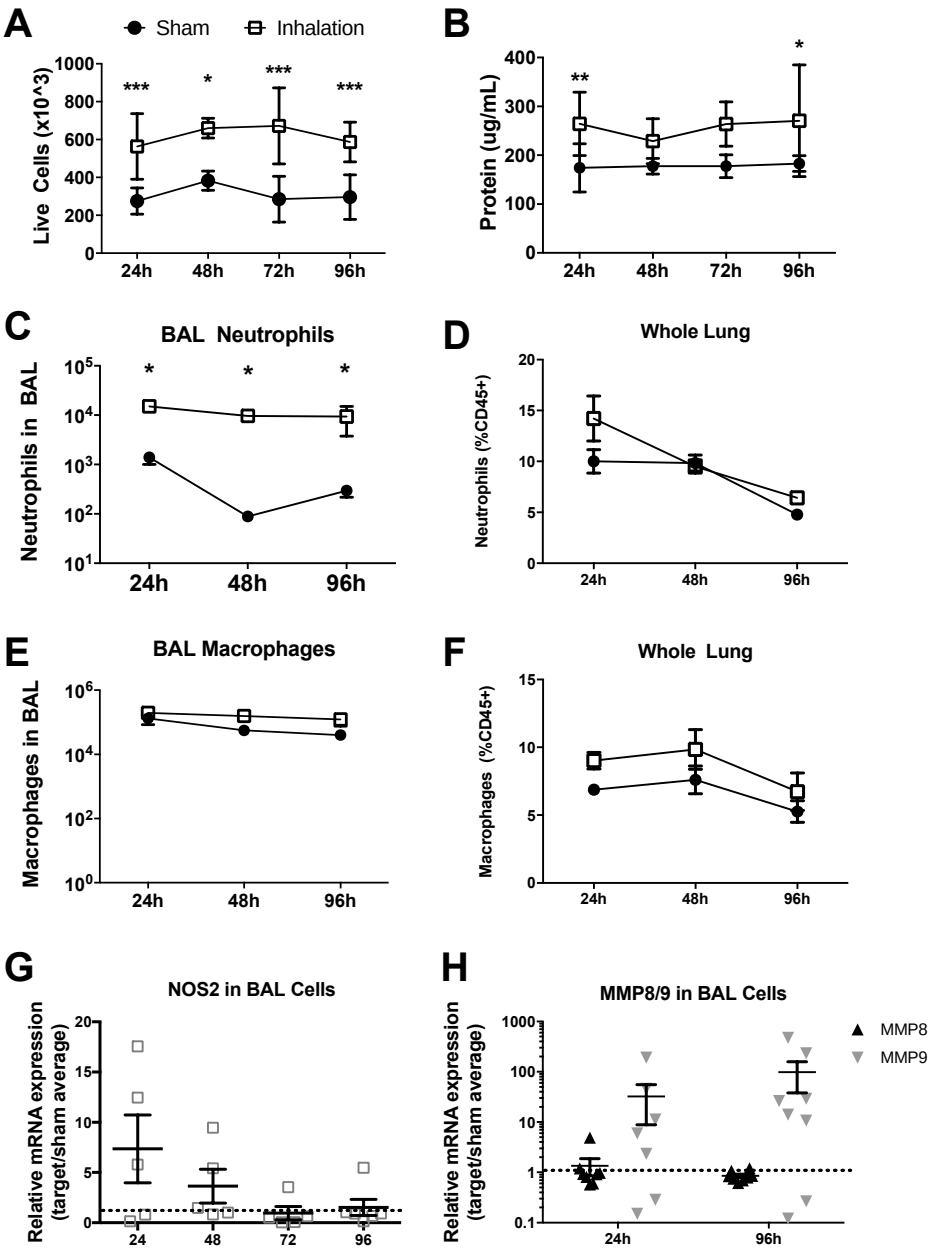

Figure 5.2: Neutrophilic inflammation following acute wood smoke inhalation. (A) Total live cells were enumerated in BALF at indicated time points following smoke or sham procedure. (B) Protein concentration in BALF cell-free supernatant was measured by Bradford assay. (C-D) Neutrophils and (E-F) macrophages were quantified by flow cytometry and normalized to live cell counts in BAL and whole lung following injury. (G) MMP8 and (H) MMP9 expression in BAL cells and whole lung tissue normalized to sham average at 24h and 96h after injury. Data were analyzed by two-way ANOVA with Bonferroni post-test and significance is indicated as * $p < 0.05$, ** $p < 0.005$, *** $p < 0.001$.

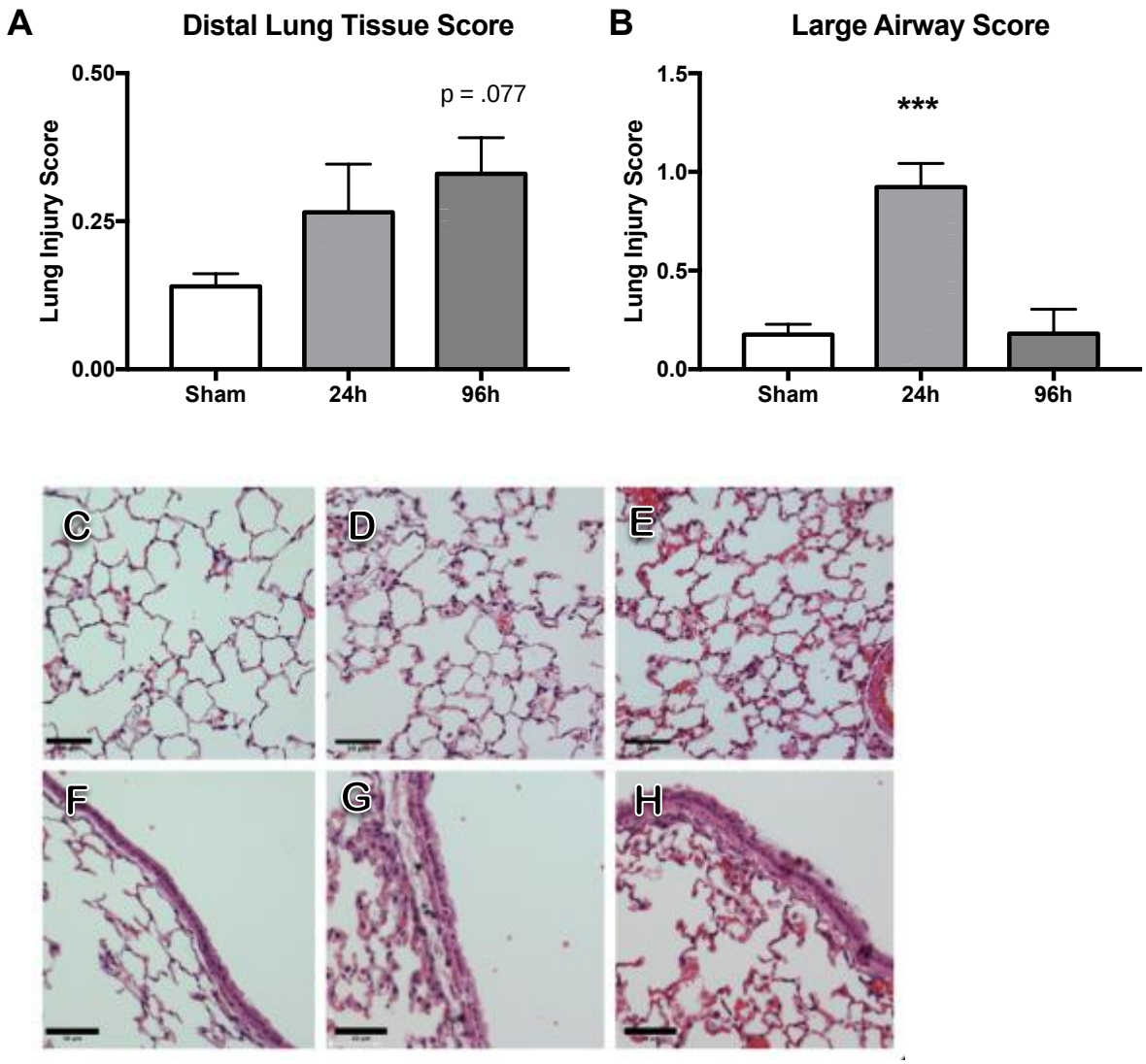

Figure 5.3: Histological evidence of lung injury following acute smoke exposure. Sections of lung tissue were analyzed by histology and scored by blinded individuals. (A) Tissue injury score in sections of distal lung tissue sections (A) and large airway sections (B) in pooled sham mice and smoke treated mice at two time points. p-value represents Tukey post-test following a one-way ANOVA. Representative images of sham distal lung tissue (C) and large airway (F) are shown, as well as smoke-treated distal lung tissue (D, 24h; E, 96h) and large airway (G, 24h; H, 96h). Scale bars correspond to 50um. Data were analyzed by one-way ANOVA with Tukey post-test and significance is indicated by *** $p < 0.001$.

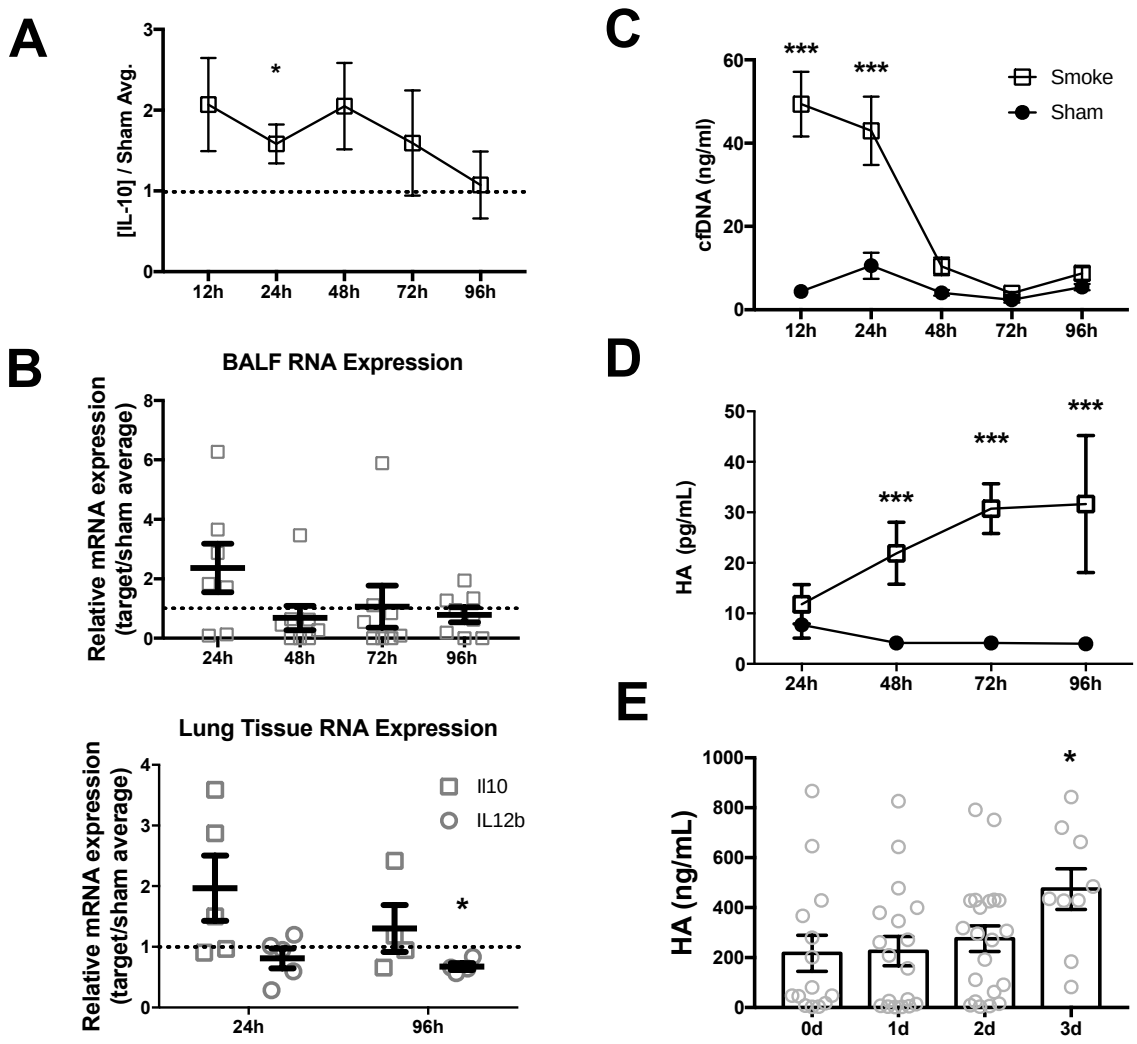

Figure 5.4: Temporal regulation of IL-10 and DAMP release following smoke inhalation. (A) IL-10 concentration in primary BALF cell-free supernatant following inhalational injury, normalized to sham average concentrations at each time point. (B) IL-10 expression in BALF cells and IL-10 and IL-12 expression in interstitial lung tissue normalized to sham average at indicated time points after injury, normalized to sham average expression at each time. (C) cfDNA concentration in secondary BALF supernatant. (D) Hyaluronic acid concentration in primary BALF supernatant following inhalational injury. (E) Hyaluronic acid concentration in BALF samples from patients diagnosed with inhalational injury. Data were analyzed by Student's T-test or two-way ANOVA with Bonferroni post-test, as appropriate, and significance was indicated by * $p < 0.05$, *** $p < 0.001$.

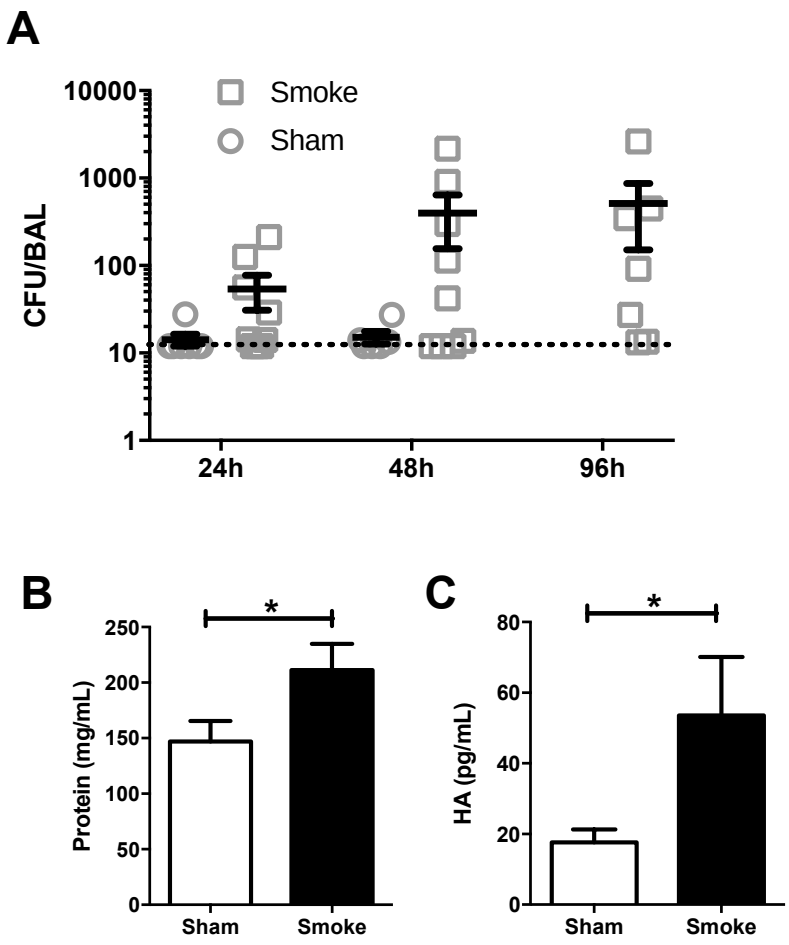

Figure 5.5: Pneumonia develops subsequent to systemic infection in mice following smoke inhalation. (A) CFU recovery from BAL of mice infected with $1x10^6$ CFU PA01 at 48h after sham or smoke procedure and harvested at various timepoints following infection. (B) Protein concentration and (C) Hyaluronic acid concentration in BAL cell-free supernatant of mice infected with $1x10^6$ CFU PA01 at 48h after sham or smoke procedure and harvested 48h after infection. Data were analyzed by Student's T-test between treatment groups at each time-point and significance is indicated by * $p < 0.05$.

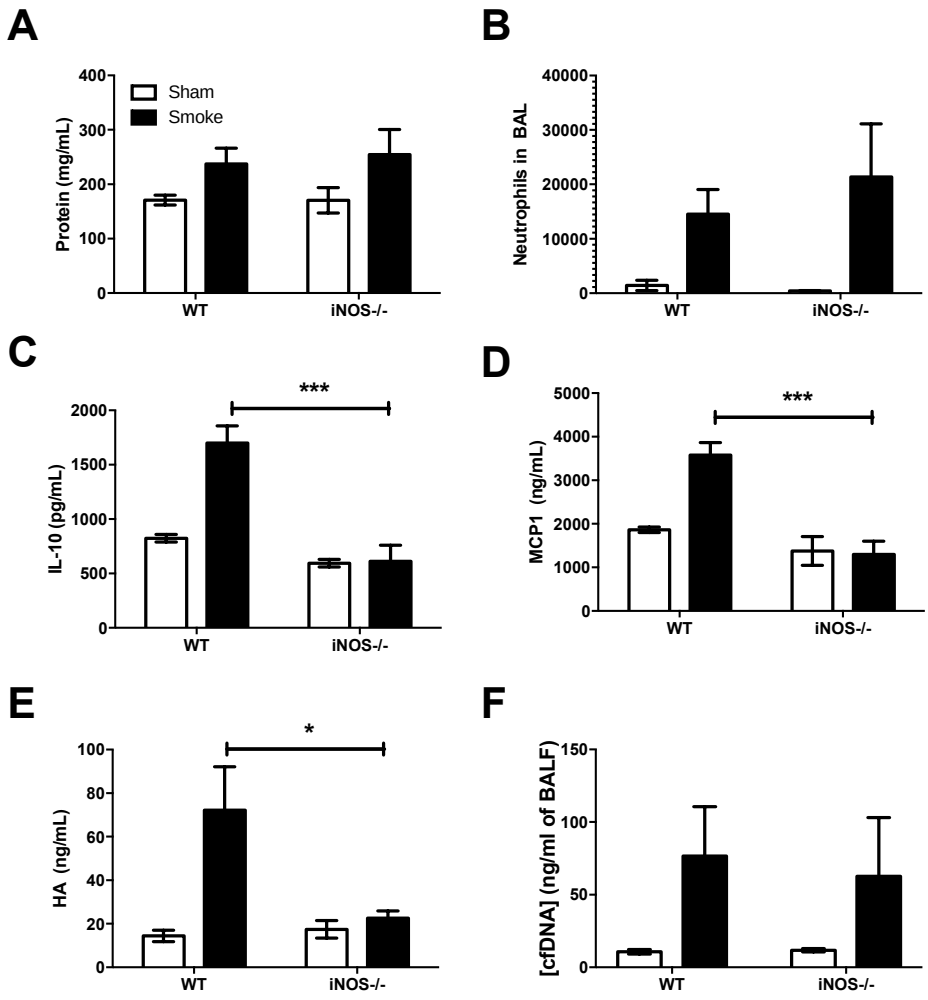

Figure 5.6: iNOS deficiency prevents cytokine production but not inflammation after smoke inhalation. (A) Protein concentration in BALF at 96h following sham or injury procedure. (B) Neutrophils quantified by flow cytometry and normalized to live cell counts in BAL at 96h following injury. (C) IL-10 and (D) MCP-1 concentration in BALF at 24h following sham or injury procedure. (E) Hyaluronic acid concentration in BALF at 96h following sham or smoke procedure. (F) cfDNA concentration in BALF 24h after sham or smoke treatment. Data were analyzed by two-way ANOVA with Bonferroni post-test and significance is indicated by * $p < 0.05$, *** $p < 0.001$.

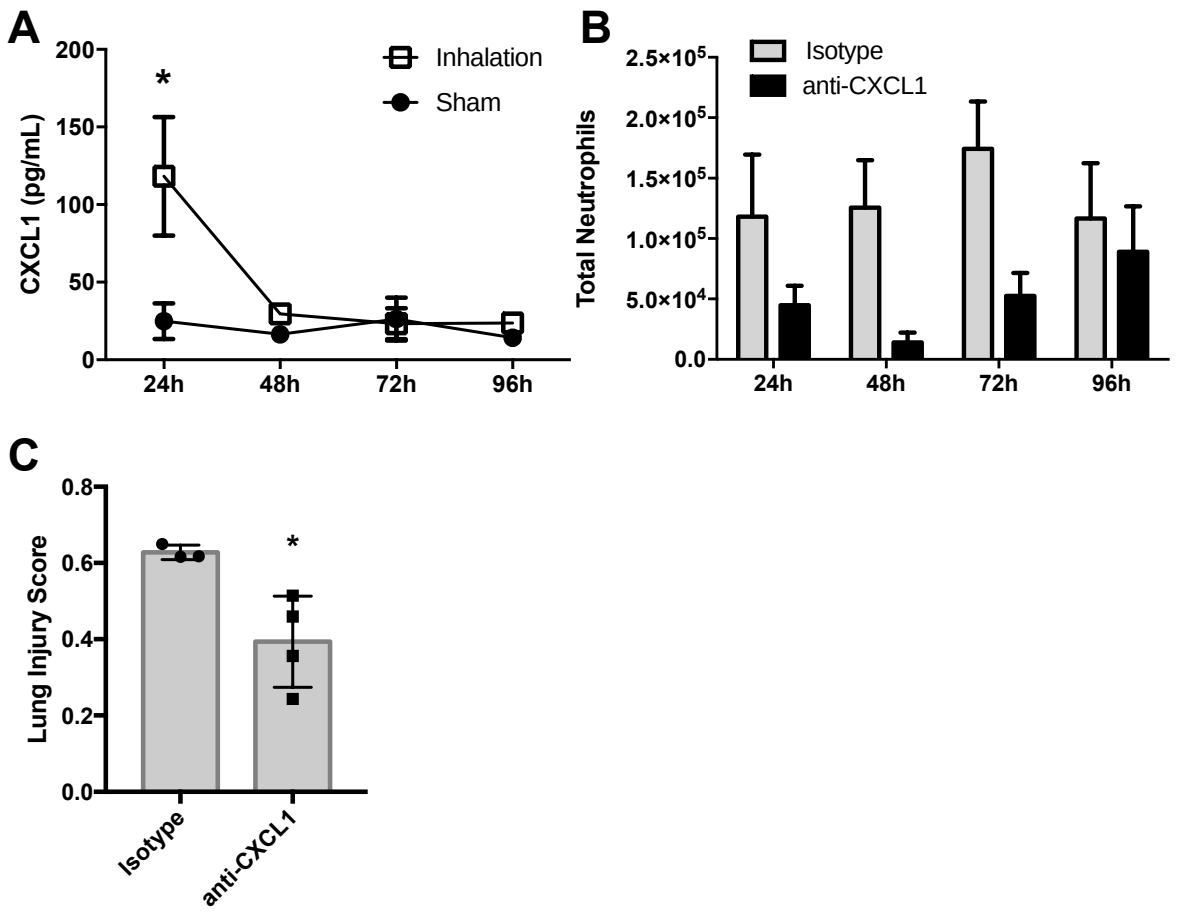

Figure 5.7: CXCL1 drives neutrophilia following smoke exposure. (A) CXCL1 concentration in BALF at 1-4 days following sham or smoke procedure. (B) Mice were treated with anti-CXCL1 or isotype control at 0h and 24h following injury. Neutrophils were quantified by flow cytometry and normalized to live cell counts in BAL at 24h and 48h following injury. (C) Tissue injury scores from distal airway sections of smoke-treated mice who received anti-CXCL1 or isotype control and harvested 24h later. Data were analyzed by Student's T-test (A,C) and two-way ANOVA (B) and significance are represented as * $p < 0.05$.

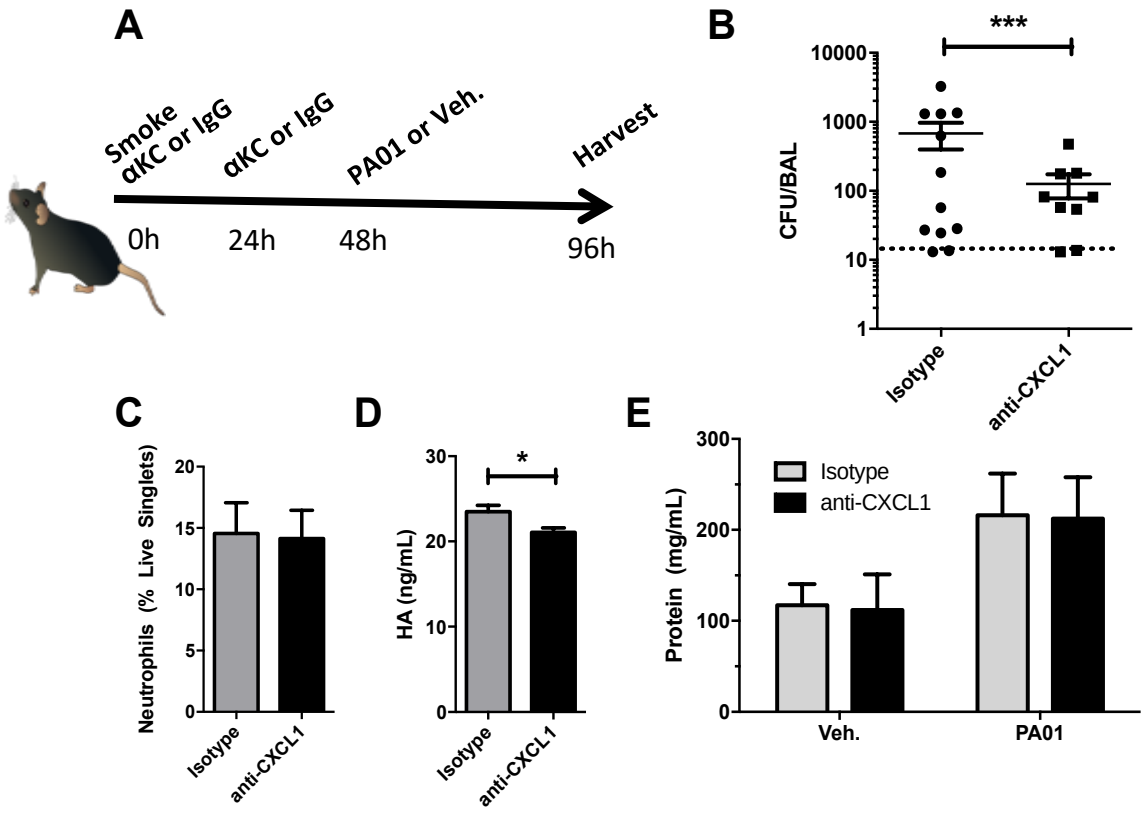

Figure 5.8: Early inhibition of neutrophil migration protects against infection and HA release. (A) Experimental design. Mice were treated with anti-CXCL1 or isotype control antibody via tail-vein injection at 0h and 24h following smoke exposure. At 48h mice were inoculated with PA01 or vehicle control via tail vein injection. Samples were collected at 48h following infection, 96h following injury. (B) CFU recovery from BAL of smoke-treated mice treated with anti-CXCL1 or isotype control prior to infection with PA01. (C) Neutrophils from BALF quantified by flow cytometry and (D) hyaluronic acid concentration in BALF following smoke and infection in mice treated with anti-CXCL1 or isotype control. (D) Protein concentration in BALF of infected vs. uninfected mice treated with anti-CXCL1 or isotype control. Data were analyzed by Student's T-test and significance is indicated by * $p < 0.05$, *** $p < 0.001$.

REFERENCES

1. Ahn CS, Maitz PK. The true cost of burn. Burns. 2012;38(7):967-74. doi: 10.1016/j.burns.2012.05.016. PubMed PMID: 22795515.

2. Rehberg S, Maybauer MO, Enkhbaatar P, Maybauer DM, Yamamoto Y, Traber DL. Pathophysiology, management and treatment of smoke inhalation injury. Expert Rev Respir Med. 2009;3(3):283-97. doi: 10.1586/ERS.09.21. PubMed PMID: 20161170; PMCID: PMC2722076.

3. Mosier MJ, Pham TN, Park DR, Simmons J, Klein MB, Gibran NS. Predictive value of bronchoscopy in assessing the severity of inhalation injury. J Burn Care Res. 2012;33(1):65-73. doi: 10.1097/BCR.0b013e318234d92f. PubMed PMID: 21941194.

4. Finnerty CC, Herndon DN, Jeschke MG. Inhalation injury in severely burned children does not augment the systemic inflammatory response. Crit Care. 2007;11(1):R22. doi: 10.1186/cc5698. PubMed PMID: 17306027; PMCID: PMC2151855.

5. Jones SW, Zhou H, Ortiz-Pujols SM, Maile R, Herbst M, Joyner BL, Jr., Zhang H, Kesic M, Jaspers I, Short KA, Meyer AA, Peden DB, Cairns BA, Noah TL. Bronchoscopy-derived correlates of lung injury following inhalational injuries: a prospective observational study. PLoS One. 2013;8(5):e64250. doi: 10.1371/journal.pone.0064250. PubMed PMID: 23691180; PMCID: PMC3656836.

6. Wurtz R, Karajovic M, Dacumos E, Jovanovic B, Hanumadass M. Nosocomial infections in a burn intensive care unit. Burns. 1995;21(3):181-4. PubMed PMID: 7794498.

7. Maile R, Jones S, Pan Y, Zhou H, Jaspers I, Peden DB, Cairns BA, Noah TL. Association between early airway damage-associated molecular patterns and subsequent bacterial infection in patients with inhalational and burn injury. Am J Physiol Lung Cell Mol Physiol. 2015;308(9):L855-60. doi: 10.1152/ajplung.00321.2014. PubMed PMID: 25770180; PMCID: PMC4421787.

8. Davis CS, Albright JM, Carter SR, Ramirez L, Kim H, Gamelli RL, Kovacs EJ. Early pulmonary immune hyporesponsiveness is associated with mortality after burn and smoke inhalation injury. J Burn Care Res. 2012;33(1):26-35. doi: 10.1097/BCR.0b013e318234d903. PubMed PMID: 21979852; PMCID: PMC3253958.

9. Copeland S, Warren HS, Lowry SF, Calvano SE, Remick D, Inflammation, the Host Response to Injury I. Acute inflammatory response to endotoxin in mice and humans. Clin Diagn Lab Immunol. 2005;12(1):60-7. doi: 10.1128/CDLI.12.1.60-67.2005. PubMed PMID: 15642986; PMCID: PMC540200.

10. Zawacki BE, Jung RC, Joyce J, Rincon E. Smoke, burns, and the natural history of inhalation injury in fire victims: a correlation of experimental and clinical data. Ann Surg. 1977;185(1):100-10. PubMed PMID: 831629; PMCID: PMC1396243.

11. Matthew E, Warden G, Dedman J. A murine model of smoke inhalation. Am J Physiol Lung Cell Mol Physiol. 2001;280(4):L716-23. PubMed PMID: 11238012.

12. Esechie A, Kiss L, Olah G, Horvath EM, Hawkins H, Szabo C, Traber DL. Protective effect of hydrogen sulfide in a murine model of acute lung injury induced by combined burn and smoke

inhalation. Clin Sci (Lond). 2008;115(3):91-7. doi: 10.1042/CS20080021. PubMed PMID: 18315525.

13. Mizutani A, Enkhbaatar P, Esechie A, Traber LD, Cox RA, Hawkins HK, Deyo DJ, Murakami K, Noguchi T, Traber DL. Pulmonary changes in a mouse model of combined burn and smoke inhalation-induced injury. J Appl Physiol (1985). 2008;105(2):678-84. doi: 10.1152/japplphysiol.00232.2007. PubMed PMID: 18436699.

14. Lange M, Hamahata A, Traber DL, Connelly R, Nakano Y, Traber LD, Schmalstieg FC, Herndon DN, Enkhbaatar P. Pulmonary microvascular hyperpermeability and expression of vascular endothelial growth factor in smoke inhalation- and pneumonia-induced acute lung injury. Burns. 2012;38(7):1072-8. doi: 10.1016/j.burns.2012.02.019. PubMed PMID: 22647495; PMCID: PMC3893691.

15. Lange M, Szabo C, Traber DL, Horvath E, Hamahata A, Nakano Y, Traber LD, Cox RA, Schmalstieg FC, Herndon DN, Enkhbaatar P. Time profile of oxidative stress and neutrophil activation in ovine acute lung injury and sepsis. Shock. 2012;37(5):468-72. doi: 10.1097/SHK.0b013e31824b1793. PubMed PMID: 22266977; PMCID: PMC4646062.

16. Soejima K, Traber LD, Schmalstieg FC, Hawkins H, Jodoin JM, Szabo C, Szabo E, Virag L, Salzman A, Traber DL. Role of nitric oxide in vascular permeability after combined burns and smoke inhalation injury. Am J Respir Crit Care Med. 2001;163(3 Pt 1):745-52. doi: 10.1164/ajrccm.163.3.9912052. PubMed PMID: 11254534.

17. Matute-Bello G, Downey G, Moore BB, Groshong SD, Matthay MA, Slutsky AS, Kuebler WM, Acute Lung Injury in Animals Study G. An official American Thoracic Society workshop report: features and measurements of experimental acute lung injury in animals. Am J Respir Cell Mol Biol. 2011;44(5):725-38. doi: 10.1165/rcmb.2009-0210ST. PubMed PMID: 21531958.

18. Armstrong R. The physiological role and pharmacological potential of nitric oxide in neutrophil activation. Int Immunopharmacol. 2001;1(8):1501-12. PubMed PMID: 11515815.

19. Johnson ER, Matthay MA. Acute lung injury: epidemiology, pathogenesis, and treatment. J Aerosol Med Pulm Drug Deliv. 2010;23(4):243-52. doi: 10.1089/jamp.2009.0775. PubMed PMID: 20073554; PMCID: PMC3133560.

20. Reiss LK, Uhlig U, Uhlig S. Models and mechanisms of acute lung injury caused by direct insults. Eur J Cell Biol. 2012;91(6-7):590-601. doi: 10.1016/j.ejcb.2011.11.004. PubMed PMID: 22284832.

21. Liu F, Li W, Pauluhn J, Trubel H, Wang C. Rat models of acute lung injury: exhaled nitric oxide as a sensitive, noninvasive real-time biomarker of prognosis and efficacy of intervention. Toxicology. 2013;310:104-14. doi: 10.1016/j.tox.2013.05.016. PubMed PMID: 23770417.

22. Dong H, Li J, Lv Y, Zhou Y, Wang G, Hu S, He X, Yang P, Zhou Z, Xiang X, Wang CY. Comparative analysis of the alveolar macrophage proteome in ALI/ARDS patients between the exudative phase and recovery phase. BMC Immunol. 2013;14:25. doi: 10.1186/1471-2172-14-25. PubMed PMID: 23773529; PMCID: PMC3727986.

23. Carraway MS, Piantadosi CA, Jenkinson CP, Huang Y-CT. Differential Expression of Arginase and iNOS in the Lung in Sepsis. Experimental Lung Research. 2009;24(3):253-68. doi: 10.3109/01902149809041533.

24. Bogdan C. Nitric oxide and the immune response. Nat Immunol. 2001;2(10):907-16. doi: 10.1038/ni1001-907. PubMed PMID: 11577346.

25. Vindenes H, Ulvestad E, Bjerknes R. Increased levels of circulating interleukin-8 in patients with large burns: relation to burn size and sepsis. J Trauma. 1995;39(4):635-40. PubMed PMID: 7473946.

26. Zheng H, Chen XL, Han ZX, Zhang Z, Wang SY, Xu QL. Ligustrazine attenuates acute lung injury after burn trauma. Burns. 2005;31(4):453-8. doi: 10.1016/j.burns.2004.10.023. PubMed PMID: 15896507.

27. Cairns B, Maile R, Barnes CM, Frelinger JA, Meyer AA. Increased Toll-like receptor 4 expression on T cells may be a mechanism for enhanced T cell response late after burn injury. J Trauma. 2006;61(2):293-8; discussion 8-9. doi: 10.1097/01.ta.0000228969.46633.bb. PubMed PMID: 16917441.

28. Cairns BA, Barnes CM, Mlot S, Meyer AA, Maile R. Toll-like receptor 2 and 4 ligation results in complex altered cytokine profiles early and late after burn injury. J Trauma. 2008;64(4):1069-77; discussion 77-8. doi: 10.1097/TA.0b013e318166b7d9. PubMed PMID: 18404077.

29. Neely CJ, Kartchner LB, Mendoza AE, Linz BM, Frelinger JA, Wolfgang MC, Maile R, Cairns BA. Flagellin treatment prevents increased susceptibility to systemic bacterial infection after injury by inhibiting anti-inflammatory IL-10+ IL-12- neutrophil polarization. PLoS One. 2014;9(1):e85623. doi: 10.1371/journal.pone.0085623. PubMed PMID: 24454904; PMCID: PMC3893295.

30. Xiao W, Mindrinos MN, Seok J, Cuschieri J, Cuenca AG, Gao H, Hayden DL, Hennessy L, Moore EE, Minei JP, Bankey PE, Johnson JL, Sperry J, Nathens AB, Billiar TR, West MA, Brownstein BH, Mason PH, Baker HV, Finnerty CC, Jeschke MG, Lopez MC, Klein MB, Gamelli RL, Gibran NS, Arnoldo B, Xu W, Zhang Y, Calvano SE, McDonald-Smith GP, Schoenfeld DA, Storey JD, Cobb JP, Warren HS, Moldawer LL, Herndon DN, Lowry SF, Maier RV, Davis RW, Tompkins RG, Inflammation, Host Response to Injury Large-Scale Collaborative Research P. A genomic storm in critically injured humans. J Exp Med. 2011;208(13):2581-90. doi: 10.1084/jem.20111354. PubMed PMID: 22110166; PMCID: PMC3244029.

31. Faure K, Sawa T, Ajayi T, Fujimoto J, Moriyama K, Shime N, Wiener-Kronish JP. TLR4 signaling is essential for survival in acute lung injury induced by virulent Pseudomonas aeruginosa secreting type III secretory toxins. Respir Res. 2004;5:1. doi: 10.1186/1465-9921-5-1. PubMed PMID: 15040820; PMCID: PMC389879.

32. Imai Y, Kuba K, Neely GG, Yaghubian-Malhami R, Perkmann T, van Loo G, Ermolaeva M, Veldhuizen R, Leung YH, Wang H, Liu H, Sun Y, Pasparakis M, Kopf M, Mech C, Bavari S, Peiris JS, Slutsky AS, Akira S, Hultqvist M, Holmdahl R, Nicholls J, Jiang C, Binder CJ, Penninger JM. Identification of oxidative stress and Toll-like receptor 4 signaling as a key pathway of acute lung injury. Cell. 2008;133(2):235-49. doi: 10.1016/j.cell.2008.02.043. PubMed PMID: 18423196.

CHAPTER 6: NOX2 ACTIVITY PROMOTES RESOLUTION OF INFLAMMATION AFTER ACUTE WOOD SMOKE INHALATION.[1]

Summary

Reactive oxygen species (ROS) potently induce tissue damage during inflammation, and antioxidant administration has been used extensively in animal studies of smoke inhalation to attenuate pathology; however, activity of granulocyte NADPH oxidase (NOX2) triggers anti-inflammatory, pro-resolution pathways that offset oxidative tissue damage. In this study, we set out to determine whether NOX2-dependent anti-inflammatory signals played a role in the onset and resolution of inflammation following acute smoke exposure. Protein concentration and neutrophil recruitment to the lung were significantly aggravated in NOX-2 deficient (CGD) mice after smoke exposure. Increased neutrophil recruitment may be attributable to increased production of neutrophil chemoattractants, CXCL1 and LTB4, in CGD mice compared to WT controls. Finally, we tested one established mechanism by which NOX2 activity promotes anti-inflammatory signaling, specifically stabilization of HIF1α, by treating mice with dimethyloxalylglycine (DMOG) to activate HIF1α *in vivo*. Although DMOG treatment did not reverse the hyper-inflammatory state of CGD mice after smoke inhalation, it did attenuate inflammation in WT mice. The data presented herein clearly establish a role for NOX2 activity in promoting resolution of inflammation after smoke inhalation.

Introduction

Oxidative tissue damage has been identified as a key determinant of inflammation and outcomes following smoke inhalation and burn injury (1-3). Formation of carbonyl adducts on proteins in the

[1] Attribution: Julia Dunn performed all of the experiments, analyzed data, and prepared graphs. Madison Malfitano, Laurel Kartchner, and Lindsey Glenn performed smoke inhalation experiments.

presence of reactive oxygen species (ROS) interferes with enzymatic function, leading to changes in metabolic activity and ultimately cell death (4). Carbonylated proteins have been observed in animal models of smoke inhalation and burn injury (3). Protein carbonylation was inhibited in a sheep burn and smoke inhalation model by administration of H_2S, a molecule that scavenges peroxynitrite, and this was associated with decreased tissue damage and an increase in IL-10 expression (3).

In vivo ROS are scavenged by antioxidants derived from Vitamin E, specifically α- and γ-tocopherol (aT and gT), with gT additionally able to scavenge peroxynitrite (5). Physiological concentrations of aT were depleted in a sheep model of burn and smoke inhalation; administration of Vitamin E replenished aT concentrations and resulted in decreased inflammation and improved lung function (6). Administration of gT blocked increases in lung tissue and serum concentrations of IL-8 and IL-6, suggesting a direct connection between oxidative stress and pro-inflammatory cytokine release (7).

Although several molecular mechanisms are capable of producing extracellular ROS after injury or infection, recruitment and activation of neutrophils has been identified as a key determinant of oxidative tissue damage in inhalational injury (2, 3). Granulocyte NADPH oxidase (NOX2) is a potent source of ROS in neutrophils, macrophages, and eosinophils. During recruitment, integrin ligation causes several biological changes in neutrophils, some of which promote actin remodeling to allow transmigration and chemotaxis, while others initiate a cascade that enables subsequent NOX2 activation (8, 9). gp91phox is a transmembrane protein and is the main scaffolding subunit of the NOX2 machinery that resides in the plasma membrane. Folding of the plasma membrane during phagocytosis and subsequent recruitment of the remaining subunits result in active NOX2 that pumps superoxide into phagocytic vesicles to destroy microbes or debris (10). Assembly of the NOX2 machinery at the cytoplasmic membrane results in extracellular ROS. Despite the ability of NOX2-derived ROS to induce oxidative tissue damage, an ever-growing body of evidence suggests that NOX2 activity is indispensable for promoting resolution of inflammation (11-16).

Rather than relieving tissue damage due to oxidative stress, NOX2 deficiency prevents the resolution of inflammation through a variety of mechanisms (12-16). Chronic granulomatous disease (CGD) is an inflammatory disease caused by deficient NOX2 activity attributable to mutations in any of the enzyme's subunits. Patients exhibit failure to resolve inflammation following infection, resulting in the formation of granulomas. Several knockout models of CGD have been described in mice, the most common of which are gp91phox-/- and gp47phox-/-. Deficient NOX2 signaling causes activation of NFkB and production of TNFa, IL-17, and G-CSF in macrophages (17). Moreover, NOX2 activity promotes translocation of Nrf2 to the nucleus within the first 4 hours of inflammation, leading to transcription of genes that suppress inflammation and reverse oxidative stress(16).

Neutrophils in CGD mice exhibit delayed induction of apoptosis as well as failure to modify PS to lyso-PS, which led to suppressed clearance through efferocytosis, and failure to resolve inflammation (14, 15). Characterization of neutrophils from CGD patients illuminated a role of mitochondrial-derived ROS in NET formation, and furthermore indicate an increased incidence of spontaneous NETosis (11). In these models of injury or infection, studies of CGD mice have illuminated the varied roles of NOX2 in promoting resolution of inflammation that can be amplified in WT mice.

In this study we characterized the role of NOX2 activity in the onset and resolution of inflammation in a clinically relevant murine model of acute smoke inhalation. We observed that accumulation of neutrophils, protein concentration, and the chemokine KC in BALF are elevated in CGD mice. We have previously reported elevations in IL-10, MCP1, and dsDNA at 24h after inhalational injury as well as HA at 72-96h after injury. This study indicates that these phenotypes are independent of NOX2 activity because they are not significantly altered in CGD mice. Finally, we show that stabilization of HIF1a with DMOG, which reversed the hyperinflammatory state of CGD mice in an intestinal damage model, did not substantially improve inflammation in CGD mice but did attenuate neutrophilia and HA release in WT mice. Together, these results point to an important role for NOX2 in resolving inflammation after smoke inhalation.

Methods

Mice. Homozygous gp91phox-/- (CGD) mice were bred in-house alongside WT controls, and raised in a specific pathogen free facility until 9-11 weeks of age. All experiments were designed and conducted in accordance with the National Institutes of Health regulations governing the treatment of vertebrate animals in biomedical research, and protocols were approved by the Institutional Animal Care and Use Committee (IACUC) at the University of North Carolina at Chapel Hill.

Smoke inhalation. Mice were exposed to 6 total minutes of smoke generated from combusted plywood as previously described. Briefly, mice anesthetized with tribromoethanol (475mg/kg body weight; Sigma-Aldrich) and treated with subcutaneous morphine sulphate (3mg/kg body weight; Westward) were intubated and secured to a platform in a supine position, then placed in an animal induction chamber (Stoelting NC9296517). Plywood sectioned into strips (2.5cm x 8cm, Lowe's Item #12206 Model # 776391100000) was heated in a 2L side-arm flask to generate smoke. Air pumped through the flask forced smoke into the induction chamber for three exposures of 2 minutes with a 1 minute break between exposures. Mice were resuscitated with an intraperitoneal injection of lactated Ringer's solution (1mL/kg body weight; Baxter Healthcare Incorporated), and were given morphine in their drinking water ad libitum for the duration of the experiment. Sham mice were treated identically except that air was pumped into the induction chamber rather than smoke. Dimethyloxalylglycine (DMOG) was resuspended to 4 mg/mL in PBS, and 100 uL of DMOG or vehicle control was administered via intraperitoneal injection immediately after smoke exposure and each day until euthanasia. Prior to tissue collection, mice were euthanized with gaseous isofluorane.

Broncho-alveolar lavage sample acquisition and processing. To collect broncho-alveolar lavage fluid (BALF), a catheter (22G x 1", Exel) was inserted into the trachea and connected to a syringe containing 1mL 0.6mM EDTA in PBS. 0.6mL was instilled into the lungs and then withdrawn three times to obtain a primary wash –typical recovery was 0.75 mL. Two subsequent washes were combined to obtain a secondary wash, for which typical recovery was 2 mL. Cell pellets from primary and secondary

washes were combined for analysis via flow cytometry. Cell-free supernatant from primary wash was analyzed by Bradford assay and enzyme-linked immune-sorbent assay (ELISA) for IL-10, hyaluronic acid, CXCL1 (R&D), and MCP-1 (eBioscience) according to manufacturer's instructions. LTB4 activity was quantified in primary BALF using a parameter assay kit (R&D). Cell-free DNA was enriched from 500uL of secondary BALF using a cfDNA enrichment kit (Zymo Research). Total cfDNA per mL of BALF was determined using the Qubit 3.0 fluorimeter (Life Technologies) and the Qubit dsDNA high-sensitivity detection reagents (Life Technologies).

Lungs were removed from mice after BAL extraction. Minced lung tissue was digested in 4 mL PBS with 10% Fetal Bovine Serum (PBS-FBS) with 1500 u/mouse collagenase (Worthington) and 0.1 µg/mouse DNase and shaken at 250rpm at 37°C for 1 h. Samples were filtered through a 100 µm cell strainer. Red blood cells were removed with ACK Lysis Buffer and remaining cells were suspended in PBS-FBS prior to flow cytometric analysis. Live cells from lung digest and BALF were counted manually with a hemocytometer using trypan blue dye.

Flow cytometry. Following incubation with Fc Block (eBiosciences), cells were stained with labeled antibodies against CD45, CD11b, CD11c, and Ly6G (eBiosciences; BD Biosciences). Cells were fixed with 1% paraformaldehyde prior to analysis on a CyAn (Beckmann-Coulter). To quantify RONS production, stained cells were incubated with 0.75 mg Dihydrorhodamine 123 (DHR; Thermo-Fischer; Waltham, MA). Duplicate samples were either stimulated with 62.5 ng phorbol 12-myristate 13-acetate (PMA) or left unstimulated. After 30 min, reactions were quenched with a fixation buffer containing 1% paraformaldehyde and mean fluorescence intensity (MFI) was measured. Samples were analyzed with Summit 5.1 software (Beckmann-Coulter). Neutrophils were defined as CD45+CD11b+CD11c-Ly6G+, and Macrophages were defined as CD45+CD11c+Ly6G-.

Statistical Analysis. GraphPad Prism Version 5.0 for Windows was used to analyze data by Student's t-Test, One-Way Analysis of Variance (ANOVA) with Tukey post-test, or Two-Way ANOVA

with Bonferroni post-test, as appropriate. Data are represented as mean +/- standard error of the mean (SEM). Statistical significance is indicated as * $p < 0.05$.

Results

NOX2 deficiency amplifies inflammation after acute smoke inhalation. Production of ROS by neutrophils has the potential to induce oxidative tissue damage and to initiate pro-resolution signaling pathways. To differentiate between these mechanisms, we measured production of ROS and RNS by neutrophils in WT mice after smoke inhalation and also quantified inflammation in CGD mice compared to WT controls in our smoke inhalation model. We do not observe a significant increase in intracellular oxidation of Dihydrorhodamine 123 by neutrophils recovered from the BALF at 24h, 48h, or 96h after smoke inhalation, indicating that on a per-cell basis neutrophils do not exhibit an increase in reactive oxygen and nitrogen species (RONS) production (Figure 6.1 A). We observed a significant increase in protein and neutrophils in BALF of CGD mice with and without smoke inhalation injury compared to WT controls (Figure 6.1 B-C). In interstitial tissue, we observe an increase in neutrophil count after smoke inhalation in WT mice, however in CGD mice neutrophil numbers in interstitial lung tissue are elevated regardless of injury status compared to WT sham levels (Figure 6.1 D).

NOX2 deficiency is known to interfere with neutrophil clearance by blocking apoptosis and preventing recognition of apoptotic neutrophilx by macrophages (16). We therefore set out to determine whether the increased number of neutrophils observed in BALF of CGD mice after smoke inhalation was due to neutrophils failing to undergo apoptosis or an accumulation of apoptotic neutrophils that had yet to progress to secondary necrosis. We measured expression of Annexin V and internalization of 7-AAD in BALF cells form WT and CGD mice after smoke inhalation. In samples from WT mice after smoke inhalation we did not observe a change in the fraction of apoptotic neutrophils, however there was a decrease in the fraction of neutrophils undergoing secondary necrosis (Figure 6.1 E). In CGD mice, we observe a greater fraction of apoptotic neutrophils than in WT mice, with and without smoke inhalation, and a vanishingly small fraction of neutrophils undergoing secondary apoptosis.

Leukotriene B4 (LTB4) is a potent neutrophil chemoattractant whose activity is lost when it is oxidized (18). We therefore measured LTB4 activity in BALF supernatants from sham and smoke-treated WT and CGD mice using a competition assay. In WT mice we did not observe depletion in fluorescent signal from 100% after sham treatment, indicating absence of active LTB4. Similarly, we do not observe an increase in LTB4 activity after smoke inhalation in WT mice (Figure 6.1 F). By contrast, we observe a significant increase in LTB4 activity in smoke-treated CGD mice compared to WT.

NOX2 drives cytokine production but not DAMP release after smoke inhalation. We have previously reported an increase in IL-10, MCP1, and dsDNA in BALF at 24h following smoke inhalation and accumulation of HA at 72-96h after injury. At 24h after injury, we do not observe an increase in either IL-10 or MCP1 in CGD mice, however dsDNA concentrations were comparable in smoke treated CGD mice compared to WT (Figure 6.2 A-C). We observed an increase in dsDNA concentrations in uninjured CGD mice compared to WT, however there was also an injury-dependent increase in dsDNA. In contrast, there was no change in HA concentrations in CGD mice compared to WT 96h after sham or smoke treatment (Figure 6.3 D).

HIF1α stabilization attenuates smoke-dependent inflammation in WT but not CGD mice. Previous reports illustrated a role for HIF1α in resolving intestinal inflammation in WT mice and demonstrated that this mechanism was interrupted in CGD mice (19). We set out to determine whether pharmacological stabilization of HIF1α would exert a similar anti-inflammatory effect after acute smoke inhalation in WT and CGD mice using dimethyloxalylglycine (DMOG) administration, which increases HIF1α expression *in vivo* (20). In CGD mice 96h after inhalation, DMOG treatment did not change concentrations of protein or HA in the BALF compared to vehicle control (Figure 6.3 A-B). 96h after injury, DMOG treatment resulted in a decrease in CXCL1 concentration in BALF of CGD mice compared to vehicle control at 96h after injury; however, we observed a significant increase in neutrophil numbers in CGD mice treated with DMOG compared to vehicle controls (Figure 6.3 C-D). In WT mice,

DMOG administration led to a significant decrease in neutrophil recruitment and HA concentration in the BALF at 96h after injury (Figure 6.3 B-C).

Discussion

Several reports have illustrated the importance of NOX2 in resolution of inflammation by demonstrating that injuries and infections involving neutrophil recruitment result in aggravated damage in mice deficient for NOX2 (12-16, 19). These studies have highlighted important downstream targets of neutrophil-derived ROS in promoting resolution. In this study, we set out to determine if NOX2 deficiency would exert a similar pro-inflammatory effect after acute smoke inhalation. We observe substantial amplification of protein concentration and neutrophil recruitment in the BALF after smoke inhalation in CGD mice.

Increased neutrophilia may be attributable to elevated LTB4 activity and production of the neutrophil chemoattractant CXCL1 (also known as KC). Following a fungal infection, acute induction of CXCL1 mRNA expression occurred in both WT and CGD mice, however CXCL1 production was sustained for up to a week only in CGD mice (12). We similarly observed CXCL1 protein expression in WT mice has returned to baseline by 48h after smoke exposure; however, CXCL1 remains elevated in BALF of CGD mice at 96h. Furthermore, LTB4 activity after smoke exposure is significantly elevated in CGD mice compared to WT controls, suggesting that LTB4 oxidation may limit inflammation in WT mice. Sustained CXCL1 expression and LTB4 activity may account for increased neutrophilia after smoke exposure in CGD mice.

Antioxidant treatment after burn and cotton smoke inhalation has been shown to promote increased IL-10 and improved lung function (3). In a mouse model of intra-tracheal LPS administration, no change in IL-10 expression was observed in CGD mice (13). Here we show that in CGD mice IL-10 was not increased compared to sham controls after acute smoke inhalation. This result, in context of data

in the literature, suggests that NOX2 activity promotes IL-10 production through intracellular mechanisms that are not impacted by administration of antioxidants.

Although NOX2 activity is known to promote NET formation in neutrophils, in CGD neutrophils mitochondrial ROS is sufficient to induce NET formation and oxidation of extruded DNA (11). Moreover, neutrophils from CGD patients exhibit spontaneous *ex vivo* NETosis accompanied by an increase in MPO:DNA complexes in patient serum (11). Spontaneous NETosis may account for the increased cfDNA observed in BALF of CGD mice; future studies can confirm this hypothesis by quantifying relative amplification of the 16S mtDNA by PCR compared to 18S genomic DNA.

Based on published studies demonstrating the ability of pharmacological HIF1α stabilization to reduce inflammation in WT mice and reverse the hyperinflammatory state in CGD mice after intestinal damage, we expected to observe similar results in our model (19). Although we did not observe improved inflammatory readouts in CGD mice treated with DMOG, we did observe decreased neutrophil numbers and HA concentration in WT mice treated with DMOG after smoke inhalation compared to PBS-treatment.

These results suggest that although HIF1α plays a protective role in the lung after smoke inhalation, the connection between NOX2 activity and HIF1α stabilization may not be as direct as it was observed in another injury model. Future studies will continue to explore potential mechanisms for increased inflammation in CGD mice after smoke inhalation, in order to identify strategies for suppressing inflammation in CGD and WT mice. Although antioxidant administration may offset the negative effects of tissue oxidation during inflammation, this solution does not address oxidant-sensitive pro-resolution pathways that would also be suppressed. Such targets of NOX2 signaling include Nrf2, Ref1, and NFkB (17). Agonizing one or more of these targets, along with antioxidant administration to protect the lung against oxidative stress, may represent a viable option for the treatment of inhalational injury.

FIGURES

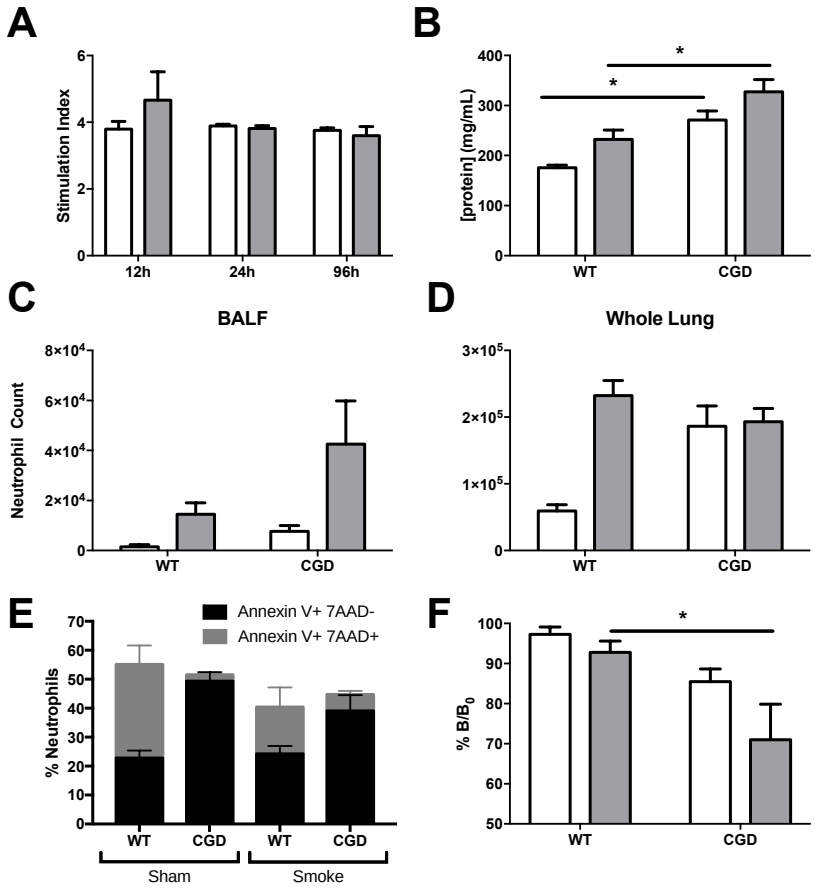

Figure 6.1: NOX2 deficiency amplifies inflammation after acute smoke inhalation. (A) Production of RO/NS in neutrophils isolated from BALF of sham (open bars) or smoke inhalation (shaded bars) treated mice was determined as fluorescence of DHR123 measured by flow cytometry. Stimulation index was calculated as MFI of PMA stimulated cells divided by the MFI of unstimulated cells. (B) Protein concentration in BALF of sham (open bars) and smoke (shaded bars) treated WT and CGD mice 96h after treatment. (C-D) Neutrophils were quantified by flow cytometry in BALF (C) and whole lung digest (D) as a percentage of live cells and normalized to total cell counts. (E) Samples prepared for flow cytometry from BALF were stained with PE-conjugated Annexin V and 7-AAD to quantify apoptotic (AnnexinV+7AAD-) and secondary necrotic (AnnexinV+7AAD+) cells within the gated neutrophil population. (F) LTB4 activity was quantified in BALF using a competition-based assay and results are represented as % signal compared to negative control. Data were analyzed by two-way ANOVA with Bonferroni post-test and significance denoted as *$p < 0.05$. 3-4 sham and 4-5 smoke-treated mice were used per treatment group, and experiments were repeated to confirm results.

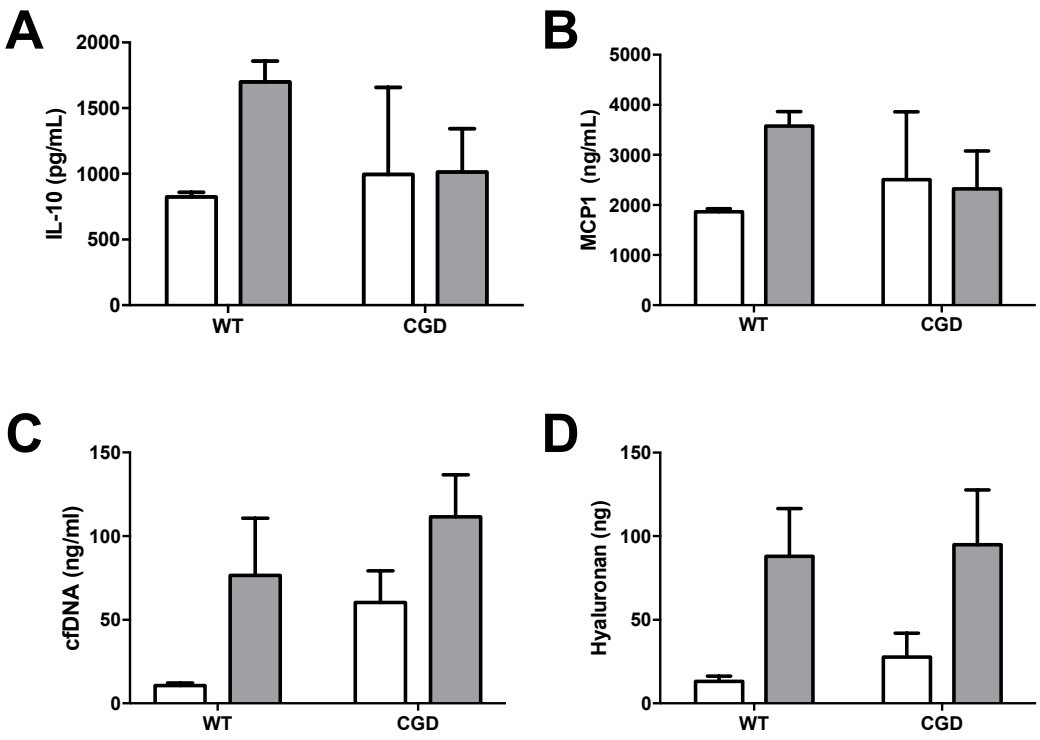

Figure 6.2: NOX2 drives cytokine production but not DAMP release after smoke inhalation. Sham samples are represented by open bars and smoke samples are represented by shaded bars. IL-10 concentration (A) and MCP-1 concentration (B) were quantified in primary BALF samples 24h after inhalational injury or sham treatment in WT and CGD mice. (C) dsDNA concentration was quantified in secondary BALF samples 24h after inhalational injury or sham treatment in WT or CGD mice. (D) Hyaluronic acid concentration was quantified in primary BALF 96h after inhalational injury or sham treatment in WT or CGD mice. Data were analyzed by two-way ANOVA with Bonferroni post-test. 3-4 sham and 4-5 smoke-treated mice were used per treatment group, and experiments were repeated to confirm results.

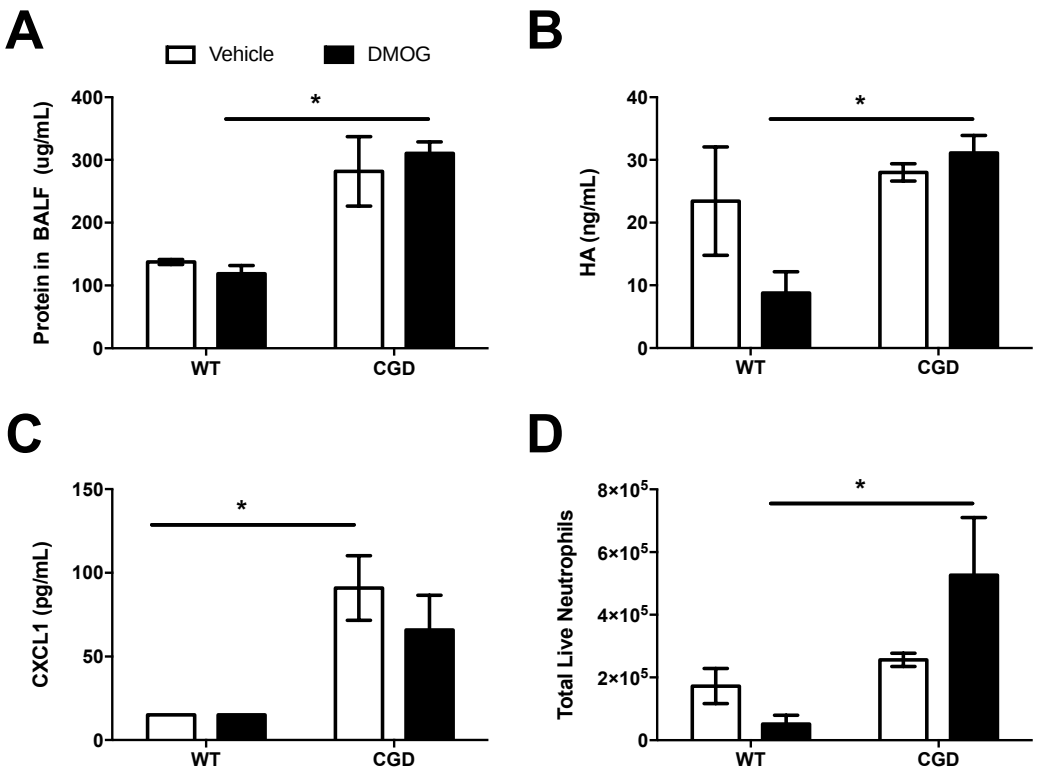

Figure 6.3: HIF1α stabilization attenuates smoke-dependent inflammation in WT but not CGD mice. Mice were treated with either DMOG (closed bars) or PBS vehicle control (open bars) immediately after and daily following inhalational injury. Concentration of protein (A) and hyaluronic acid (B) were quantified in BALF at 24h following injury. Concentraiton of CXCL1 (C) was quantified in BALF at 96h following injury. Total neutrophils (D) were measured as a percentage of live cells by flow cytometry and normalized to the total sample as determined by trypan blue staining. Data were analyzed by two-way ANOVA with Bonferroni post-test and significance indicated as * $p < 0.05$. 3-4 sham and 4-5 smoke-treated mice were used per treatment group, and experiments were repeated to confirm results.

REFERENCES

1. Rehberg S, Maybauer MO, Enkhbaatar P, Maybauer DM, Yamamoto Y, Traber DL. Pathophysiology, management and treatment of smoke inhalation injury. Expert Rev Respir Med. 2009;3(3):283-97. doi: 10.1586/ERS.09.21. PubMed PMID: 20161170; PMCID: PMC2722076.

2. Lange M, Szabo C, Traber DL, Horvath E, Hamahata A, Nakano Y, Traber LD, Cox RA, Schmalstieg FC, Herndon DN, Enkhbaatar P. Time profile of oxidative stress and neutrophil activation in ovine acute lung injury and sepsis. Shock. 2012;37(5):468-72. doi: 10.1097/SHK.0b013e31824b1793. PubMed PMID: 22266977; PMCID: PMC4646062.

3. Esechie A, Kiss L, Olah G, Horvath EM, Hawkins H, Szabo C, Traber DL. Protective effect of hydrogen sulfide in a murine model of acute lung injury induced by combined burn and smoke inhalation. Clin Sci (Lond). 2008;115(3):91-7. doi: 10.1042/CS20080021. PubMed PMID: 18315525.

4. Ciolino HP, Levine RL. Modification of proteins in endothelial cell death during oxidative stress. Free Radic Biol Med. 1997;22(7):1277-82. PubMed PMID: 9098102.

5. Galli F, Stabile AM, Betti M, Conte C, Pistilli A, Rende M, Floridi A, Azzi A. The effect of alpha- and gamma-tocopherol and their carboxyethyl hydroxychroman metabolites on prostate cancer cell proliferation. Arch Biochem Biophys. 2004;423(1):97-102. doi: 10.1016/j.abb.2003.11.014. PubMed PMID: 14871472.

6. Morita N, Traber MG, Enkhbaatar P, Westphal M, Murakami K, Leonard SW, Cox RA, Hawkins HK, Herndon D, Traber LD, Traber DL. Aerosolized alpha-tocopherol ameliorates acute lung injury following combined burn and smoke inhalation injury in sheep. Shock. 2006;25(3):277-82. doi: 10.1097/01.shk.0000208805.23182.a7. PubMed PMID: 16552360.

7. Hamahata A, Enkhbaatar P, Kraft ER, Lange M, Leonard SW, Traber MG, Cox RA, Schmalstieg FC, Hawkins HK, Whorton EB, Horvath EM, Szabo C, Traber LD, Herndon DN, Traber DL. gamma-Tocopherol nebulization by a lipid aerosolization device improves pulmonary function in sheep with burn and smoke inhalation injury. Free Radic Biol Med. 2008;45(4):425-33. doi: 10.1016/j.freeradbiomed.2008.04.037. PubMed PMID: 18503777; PMCID: PMC2555991.

8. Graham DB, Robertson CM, Bautista J, Mascarenhas F, Diacovo MJ, Montgrain V, Lam SK, Cremasco V, Dunne WM, Faccio R, Coopersmith CM, Swat W. Neutrophil-mediated oxidative burst and host defense are controlled by a Vav-PLCgamma2 signaling axis in mice. J Clin Invest. 2007;117(11):3445-52. doi: 10.1172/JCI32729. PubMed PMID: 17932569; PMCID: PMC2000813.

9. Mocsai A, Zhou M, Meng F, Tybulewicz VL, Lowell CA. Syk is required for integrin signaling in neutrophils. Immunity. 2002;16(4):547-58. PubMed PMID: 11970878.

10. Panday A, Sahoo MK, Osorio D, Batra S. NADPH oxidases: an overview from structure to innate immunity-associated pathologies. Cell Mol Immunol. 2015;12(1):5-23. doi: 10.1038/cmi.2014.89. PubMed PMID: 25263488; PMCID: PMC4654378.

11. Lood C, Blanco LP, Purmalek MM, Carmona-Rivera C, De Ravin SS, Smith CK, Malech HL, Ledbetter JA, Elkon KB, Kaplan MJ. Neutrophil extracellular traps enriched in oxidized

mitochondrial DNA are interferogenic and contribute to lupus-like disease. Nat Med. 2016;22(2):146-53. doi: 10.1038/nm.4027. PubMed PMID: 26779811; PMCID: PMC4742415.

12. Morgenstern DE, Gifford MA, Li LL, Doerschuk CM, Dinauer MC. Absence of respiratory burst in X-linked chronic granulomatous disease mice leads to abnormalities in both host defense and inflammatory response to Aspergillus fumigatus. J Exp Med. 1997;185(2):207-18. PubMed PMID: 9016870; PMCID: PMC2196125.

13. Han HJ, Lee YJ, Park SH, Lee JH, Taub M. High glucose-induced oxidative stress inhibits Na+/glucose cotransporter activity in renal proximal tubule cells. Am J Physiol Renal Physiol. 2005;288(5):F988-96. doi: 10.1152/ajprenal.00327.2004. PubMed PMID: 15598843.

14. Frasch SC, Fernandez-Boyanapalli RF, Berry KA, Murphy RC, Leslie CC, Nick JA, Henson PM, Bratton DL. Neutrophils regulate tissue Neutrophilia in inflammation via the oxidant-modified lipid lysophosphatidylserine. J Biol Chem. 2013;288(7):4583-93. doi: 10.1074/jbc.M112.438507. PubMed PMID: 23293064; PMCID: PMC3576064.

15. Rohm M, Grimm MJ, D'Auria AC, Almyroudis NG, Segal BH, Urban CF. NADPH oxidase promotes neutrophil extracellular trap formation in pulmonary aspergillosis. Infect Immun. 2014;82(5):1766-77. doi: 10.1128/IAI.00096-14. PubMed PMID: 24549323; PMCID: PMC3993456.

16. Segal BH, Han W, Bushey JJ, Joo M, Bhatti Z, Feminella J, Dennis CG, Vethanayagam RR, Yull FE, Capitano M, Wallace PK, Minderman H, Christman JW, Sporn MB, Chan J, Vinh DC, Holland SM, Romani LR, Gaffen SL, Freeman ML, Blackwell TS. NADPH oxidase limits innate immune responses in the lungs in mice. PLoS One. 2010;5(3):e9631. doi: 10.1371/journal.pone.0009631. PubMed PMID: 20300512; PMCID: PMC2838778.

17. Ward C, Chilvers ER, Lawson MF, Pryde JG, Fujihara S, Farrow SN, Haslett C, Rossi AG. NF-kappaB activation is a critical regulator of human granulocyte apoptosis in vitro. J Biol Chem. 1999;274(7):4309-18. PubMed PMID: 9933632.

18. Sumimoto H, Minakami S. Oxidation of 20-hydroxyleukotriene B4 to 20-carboxyleukotriene B4 by human neutrophil microsomes. Role of aldehyde dehydrogenase and leukotriene B4 omega-hydroxylase (cytochrome P-450LTB omega) in leukotriene B4 omega-oxidation. J Biol Chem. 1990;265(8):4348-53. PubMed PMID: 2155225.

19. Campbell EL, Bruyninckx WJ, Kelly CJ, Glover LE, McNamee EN, Bowers BE, Bayless AJ, Scully M, Saeedi BJ, Golden-Mason L, Ehrentraut SF, Curtis VF, Burgess A, Garvey JF, Sorensen A, Nemenoff R, Jedlicka P, Taylor CT, Kominsky DJ, Colgan SP. Transmigrating neutrophils shape the mucosal microenvironment through localized oxygen depletion to influence resolution of inflammation. Immunity. 2014;40(1):66-77. doi: 10.1016/j.immuni.2013.11.020. PubMed PMID: 24412613; PMCID: PMC3951457.

20. Peng X, Gong F, Chen Y, Jiang Y, Liu J, Yu M, Zhang S, Wang M, Xiao G, Liao H. Autophagy promotes paclitaxel resistance of cervical cancer cells: involvement of Warburg effect activated hypoxia-induced factor 1-alpha-mediated signaling. Cell Death Dis. 2014;5:e1367. doi: 10.1038/cddis.2014.297. PubMed PMID: 25118927; PMCID: PMC4454295.

CHAPTER 7: CONCLUDING REMARKS

In traumatic injury, what goes up must come down.

Survival after traumatic injury requires the body to create order form chaos, and the innate immune system is capable of acting as an asset or a hindrance in this process. By their nature, injuries break barriers that normally hold microbes at bay, and the body is exposed to high concentrations of both damage-associated molecular patterns (DAMPs) from the injury and pathogen-associated molecular patterns (PAMPs) from microbes. The immune system is designed to rapidly induce a pro-inflammatory response to neutralize microbes and then transition to an anti-inflammatory phenotype to promote wound closure and revascularization as PAMPs subside and DAMPs from the original injury and subsequent inflammation become prominent. With severe injuries, especially burns, wound closure takes an exceptionally long time and the body must therefore juggle conflicting signals for weeks.

Until the early 20th century, severe injuries often caused mortality in the acute, pro-inflammatory phase due to inflammation that caused edema and disrupted function of critical organs, especially the heart and lungs. Novel resuscitation strategies designed to balance blood pressure and maintain circulation increased the fraction of patients who survived initial shock, and the next great obstacle was wound infections. Wound care and cleaning, antimicrobials, and early excision and grafting have significantly attenuated this threat. Today the greatest threat to patients in burn units is pulmonary infection occurring several days after hospitalization resulting from failure of immunological surveillance and protection in the lung. Poor immune activity in the lung has been attributed to a predominantly anti-inflammatory environment of a body trying to heal that suppresses antimicrobial innate immune function. Our objective is to investigate the immune mechanisms at play in the lung after trauma in order to tackle

this significant challenge to patient survival with a translational approach using both human samples and mouse models.

Here we report that the innate immune response to bacterial challenge is severely impaired after injury, and that despite significant pulmonary inflammation the lung remains a target for infection. First, we demonstrated that in uninjured mice blood NO concentrations are elevated following pulmonary bacterial challenge and that this response is absent in injured mice. We then showed that lack of NO response is not indicative of a muted innate immune response –in fact, burn injury leads to significant innate immune infiltration to the lung. Burn injury leads to rapid accumulation of neutrophils in the pulmonary microvasculature, which may be driven by circulating DAMPs, since we show that intravenous DAMP administration amplified acute neutrophilia and prompted perturbation of the alveolar/capillary barrier. Moreover, we present evidence that neutrophil activity *in situ* is a significant determinant of their antimicrobial efficacy, since inhibiting activation of mTOR suppressed production of RONS production and TLR expression on neutrophils and was accompanied by failure to control *Pseudomonas aeruginosa* infection despite significant neutrophil recruitment.

To continue and expand our investigation of pulmonary damage and inflammation after traumatic injury, we developed a novel model of acute wood smoke exposure (Figure 7.1). After validating the utility of the model system for studying phenotypes that are relevant to patient outcomes, we again observed that neutrophil recruitment is not protective against infection and may, in fact, promote immunopathology. We arrived at this assessment through two sets of experiments. First, we partially attenuated neutrophil trafficking to the lung after smoke inhalation but did not target neutrophil function, and we observed that this attenuated pathological inflammation without increasing susceptibility to bacterial challenge. Next, to address the role of neutrophil function, we quantified the onset and resolution of inflammation in mice deficient for granulocyte NADPH oxidase, NOX2, compared to WT counterparts. In the absence of neutrophil-derived ROS, tissue damage was not attenuated and inflammation was exaggerated, pointing to a failure to resolve inflammation.

iNOS and NOX2 drive inflammation in ALI

Mechanistic findings in our smoke inhalation model reflect the current literature around ALI in a novel, translationally relevant context. iNOS expression has been noted in several animal studies of acute smoke inhalation (1-3). In other models of ALI, iNOS plays a role in cytokine and chemokine production (4, 5). We observed that iNOS was required for increases in IL-10, MCP1, and HA following injury. Our finding that clearance of PA01 was unchanged in iNOS-/- mice after smoke inhalation reflects previous data showing that iNOS activity is dispensable for *P. aeruginosa* (3).

Similarly, our results about the impact of NOX2 activity on inflammation and resolution are in agreement with the literature. NOX2 deficiency leads to unresolved inflammation following infection or injury that results in granulomas in patients, hence the disorder is named chronic granulomatous disease (CGD). Mouse models of CGD suggest that neutrophil-derived ROS play an important role in activating signaling cascades that promote resolution and may therefore act as a natural fail-safe to promote resolution (6-9). In other studies, the observation that pathology is more severe in NOX2 deficient mice led to the identification of downstream targets of NOX2 activity, such as Ref1, Nrf2, HIF1α, and NFκB, that can be targeted in WT animals to promote efficient resolution (6, 9, 10).

Targeting NOX2 signaling partners to resolve ALI

A role for neutrophil extracellular traps (NETs) in patients after burn and inhalational injuries has yet to be established; however, several mechanisms known to occur up- and down-stream of NETosis have been observed in patients and in our model of inhalational injury. ROS generation and NOX2 activity promote NETosis, which consist of DNA conjugated to enzymes and antimicrobial molecules that sequester and neutralize extracellular pathogens (7, 10, 11). Both apoptosis and NETosis begin with decondensation of the nuclear contents, after which point Caspase 3 cleavage and activation directs a cell toward apoptosis and failure to activate Caspase 3 predisposes a cell toward NETosis (10). Deficient NOX2 activity may polarize neutrophils toward NETosis rather than apoptosis, resulting in amplified inflammation (10). Cell-free dsDNA is elevated in serum and BALF from patients after traumatic injury,

which could be the result of NETosis (12, 13). To confirm NETosis as a source of the DNA, future studies can determine whether DNA is conjugated to myeloperoxidase (MPO) or neutrophil elastase (7). We furthermore propose that it would be valuable to examine *in vitro* NETosis in neutrophils from blood and BALF of trauma patients, to determine whether they are predisposed to spontaneous NET formation, as has been observed in CGD patients (7).

Previous studies in CGD mice have demonstrated that NOX2-/- delays the onset of neutrophil apoptosis and decreases signals that promote clearance of apopototic neutrophils (6, 9, 10, 14). Harnessing these mechanisms in WT mice to improve neutrophil clearance, and the anti-inflammatory events that accompany normal resolution, may be an effective strategy to decrease lung damage in our mouse model and eventually in the patient population. NFκB activity delays neutrophil apoptosis, extending neutrophil lifespan and promoting further inflammation (9, 15). NOX2 activity suppresses NFκB activity to effectively promote progression to apoptosis, and in NOX2-deficient neutrophils administration of hydrogen peroxide (H_2O_2) is sufficient to achieve the same effect (14). A variety of approaches are available to determine the extent to which these mechanisms are at play in WT and CGD mice after smoke inhalation. Several NFκB inhibitors exist that promote neutrophil apoptosis; such treatment might offset the increased neutrophilia in CGD mice compared to WT, and may decrease inflammation after smoke inhalation in WT mice (14).

During proper resolution, apoptotic neutrophils are cleared by macrophages, which phagocytose apoptotic neutrophils through a process called efferocytosis. NOX2 activity in neutrophils promotes the translocation of a modified phosphatidylserine (lyso-PS) to the surface, which engages G2A on the surface of resident macrophages to induce efferocytosis (9) Efferocytosis triggers anti-inflammatory programs in macrophages, leading to decreased production of IL-6 and CXCL1/KC. Neutrophils that are not efferocytosed after apoptosis progress to secondary necrosis, which promotes further inflammation by the release of intracellular contents.

Observational studies in humans and mechanistic studies in mice could determine the extent to which efferocytosis is occurring in the lung after smoke inhalation and whether promoting or inhibiting efferocytosis alters the long term inflammatory phenotype. *Ex vivo* efferocytosis assays have been described, and it would also be useful to evaluate macrophage expression of G2A, which recognizes signals on the surface of apopototic cells, and CD206, which is highly expressed on efferocytotic macrophages (16). These readouts can be measured in WT and CGD mice and in cells derived from BALF of patients diagnosed with inhalational injury. To assess the utility of promoting efferocytosis in promoting healthy resolution after inhalational injury, mice can be treated with antibodies that neutralize G2A, which block efferocytosis. If our hypothesis is correct and efferocytosis is critical for removing neutrophils and promoting anti-inflammatory cytokine production in tissue-resident macrophages, then G2A blockade should increase the number of inflammatory cells and DAMPs present in the BALF after smoke inhalation.

Where there's smoke, there's fire.

Given the established utility of our inhalational injury model for mimicking patient phenotypes after smoke inhalation, an important application for this model is to test the role of injury-related variables. Combined burn and smoke inhalational injuries lead to increased mortality, and studies are currently underway in our laboratory to examine the compounded effect of these two injuries. Furthermore, because clinical outcomes are driven by comorbidities including age, BMI, and smoker status, these variables should be incorporated into future studies of acute smoke inhalation in mice. Finally, the severity of inhalational injuries depends largely on the type of structure in which smoke was generated. Although this may have to do with ventilation in the structure, we propose that this distinction is also driven by the chemical makeup of the smoke, which can be more clearly elucidated using our experimental setup. Any of these studies, if successful, would have a significant positive impact on patient outcomes.

FIGURES

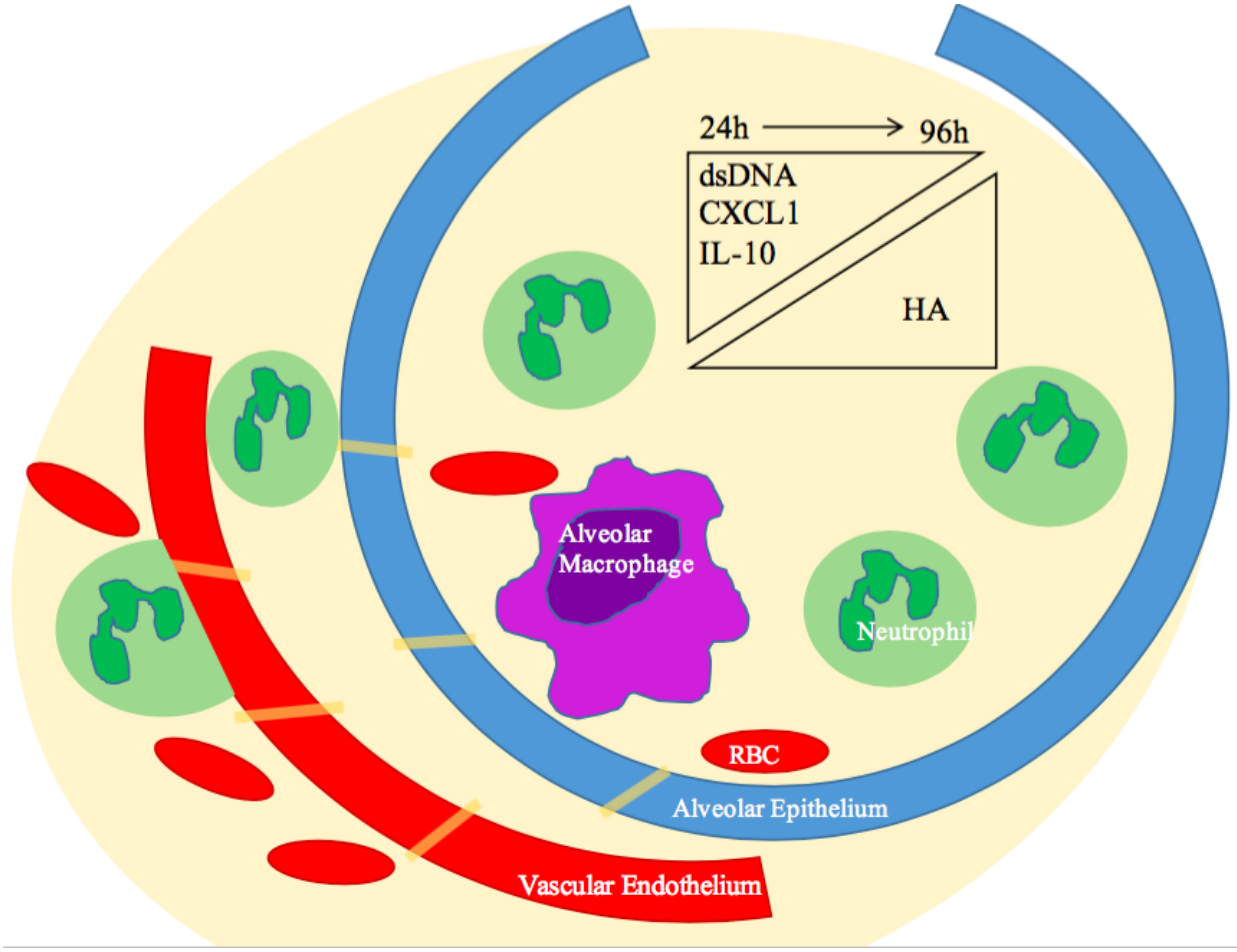

Figure 7.1: ALI following wood smoke inhalation. Like other models of ALI, wood smoke inhalation results in protein buildup, immune cells (neutrophils), and cytokines (MCP1, IL-10) in BALF following smoke inhalation, as well as congestion of microvasculature. We have demonstrated that neutrophilia is largely driven by CXCL1 accumulation in the BALF and that IL-10 is derived from macrophages. Future studies will determine the cellular source of CXCL1 as well as the molecular mechanisms that cause increases in dsDNA and HA following smoke inhalation. Abbreviations: acute lung injury (ALI); broncho-alveolar lavage fluid (BALF); double-stranded deoxyribonucleic acid (dsDNA); chemokine (c-x-c motif) ligand 1 (CXCL1); hyaluronic acid (HA); interleukin 10 (IL-10); monocyte chemotactic protein 1 (MCP1); red blood cell (RBC).

REFERENCES

1. Esechie A, Kiss L, Olah G, Horvath EM, Hawkins H, Szabo C, Traber DL. Protective effect of hydrogen sulfide in a murine model of acute lung injury induced by combined burn and smoke inhalation. Clin Sci (Lond). 2008;115(3):91-7. doi: 10.1042/CS20080021. PubMed PMID: 18315525.

2. Carraway MS, Piantadosi CA, Jenkinson CP, Huang Y-CT. Differential Expression of Arginase and iNOS in the Lung in Sepsis. Experimental Lung Research. 2009;24(3):253-68. doi: 10.3109/01902149809041533.

3. Bogdan C. Nitric oxide and the immune response. Nat Immunol. 2001;2(10):907-16. doi: 10.1038/ni1001-907. PubMed PMID: 11577346.

4. Trifilieff A, Fujitani Y, Mentz F, Dugas B, Fuentes M, Bertrand C. Inducible Nitric Oxide Synthase Inhibitors Suppress Airway Inflammation in Mice Through Down-Regulation of Chemokine Expression. The Journal of Immunology. 2000;165(3):1526-33. doi: 10.4049/jimmunol.165.3.1526.

5. Mizutani A, Enkhbaatar P, Esechie A, Traber LD, Cox RA, Hawkins HK, Deyo DJ, Murakami K, Noguchi T, Traber DL. Pulmonary changes in a mouse model of combined burn and smoke inhalation-induced injury. J Appl Physiol (1985). 2008;105(2):678-84. doi: 10.1152/japplphysiol.00232.2007. PubMed PMID: 18436699.

6. Campbell EL, Bruyninckx WJ, Kelly CJ, Glover LE, McNamee EN, Bowers BE, Bayless AJ, Scully M, Saeedi BJ, Golden-Mason L, Ehrentraut SF, Curtis VF, Burgess A, Garvey JF, Sorensen A, Nemenoff R, Jedlicka P, Taylor CT, Kominsky DJ, Colgan SP. Transmigrating neutrophils shape the mucosal microenvironment through localized oxygen depletion to influence resolution of inflammation. Immunity. 2014;40(1):66-77. doi: 10.1016/j.immuni.2013.11.020. PubMed PMID: 24412613; PMCID: PMC3951457.

7. Lood C, Blanco LP, Purmalek MM, Carmona-Rivera C, De Ravin SS, Smith CK, Malech HL, Ledbetter JA, Elkon KB, Kaplan MJ. Neutrophil extracellular traps enriched in oxidized mitochondrial DNA are interferogenic and contribute to lupus-like disease. Nat Med. 2016;22(2):146-53. doi: 10.1038/nm.4027. PubMed PMID: 26779811; PMCID: PMC4742415.

8. Morgenstern DE, Gifford MA, Li LL, Doerschuk CM, Dinauer MC. Absence of respiratory burst in X-linked chronic granulomatous disease mice leads to abnormalities in both host defense and inflammatory response to Aspergillus fumigatus. J Exp Med. 1997;185(2):207-18. PubMed PMID: 9016870; PMCID: PMC2196125.

9. Frasch SC, Fernandez-Boyanapalli RF, Berry KA, Murphy RC, Leslie CC, Nick JA, Henson PM, Bratton DL. Neutrophils regulate tissue Neutrophilia in inflammation via the oxidant-modified lipid lysophosphatidylserine. J Biol Chem. 2013;288(7):4583-93. doi: 10.1074/jbc.M112.438507. PubMed PMID: 23293064; PMCID: PMC3576064.

10. Rohm M, Grimm MJ, D'Auria AC, Almyroudis NG, Segal BH, Urban CF. NADPH oxidase promotes neutrophil extracellular trap formation in pulmonary aspergillosis. Infect Immun. 2014;82(5):1766-77. doi: 10.1128/IAI.00096-14. PubMed PMID: 24549323; PMCID: PMC3993456.

11. Brinkmann V, Laube B, Abu Abed U, Goosmann C, Zychlinsky A. Neutrophil extracellular traps: how to generate and visualize them. J Vis Exp. 2010(36). doi: 10.3791/1724. PubMed PMID: 20182410; PMCID: PMC3125121.

12. Jones SW, Zhou H, Ortiz-Pujols SM, Maile R, Herbst M, Joyner BL, Jr., Zhang H, Kesic M, Jaspers I, Short KA, Meyer AA, Peden DB, Cairns BA, Noah TL. Bronchoscopy-derived correlates of lung injury following inhalational injuries: a prospective observational study. PLoS One. 2013;8(5):e64250. doi: 10.1371/journal.pone.0064250. PubMed PMID: 23691180; PMCID: PMC3656836.

13. Simmons JD, Lee YL, Mulekar S, Kuck JL, Brevard SB, Gonzalez RP, Gillespie MN, Richards WO. Elevated levels of plasma mitochondrial DNA DAMPs are linked to clinical outcome in severely injured human subjects. Ann Surg. 2013;258(4):591-6; discussion 6-8. doi: 10.1097/SLA.0b013e3182a4ea46. PubMed PMID: 23979273; PMCID: PMC3935616.

14. Ward C, Chilvers ER, Lawson MF, Pryde JG, Fujihara S, Farrow SN, Haslett C, Rossi AG. NF-kappaB activation is a critical regulator of human granulocyte apoptosis in vitro. J Biol Chem. 1999;274(7):4309-18. PubMed PMID: 9933632.

15. Han HJ, Lee YJ, Park SH, Lee JH, Taub M. High glucose-induced oxidative stress inhibits Na+/glucose cotransporter activity in renal proximal tubule cells. Am J Physiol Renal Physiol. 2005;288(5):F988-96. doi: 10.1152/ajprenal.00327.2004. PubMed PMID: 15598843.

16. Segal BH, Han W, Bushey JJ, Joo M, Bhatti Z, Feminella J, Dennis CG, Vethanayagam RR, Yull FE, Capitano M, Wallace PK, Minderman H, Christman JW, Sporn MB, Chan J, Vinh DC, Holland SM, Romani LR, Gaffen SL, Freeman ML, Blackwell TS. NADPH oxidase limits innate immune responses in the lungs in mice. PLoS One. 2010;5(3):e9631. doi: 10.1371/journal.pone.0009631. PubMed PMID: 20300512; PMCID: PMC2838778.